Analysis of Cross-talk and Discontinuity Problems in Microstrip Lines

Ahmed Ali Hussein

Submitted to the
Institute of Graduate Studies and Research
in partial fulfillment of the requirements for the Degree of

Master of Science
in
Electrical and Electronic Engineering

Eastern Mediterranean University
February 2014
Gazimağusa, North Cyprus

Approval of the Institute of Graduate Studies and Research

Prof. Dr. Elvan Yılmaz
Director

I certify that this thesis satisfies the requirements as a thesis for the degree of Master of Science in Electrical and Electronic Engineering.

Prof. Dr. Aykut Hocanın
Chair, Department of Electrical and Electronic Engineering

We certify that we have read this thesis and that in our opinion it is fully adequate in scope and quality as a thesis for the degree of Master of Science in Electrical and Electronic Engineering.

Assist. Prof. Dr. Rasime Uyguroğlu
Supervisor

Examining Committee

1. Prof. Dr. Hasan Amca
2. Asst. Prof. Dr. Hasan Demirel
3. Asst. Prof. Dr. Rasime Uyguroğlu

ABSTRACT

In this thesis, microstrip line problems such as crosstalk and discontinuity that may occur in the microwave circuits have been studied in line with the literature and simulations have been carried out by using FEKO 5.5 full wave simulation software. The crosstalk problem is studied in three sections. The first section deals with the effect of placing rectangular trace between the strips, which is connected to the ground. With the proposed design 7dB of reduction has been observed in the Far-End crosstalk (FEXT). In the second section, perpendicular rectangular metals with Via fences connected to the Guard trace (RVG) have been used and FEXT enhancement of 7dB was observed. In the last section, Cross shape metals with via fence were connected by Guard trace (CVG) and The FEXT was reduced by 8dB. The results are compared with spacing rule results for S = 3W.

The discontinuity problem that occurs in right angle and step-width microstrip lines may be reduced by two types of chamfered methods. i.e. angle chamfered and tapered chamfered methods. In this study, a novel design has been applied to reduce the discontinuity problem by using tapered line on both sides of transmission lines. Simulation results show an improvement in reflection coefficient for 23 GHz (7-30) GHz bandwidth (BW) when compared with the step-width without chamfered. For the bend discontinuity, it was found out that the improvement in the reflection coefficient with a 70% chamfered ratio compared with 50% ratio is about 4dB for 70 GHz BW.

Keywords: Coupling, FEXT, NEXT, Microstrip discontinuity, FEKO, RVG, CVG, Chamfer, taper, Via fence

ÖZ

Bu tez çalışmasında, mikroşerit devrelerdeki iletim hatlarında görülen çapraz girişim ve kesintilerden oluşan problemler ele alınmış; FEKO 5.5 yazılım paketi ile benzetişim yapılmış ve sonuçlar yayınlanmış sonuşlarara gore değerlendirilmiştir. Çapraz girişimle ilgili çalışma üç bölümden oluşmaktadır. Öncelikle, iki şerit arasına, referans metale temas edecek şekilde metal bar yerleştirilerek bir çalışma yapılmıştır. Daha sonra, iki mikrpşerit arasına yerleştirilmiş şerite, dik (dielektrik içerisine konmuş) silindirik yapılı metalik korumanın etkisi incelenmiştir.Önerilen şerit uzunluğu ve bağıl permitivite için FEXT değerinde 7dB'lik azalma görülmüştür. İkinci çalışmada, önceki tasarıma ek olarak şerit düzleminde metal dikdörtgen (RGV) eklenmiş ve FEXT değerinde 7dB'lik, dikdörtgen yerine çapraz şeritler kullanıldığı zaman ise 8dB'lik azalma tespit edilmiştir. Bu değerlendirme, şeritler arası mesafenin, şerit genişliğinin üç katı olduğu durumla karşılaştırılmıştır.

Ayrıca, mikroşerit iletim hatlarındaki dik açılı kıvrık ve merdiven türü genişleyen kesintilerden kaynaklanan empedans uyum sorunları,iki tür mikroşerit kesinti (chamfered) yöntemi ile azaltılmıştır; açı kesit ve konik kesit. Kesinti problemini azaltmak için mikroşeritin her iki yanına konik yöntemi ile empedans uyumlaması yapılmıştır. Simülasyon sonuçlarına göre, merdiven türü genişlemeli iletim hatlarına uygulanan kesintili uygumlaştırma yönteminin kesintisize göre 23GHz'(7-30) GHz lik BW için, yansıma katsayısı bakımından daha iyi olduğu görülmüştür. Kıvrık kesintili şeritlerde ise 70GHz BW için yansıma katsayısının 70%'lik oyuk oranıda, 50%'ye gore 4dB'lik bir iyileşme tesbit edilmiştir.

Anahtar Kelimeler: çabraz girişim**,** FEXT, NEXT, kesintili mikroşerit, FEKO, RVG, CVG kesit, konik, metalik koruma yolu (via fence)

ACKNOWLEDGMENTS

I wish to express my thanks and appreciation to my supervisor in the person of Asst. Prof. Dr. Rasime Uyguroğlu for helping me to complete my research work, his relentless help and support towards me helps me overcome the difficulties in studying the length of the search.

My sincere appreciation goes to all employees in the department, the members of the Administration Faculty and the Head of the Department. More importantly, Prof. Dr. Aykut Hocanın, and Vice Chairman of the Department, Asst. Prof. Dr. Hasan Demirel.

I will also like to appreciate my family for their help and support. They encouraged me all through my studies; it's a great source of motivation towards my success today.

Also extend sincere thanks to all my friends here in Eastern Mediterranean University and in my country Iraq.

TABLE OF CONTENTS

ABSTRA CT iii

ÖZ v

ACKNOWLEDGMENTS vii

LIST OF TABLES x

LIST OF FIGURES xi

LIST OF SYMBOLS /ABBREVIATIONS xvi

1 INTRODUCTION AND BACKGROUND 1

1.1 Introduction 1

1.2 Thesis overview 2

2 BACKGROUND INFORMATION 3

2.1 Background 3

2.1.1 The definition of the Transmission Line 3

2.1.2 Transmission line parameters 4

2.1.3 Transmission line equations 4

2.1.4 Microstrip Line (MSL) 6

2.1.5 Special TL Loads 9

2.1.6 Scattering Parameters (S-parameters) 10

2.2 Microstrip Line Simulations 12

2.2.1 Effective Relative Permativity ($\boldsymbol{\varepsilon_{eff}}$) 12

2.2.2 Characteristic Impedance $\boldsymbol{Z_o}$ 14

2.2.3 Scattering Parameter 16

3 Crosstalk problem between microstrip lines 19

3.1 Introduction 19

3.2 Crosstalk or Coupling 19
3.2.1 Simulation of a Microstrip line by FEKO 5.5 Simulator 22
3.2.2 Crosstalk between two microstrip lines 24
3.2.3 Simulation Results 29
4 DISCONTINUITY PROBLEM 67
4.1 Introduction 67
4.2 Types of Discontinuities 68
4.2.1 Step in Width Discontinuity 68
4.2.2 Right angle bend Discontinuity 69
4.3 Simulation Results 70
4.3.1 Right angle bend discontinuity 70
4.4.2 Step in Width Discontinuity 76
5 CONCLUSION AND FUTURE WORK 83
5.1 Conclusion 83
5.2 Future Work 84
REFERENCES 85

LIST OF TABLES

Table 3.1: Dimensions of microstrip lines 24

Table 3.2: Dimension of the coating microstrip line design [1] 29

Table 3.3: Dimension of the microstrip lines in [3] 36

Table 3.4: Dimensions of the coupled microstrip lines [4] 38

Table 3.5: Dimensions of Microstrip lines with via fences 44

Table 3.6: Dimensions of microstrip line with the Design 46

Table 3.7: Design Parameters of RVG design 54

Table 3.8: Dimensions of CVG design 59

LIST OF FIGURES

Figure 2.1: Types of Transmission lines (a) Coaxial cable (b) Two wire line (c) Wire over conducting plane (d) Planar line (e) Microstrip line (f) Stripline [8] 3

Figure 2.2: Transmission line circuit [8] 4

Figure 2.3: Microstrip line structure [10] 6

Figure 2.4: EM field in microstrip line (quasi-TEM) [10] 7

Figure 2.5: EM field in planar line [10] 8

Figure 2.6: Two port T-network 11

Figure 2.7: Short circuit microstrip line (a) Side view (b) Top view 12

Figure 2.8: Standing wave patterns for shorted microstrip line 13

Figure 2.9: Relationship between ε_{reff} and *w/h* 14

Figure 2.10: Relationship between input impedance and ratio *w/h* 15

Figure 2.11: Relationship between Z_{in} and the transmission lines length 15

Figure 2.12: Scattering parameter for two port network 16

Figure 2.13: Reflection coefficients for short circuit line 17

Figure 2.14: Reflection coefficients for open circuit line 18

Figure 3.1: Equivalent circuit for two microstrip line [1] 22

Figure 3.2: Top view microstrip line stricture 23

Figure 3.3: S_{11} and S_{21} for one microstrip line 23

Figure 3.4: (a) Top view of the lines without coating (b) side view with Coating [1] 25

Figure 3.5: S_{11} and S_{21} two microstrip line 25

Figure 3.6: Comparison between the diract coupling and Far-End coupling for $S=W$ 28

Figure 3.7: Comparison of the Phase of S_{41} and Phase of S_{21} for $S=W$ 28

Figure 3.8: Cross section of the coupled coated lines 29

Figure 3.9: Simulation of FEXT [1] 30

Figure 3.10: NEXT simulation [1] 30

Figure 3.11: Simulated FEXT for the coated microstrip lines by FEKO 31

Figure 3.12: NEXT simulation for the coated microstrip lines by FEKO 31

Figure 3.13: Electromagnetic field when $S=W$ (a) Electric field coupled (b) Magnetic field coupled 32

Figure 3.14: Electromagnetic field coupled when $S=4W$ (a) Electric field (b) Magnetic field 33

Figure 3.15: Microstrip lines (a) Tope view (b) Side view [9] 34

Figure 3.16: Effect of changing length of lines on the FEXT [2] 35

Figure 3.17: FEKO Simulation FEXT results for different line lengths 35

Figure 3.18: (a) $3W$ rule (b) Shorting via (c) RSR construction [3] 36

Figure 3.19: FEXT simulations to compare among RSR, $3W$ rules and shorting via[3] 37

Figure 3.20: FEXT simulation by FEKO 37

Figure 3.21: Microstrip lines structure with via (a) via without connection to metal (b) via connected to metal (b) Side view 38

Figure 3.22: Coupling between microstrip lines (FEXT S_{41}) [4] 39

Figure 3.23: FEXT as a function of frequency by FEKO 40

Figure 3.24: Electromagnetic coupling between double lines (a) Electric field (b) Magnetic field 41

Figure 3.25: Electromagnetic coupled use via fences (a) Electric field (b) Magnetic field 42

Figure 3.26: Electromagnatic field use guard trace and via (a) Electric field (b) Magnetic field 43
Figure 3.27: Comparison of the direct coupling between using via fences and 3*W* rule 44
Figure 3.28: Compare the FEXT between using via fences and 3W rule 45
Figure 3.29: Compare the NEXT between using via fences and 3*W* rule 45
Figure 3.30: Double microstrip lines with rectangular Trace (a) Tope view (b) Side view 46
Figure 3.31: Comparison of the direct coupling S_{21} for rectangular trace, use via fences and with 3*W* rule, with *S*=3*W* 47
Figure 3.32: Description of FEXT among use rectangular trace, use via fences and with 3*W* rule, with *S*=3*W* 48
Figure 3.33: NEXT for rectangular trace, use via fences and with 3*W* rule, with *S*=3*W* 49
Figure 3.34: Direct coupling for two different lengths 15*mm* and 50*mm* 50
Figure 3.35: FEXT for two different lengths 15*mm* and 50*mm* 50
Figure 3.36: The electromagnetic field of the double microstrip lines with rectangular trace (a) Electric field (b) Magnetic field 51
Figure 3.37: Direct coupling S_{21} for different dielectric constants 52
Figure 3.38: Simulated FEXT for different dielectric constants 53
Figure 3.39: Simulated NEXT for different dielectric constants 53
Figure 3.40: Double microstrip lines with RVG (a) Top view (b) Side view 54
Figure 3.41: Comparison the direct couple S_{21} between use RVG and 3*W* rule 55
Figure 3.42: Comparison of FEXT between RVG and 3*W* rule 55
Figure 3.43: Comparison of NEXT between RVG and 3*W* rule 56

Figure 3.44: Direct couple S_{21} for two different line lengths 56

Figure 3.45: FEXT for two different line lengths 57

Figure 3.46: Electromagnetic field at 10 GHz for length15mm (a) Electric field (b) Magnetic field 58

Figure 3.47: CVG structure (a) Top view (b) Side view for double microstrip lines 59

Figure 3.48: Direct couple S_{21} for CVG and 3*W*, 4*W*, when *L*=50mm 60

Figure 3.49: FEXT for CVG and 3*W*, 4*W* rule when length 50*mm* 61

Figure 3.50: NEXT for CVG, 3*W*, *4W* with length 50*mm* 61

Figure 3.51: CVG results for direct couple when *L*=50*mm* and 15*mm*, *3W*spacing .. 62

Figure 3.52: Compare CVG results of FEXT when *L*=50*mm* and 15*mm*, *with 3W* spacing 63

Figure 3.53: Electromagnetic coupling, *L*=15*mm* (a) Electric field (b) Magnetic field 64

Figure 3.54: Comparing the direct couple among CVG, RVG and use Rectangular trace, when *L*=15*mm* 65

Figure 3.55: Comparing the FEXT among CVG, RVG and use Rectangular trace , when *L*=15*mm* 65

Figure 3.56: Comparing NEXT among CVG, RVG and use Rectangular trace, when *L*=15mm 66

Figure 4.1: The equivalent circuit of the Step in width MSL [10] 68

Figure 4.2: Step in width with chamfered step 69

Figure 4.3: Equivalent circuit for bending microstrip line [10] 69

Figure 4.4: Top view of (a) The bending (b) Step-width microstrip lines [7] 70

Figure 4.5: Top view structure of the bending (a) without chamfered (b) with chamfered 71

Figure 4.6: Comparing S-parameters between chamfered and non-chamfered line [7] 71
Figure 4.7: Comparing between chamfered and Non-chamfered bend line by FEKO 72
Figure 4.8: Effect of chamfered bend line by 70% 73
Figure 4.9: Electric field (a) At source (b) At bend (c) At load 74
Figure 4.10: Magnetic field, non-chamfered line 75
Figure 4.11: Electric field (a) At source (b) At chamfered bend (c) At load 76
Figure 4.12: Magnetic field, chamfered bend 76
Figure 4.13: Step width structure for different angles 77
Figure 4.14: Comparsion of the S_{11} between chamfered and non-chamfered line [7] 77
Figure 4.15: Comparison of S-parameters between non-chamfered and chamfered line 78
Figure 4.16: Electric field (a) At source step (b) At load step 79
Figure 4.17: Magnetic field non-chamfered step 79
Figure 4.18: Electric field for chamfered step off line 80
Figure 4.19: Magnetic field for chamfered step 80
Figure 4.20: Step in width with all step chamfered (a) Two side (b) One side 81
Figure 4.21: Comparing S_{11} between angles and all step chamfered 81
Figure 4.22: Electric field for all step chamfered 82
Figure 4.23: Magnetic field for all step chamfered 82

LIST OF SYMBOLS /ABBREVIATIONS

C	Transmission line capacitance
C_m	Mutual capacitance
C_s	Self-Capacitance
c_o	Speed Light
d_v	diameter of via
E	Electrical Field
f	Frequency
H	Magnetic field
H_c	thickness of coat substrate
h	Thickness of Substrate
G	Transmission line conductance
I	Circuit current
L	Length of transmission line
L_m	Mutual inductance
L_R	Length of Rectangular shape metal in RVG structure
L_r	Length rib of the slot in CVG structure
L_s	Self-inductance
L_x	Length of cross Shape metal in CVG structure
R_g	generator or source resistance
R_L	Load Resistance
R_o	Characteristic Resistance
S	Spacing between double Microstrip Line
S_R	Distance between rectangular shape metal in RVG structure

S_{11}	Scattering Parameter of Port 1reflection coefficient
S_{21}	Scattering Parameter of Port 2 or direct couple
S_{31}	Scattering Parameter of Port 3 or near-end crosstalk
S_{41}	Scattering Parameter of Port 4 or far-end crosstalk
u	wave velocity
W_R	Width of Rectangular shape metal in RVG structure
W_x	Width of cross shape metal in CVG structure
X_0	Transmission Line Reactance
Z_{in}	Input Impedance
Z_L	Load Impedance
Z_o	Characteristic Impedance
$Z_{o.c}$	Open circuit impedance
$Z_{s.c}$	Short circuit impedance
α	Attenuation constant
β	Phase Constant
β_e	Even Phase constant
β_o	Odd phase constant
γ	Propagation Constant
ε	Permittivity
εr	Relative Permittivity
εo	Permittivity of Free Space
ε_{eff}	Effective Dielectric Permittivity
λ	Wavelength
λ	Guided Wavelength
λ_o	Wavelength at Free Space

μ	Permeability
μ_r	Relative Permeability
μ_o	Permeability of Free Space
π	PI
Γ	Reflection Coefficient
Γ_L	Reflection Coefficient at load
σ_c	Conductivity of line
$B.W$	Bandwidth
CSR	Cross-Shape Resonator
CVG	Cross Shape With Via Fence Connected By Guard Trace
ECT	Electric Circuit Theory
EM	Electromagnetic
EMT	Electromagnetic Theory
FEXT	Far-End Crosstalk
FDTD	Finite Difference Time Domain
FEM	Finite Element Method
FR4	Flame Retardant 4
HFSS	High Frequency Structures Simulators
MOM	Method of Moment
MSL	Microstrip line
NEXT	Near-End Crosstalk
PCB	Printed Circuit Board
PL	Planar Line
Quasi-TEM	Quasi-Transvers Electromagnetic
RSR	Rectangular Shape Resonator

RVG	Rectangular Shape With Via Fence Connected By GuardTrace
SI	Signal Integrity
SL	Stripline
SWR	Standing Wave Ratio
TEM	Transvers Electromagnetic
T.L	Transition Line
VSWR	Voltage Standing Ratio
WB	Wide Band
XT	Crosstalk

Chapter 1

INTRODUCTION AND BACKGROUND

1.1 Introduction

In microwave circuit, the microstrip line has many problems such as crosstalk (coupling), discontinuity, overshot and delay. This thesis work only addresses the crosstalk and the discontinuity problems in microstrip lines.

Coupling is an important problem for the circuits that have multi-lines. The coupling effect as a problem has been studied for microstrip lines before by [1] [2] [3] [4]. This problem is still very important due to the usage of the Very Large Scale Integration (VLSI) circuit's technology with extremely small dimensions of micron levels [5] [6]. The study shows that microstrip lines can be easily adapted to the small dimensions. The crosstalk problem is due to the close placement of the lines which can be reduced by some design techniques which are discussed fully in this thesis.

In microwave circuits, the discontinuity problem arises when there is a transition between two lines with different characteristics (e.g. Step in Width, right angle bend, T-junction and open or short circuit). This is counted as capacitive or inductive load which creates problems for matching. This thesis includes discontinuity study in different cases e.g. step in width, right angle bend. The problem was studied previously by [7] for its analysis, and how it could be reduced.

1.2 Thesis overview

Chapter 2 includes the transmission line theory and the microstrip lines. The scattering parameters are also discussed in this chapter.

In chapter 3, the depth descriptions about crosstalk problem is included and detailed simulation results are explained in eight sections.

In chapter 4 we did more study on the discontinuity problem analysis of microstrip lines and simulation results are included.

All simulation results for the problems, crosstalk and discontinuity have been simulated by FEKO software which is a full wave simulator based on Moment solution Methods (MoM).

Chapter 5 consists of two parts, conclusions about thesis and the future work.

Chapter 2

BACKGROUND INFORMATION

2.1 Background

2.1.1 The definition of the Transmission Line

Transmission lines (TL) are used to convey energy from the source port to the load port. TL can be used for low frequency applications like power distribution, and in communication systems with high frequency. Examples of TL includes coaxial cable, two wire, wire above, planar line (PL), microstrip line (MSL) and stripline (SL) which are two or more conductor lines as represented in Figure 2.1 [8].

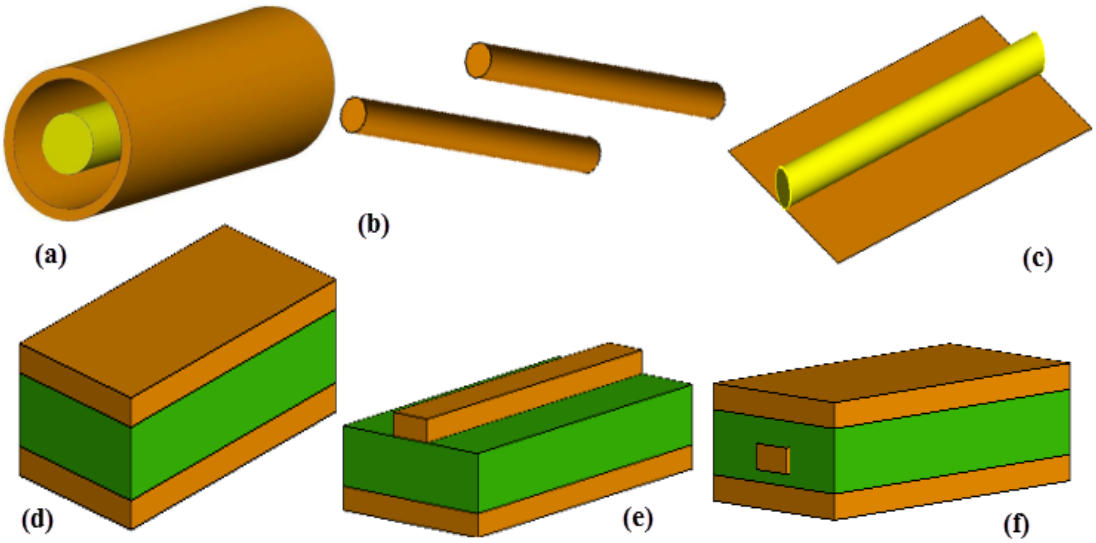

Figure 2.1: Types of Transmission lines (a) Coaxial cable (b) Two wire line (c) Wire over conducting plane (d) Planar line (e) Microstrip line (f) Stripline [8]

The problems of Transmission Lines may be solved by using electromagnetic field theory (EMT), or electric circuit theory (ECT), on which engineering relies.

2.1.2 Transmission line parameters

In this section the transmission line is characterized by three types of parameters. Firstly, the physical parameter such as the length of the line with line dimensions (thickness, width, diameter…etc.), the spacing between lines and the thickness of the substrate. Secondly, the material parameters, since the transmission line is made of conductors and dielectrics. They have the constitutive parameters like conductivity σ, permittivity ε and permeability μ. These parameters have effect on the performance of the line. Finally the electrical parameters like the resistance *R*, the capacitance *C*, the inductance *L* and the conductance *G* which is distributed parameters per unit length of the line. *R* is due to the conductivity of the conductors, *C* is due to the spacing of two plates with a dielectric, *L* is due to the inductance of the conductors and *G* is due to the dielectric losses [9]. The equivalent transmission line in terms of electrical parameters is shown in Figure 2.2.

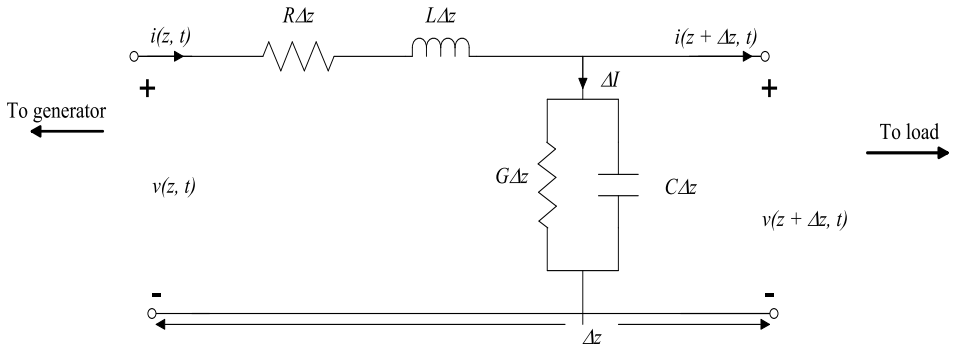

Figure 2.2: Transmission line circuit [8]

2.1.3 Transmission line equations

Transmission lines support transverse electromagnetic waves (TEM waves) when the electric and magnetic fields (orthogonal to each other) are transverse to the direction of the propagation of the wave. The *E*, *H*, and *V*, *I* relations are written as:

$$V=\int E.dl \tag{2.1}$$

$$I=\oint H.dl \tag{2.2}$$

for *TEM* waves.

Where *V* is the potential difference between two TL conductors (line and ground plane), *I* is the current flowing through one of the conductors, *E* is the electric field and *H* is the magnetic field (*V* and *I* are circuit quantities but *E* and *H*, are field quantities).

The propagation constant γ, wave velocity u and characteristic impedance Z_o are defined in the following equations respectively [8]:

$$\gamma = \alpha + j\beta = \sqrt{(R + j\omega L) * (G + j\omega C)} \tag{2.3}$$

$$u = \frac{\omega}{\beta} = f\lambda \tag{2.4}$$

Where α the attenuation is constant, β is the phase constant, f the wave frequency**,** and λ the wavelength of the wave which is equal $2\pi/\beta$.

2.1.3.1 Lossless line

For a lossless TL, the conductivity of line is σ_c=∞ (i.e. perfect conductor) and the conductivity of substrate material is $\sigma_c = 0$ and *R*= *G* = 0 (i.e. perfect dielectric).

Therefore:

$$\alpha = 0,\ \gamma = j\beta = j\omega\sqrt{LC} \tag{2.6}$$

$$u = \frac{\omega}{\beta} = \frac{1}{\sqrt{LC}} = f\lambda \tag{2.7}$$

$$X_o = 0\ , Z_o = \sqrt{\frac{L}{C}} \tag{2.8}$$

2.1.4 Microstrip Line (MSL)

Microstrip line is a parallel plate transmission line, which is vastly utilized nowadays. It is usually used for microwave integrated circuits such as filters, coupler resonators and antennas as a circuit component [8]. When a comparison is made between microstrip line and other TL's, we can see its simple geometry, small size and easy integration to the circuit, which are desirable properties in recent technologies in microwaves and communication.

A microstrip line is composed of two parallel conductors, the reference plane and the open metal conductor separated by a substrate as shown in Figure 2.2.

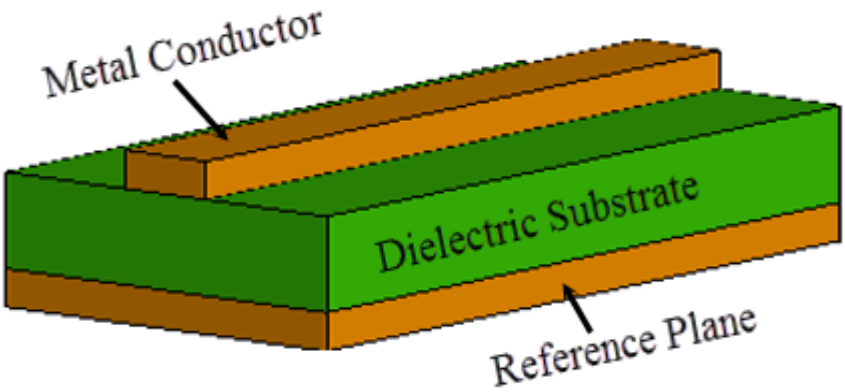

Figure 2.3: Microstrip line structure [10]

2.1.4.1 Type of Mode in MSL

The mode supported in microstrip line is a quasi-TEM mode; it has non-zero electric and magnetic fields in the direction of the wave propagation. The microstrip line has some of its fields in the dielectric and some of it in the air above the substrate and metal conductor. The phase velocity of the field in the dielectric region would be $\frac{u}{\sqrt{\varepsilon_r}}$, while in the air would be u. Figure 2.3 shows the electromagnetic waves conduct in the microstrip line [10].

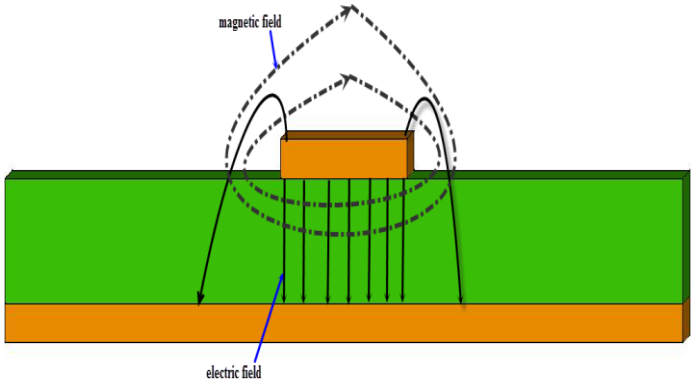

Figure 2.4: EM field in microstrip line (quasi-TEM) [10]

2.1.4.1 Fringing Effect

Due to the fringing the effective value of $\varepsilon_r$will be less than (ε_r) for such cases ε_{reff} is defined i.e. $1< \varepsilon_{reff} \leq \varepsilon_r$ as shown in Figure 2.3. This is achieved when the width of the microstrip line is less than the width of the ground plane. If $\varepsilon_r \cong \varepsilon_{eff}$ the fringing effect will be small and the EM field will be between the line and the reference plane. This happens when the width of microstrip line is the same with the width of reference plane like the parallel plates shown in Figure 2.4.

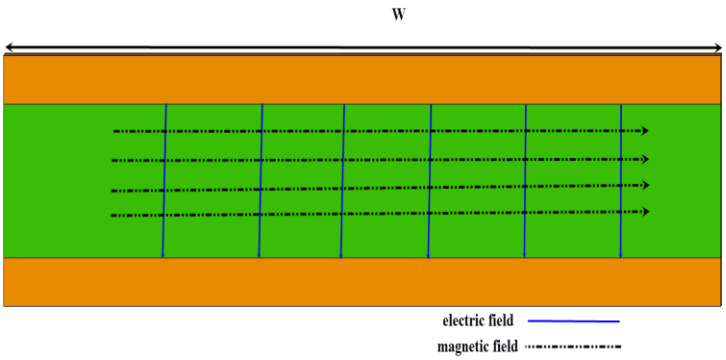

Figure 2.5: EM field in planar line [10]

There are some approximate formulas used to calculate(ε_{eff}). One of these formulas is given by Equation (2.9) [10].

$$\varepsilon_{eff} = \frac{\varepsilon_r+1}{2} + \frac{\varepsilon_r-1}{2}(1 + 12 * \frac{h}{w})^{-\frac{1}{2}} \tag{2.9}$$

Where *w* is the width of the line, *h* is the thickness of substrate and ε_r is the relative permittivity.

ε_{reff} can also be calculated by using simulation software such as FEKO 5.5 or simulation technique like FDTD. This will be explained later.

The characteristic impedance Z_o of the microstrip line is given by Equation (2.12):

$$Z_o = \begin{cases} \frac{60}{\sqrt{\varepsilon_{eff}}} \ln\left(\frac{32*h^2+w^2}{4*w*h}\right) & \text{for } \frac{w}{h} \le 1 \\ \frac{120\pi}{\left[\frac{w}{h}+1.393+0.667\ln(\frac{w}{h}+1.444)\right]*\sqrt{\varepsilon_{eff}}} & \text{for } \frac{w}{h} \ge 1 \end{cases} \tag{2.12}$$

To find the input impedance Z_{in} of the microstrip line or a transmission line having length l we can use the following equations:

$$Z_{in} = Z_o \left[\frac{Z_L + j\, Z_o \tanh \gamma l}{Z_o + j\, Z_L \tanh \gamma l}\right] \quad \text{For a lossy line} \tag{2.13}$$

for a lossy line and the Z_{in} for lossless line is given by:

$$Z_{in} = Z_o \left[\frac{Z_L + j\, Z_o \tan \beta l}{Z_o + j\, Z_L \tan \beta l}\right] \quad \text{For a lossless line} \tag{2.14}$$

2.1.5 Special TL Loads

The following three special cases can be considered for the load.

2.1.5.1 Short Circuit Line

Short circuit case occurs when $Z_L = 0$. Z_{in} can be calculated by Equation 2.15 and it will be purely imaginary.

$$Z_{in} = jZ_o tan\beta l \tag{2.15}$$

The corresponding reflection coefficient and the SWR are:

$$\Gamma_L = -1, \text{ SWR or VSWR} = \frac{1+|\Gamma_L|}{1-|\Gamma_L|} = \infty \tag{2.16}$$

where *l* is the length of line, Γ_L is load reflection coefficient; SWR or VSWR is the Voltage Stand Wave Ratio. Later the reflection coefficient calculations will be carried out by using the FEKO 5.5 simulator.

2.1.5.2 Open Circuited Line

This type of transmission line is called an open circuit line when $Z_L = \infty$. So Z_{in} and Γ_L can be calculated by the following equations:

$$Z_{oc} = Z_{in} = \frac{Z_o}{jtan\beta l} = -jZ_o\, cos\beta l \tag{2.17}$$

$$\Gamma_L = 1, \text{ SWR or VSWR } = \frac{1+|\Gamma_L|}{1-|\Gamma_L|} = \infty \quad (2.18)$$

The reflection coefficient of the open circuit line is equal 1. This will be explained later when we present the simulations of the microstrip lines.

2.1.5.3 Matched Line

Matched line is the case when ($Z_L = Z_o$) and represents the case where there is no signal reflected from the load to the source and there is no power loss. For this reason the reflection coefficient under matched load condition is nearly zero as mention in Equation 2.19 [10].

$$\Gamma = \frac{G-1}{G+1} \quad (2.19)$$

Where G is $\frac{Z_L}{Z_o}$, and for the matched line it is equal to 1 because $Z_L = Z_o$, so the reflection coefficient Γ for the matched line is zero. This can also be achieved by using FEKO 5.5 the simulation software and FDTD technique which will be clarified later.

2.1.6 Scattering Parameters (S-parameters)

Scattering parameters are representing the ratio of the incident voltage on the source port to the waves reflected from the other ports (transmitted and reflected waves) as indicated in the Figure 2.6. The scattering parameters are determined by utilized network analysis and can be measured immediately by analyzer of vector network [10].

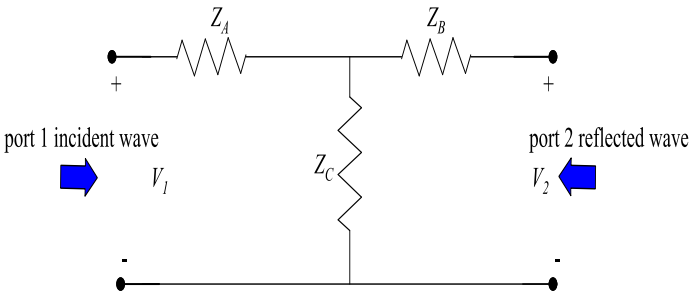

Figure 2.6: Two port T-network

For *N* port the scattering matrix S_{ij} when there are *N* ports network, that achieve depends on source voltage V_j^+ and reflected voltage V_i^- where i, j (1, 2 ...*N*) indicate the port numbers as equation (2.20) [10].

$$S_{ij} = \frac{V_i^-}{V_j^+}\Big|_{V_k^+=0} \tag{2.20}$$

Where V_k^+ is a voltage source in the load port where $k \neq j$ (i.e. incident voltage on all ports is zero except the source port).

If there is network containing two ports the scattering parameter matrix will be:

$$\begin{bmatrix} V_1^- \\ V_2^- \end{bmatrix} = \begin{bmatrix} S_{11} & S_{12} \\ S_{21} & S_{22} \end{bmatrix} \begin{bmatrix} V_1^+ \\ V_2^+ \end{bmatrix}, [V^-] = [S][V^+] \tag{2.21}$$

In the network system, the incident voltage on all ports is zero excluding source port so that all port must be terminated by matching load to prevent reflection signal. The scattering parameter for matched line (S_{11} & S_{21}) which are equal to(S_{22}& S_{12}) will be calculated in MSL simulation section.

2.2 Microstrip Line Simulations

2.2.1 Effective Relative Permativity (ε_{eff})

The effective relative permittivity (ε_{eff}) of the substrate for a microstrip line can be calculated by using the voltage standing wave pattern curve by using the short circuit case as shown in Figure 2.7.

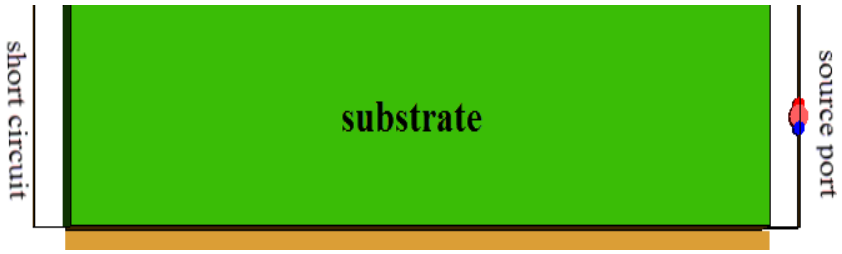

(a)

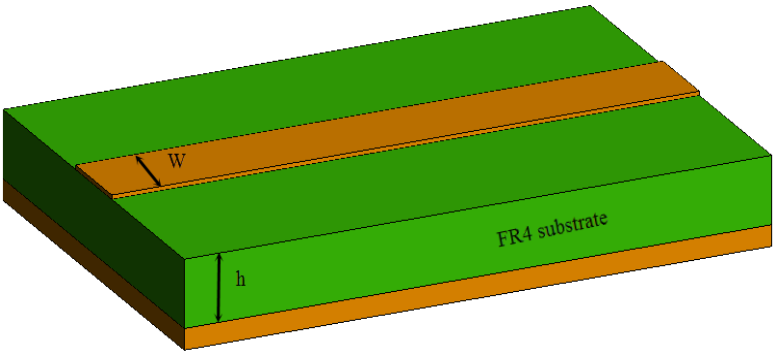

(b)

Figure 2.7: Short circuit microstrip line (a) Side view (b) Top view

The effective permittivity is calculated by finding the guided wavelength λ_g of signal line from the curve of the standing wave pattern as shown in Figure 2.8. This is represented by the distance between two peak points or minimum points in the standing wave pattern curve.

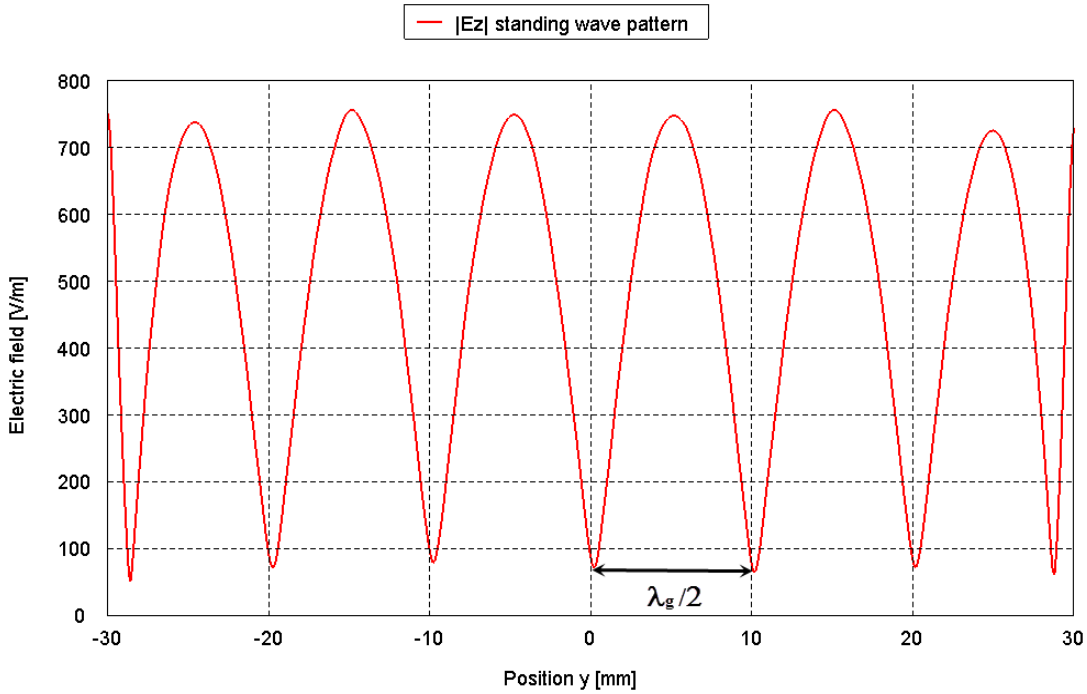

Figure 2.8: Standing wave patterns for shorted microstrip line

After finding the guided wavelength the following formulas are used to evaluate the effective permittivity.

$$\lambda_o = \frac{c_o}{f} \tag{2.22}$$

$$\varepsilon_{eff} = \left(\frac{\lambda_o}{\lambda_g}\right)^2 \tag{2.23}$$

where λ_o is the free space wavelength, c_o speed of light and f is the frequency.

Consider the case that the value to the thickness of substrate (h) is 1.6mm and is kept constant. The effective permittivity is evaluated by using the standing wave pattern obtained by FEKO. The width w varies between 1mm to 6mm and the relative permittivity is 4.5. The FEKO simulation results and the approximation results by Equation 2.9 are shown in Figure 2.9.

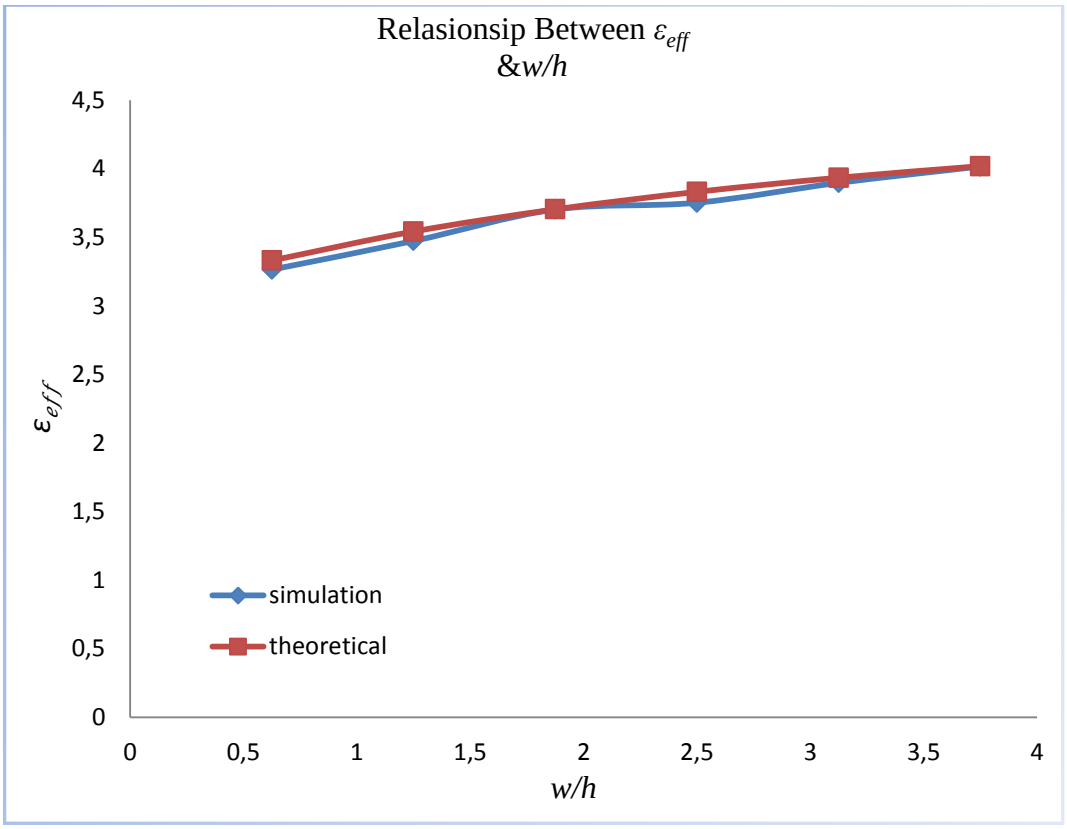

Figure 2.9: Relationship between ε_{reff} and *w/h*

If we compare the approximation results the simulation results by FEKO, they are nearly equal.

2.2.2 Characteristic Impedance Z_o

The input impedance Z_{in} with respect to the ratio $\frac{w}{h}$ for both theoretical calculations by Equations (2.12, 2.13 and 2.14) and the simulation result by FEKO 5.5 simulator are shown in Figure 2.10. All the theoretical and simulation results were carried out by considering a microstrip line on FR4 substrate 4.5 with thickness 1.6mm. The width of line differs 1mm to 10mm as shown in the Figure 2.7b.

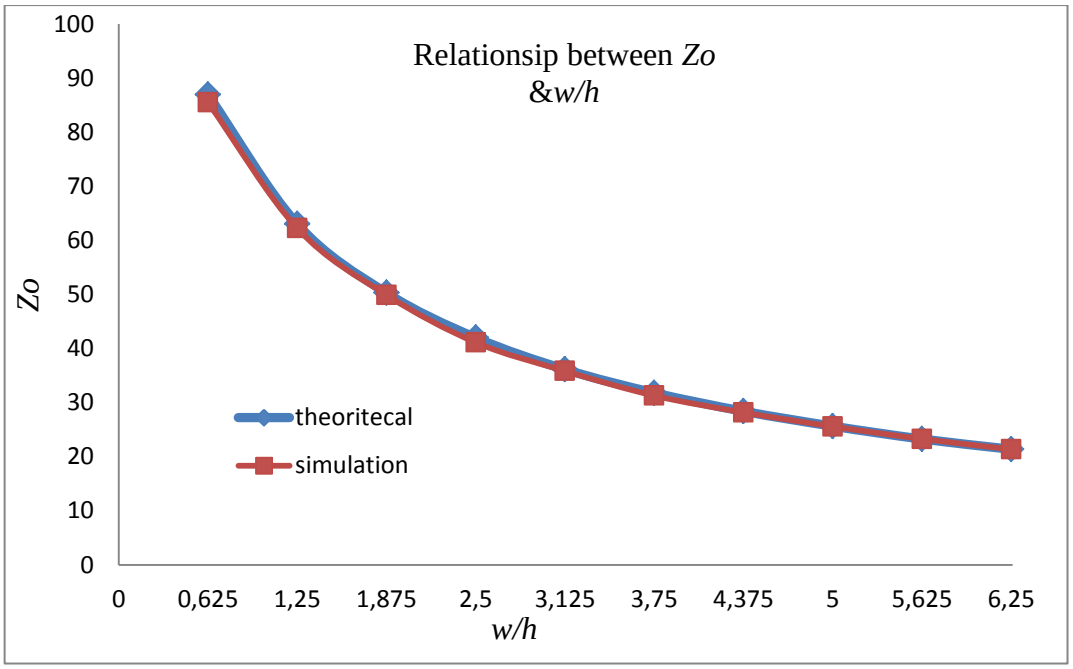

Figure 2.10: Relationship between input impedance and ratio *w/h*

The relationship between characteristic impedance and the length of line, which has 50Ω characteristic impedance under matched load conditions, is shown in Figure 2.11.

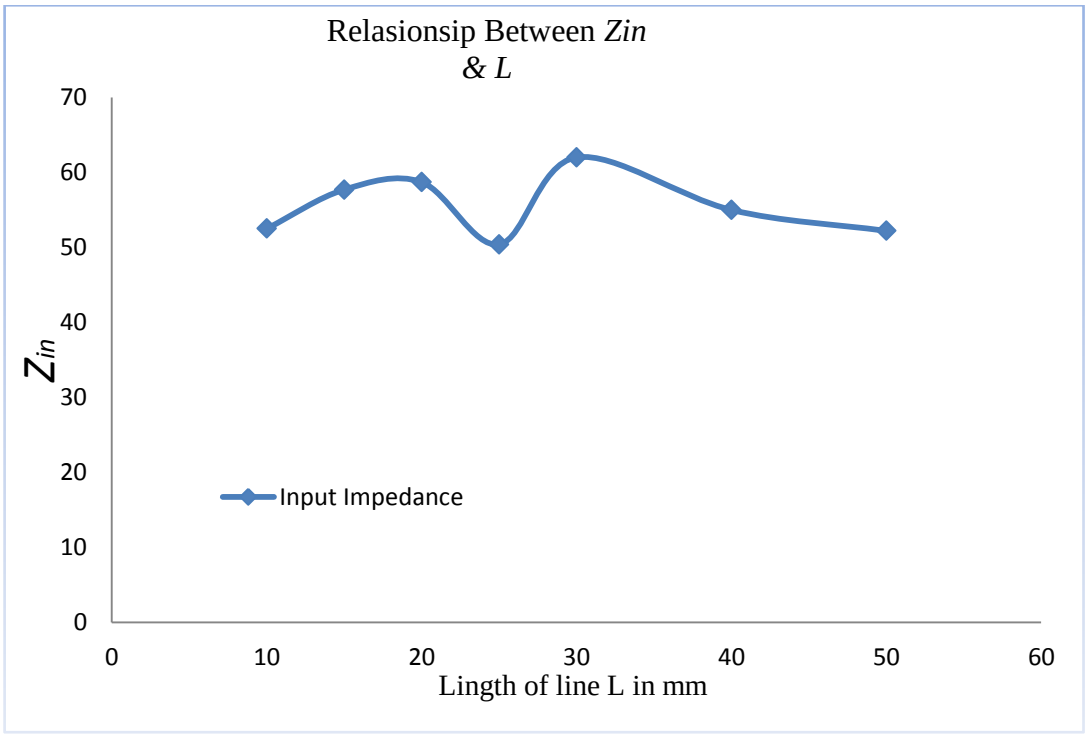

Figure 2.11: Relationship between Z_{in} and the transmission lines length

It can be observed from Figure 2.11 that the input impedance of the microstrip line is independent from the length of the line when the line length is infinity. The infinity condition is achieved by using matched load. i.e. by preventing the reflections back to the line in order to have the same impedance at every point on the line.

2.2.3 Scattering Parameter

2.2.3.1 Matched Line

The simulation results (S-parameters) for 50Ω match line are shown in Figure 2.12.

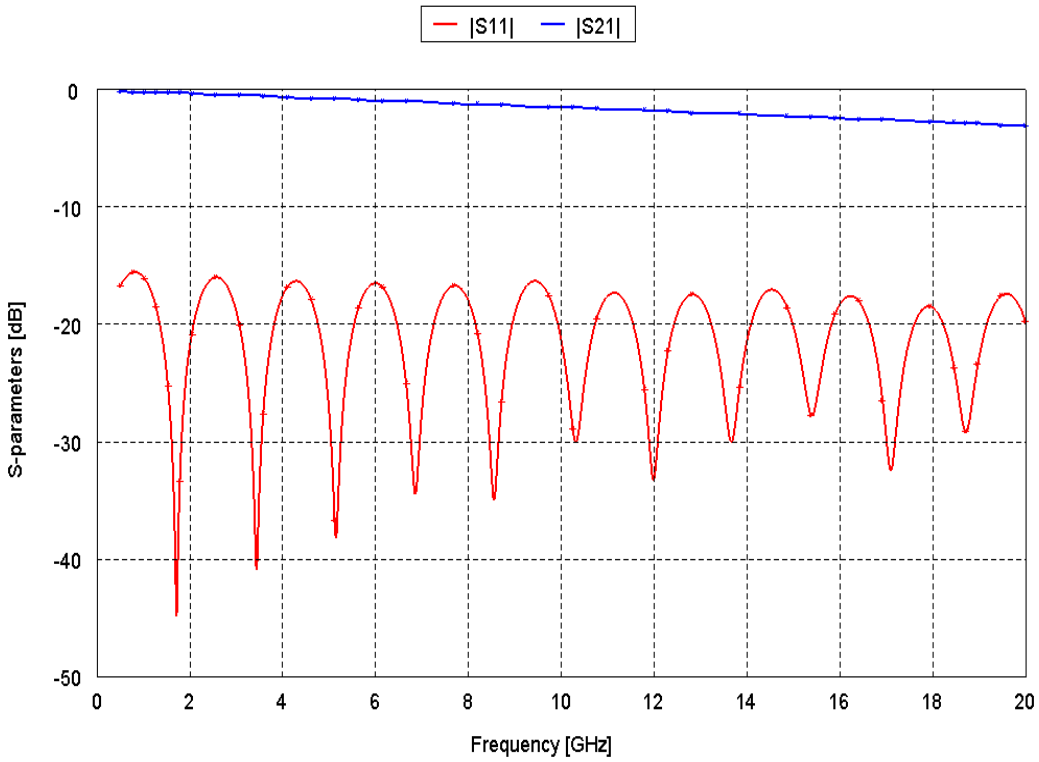

Figure 2.12: Scattering parameter for two port network

Figure 2.12 above indicates that the reflection coefficient S_{11} for the 50Ω TL is less than -10dB and the signal will be absorbed by the load. This absorption is seen from the transmission coefficientS_{21}, which is approximately equal to 0dB.

2.2.3.2 Short Circuit Line

The reflection coefficient of the short circuit line as a function of frequency shown in the Figure 2.13

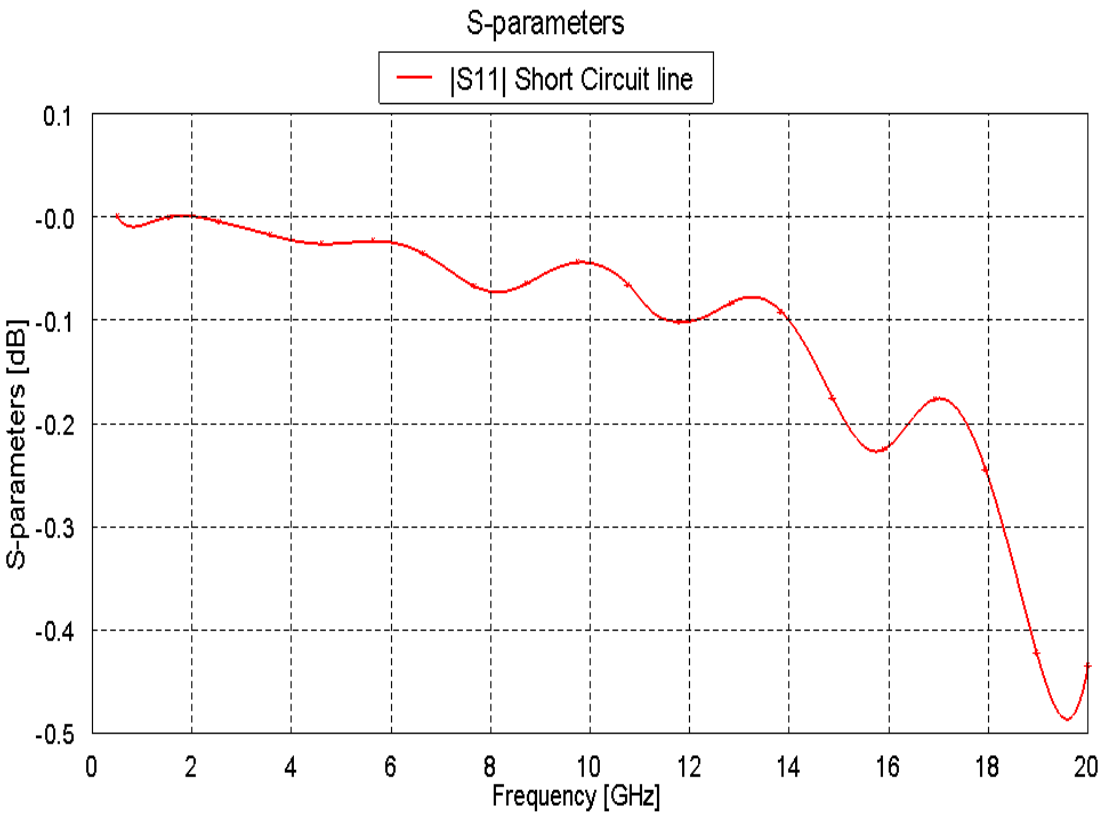

Figure 2.13: Reflection coefficients for short circuit line

This curve shows the magnitude of the reflection coefficient for short circuit line. It shows that there is a total reflection when the load is short circuit.

2.2.3.3 Open Circuit Line

The reflection coefficient of the open circuit line is shown in Figure 2.14

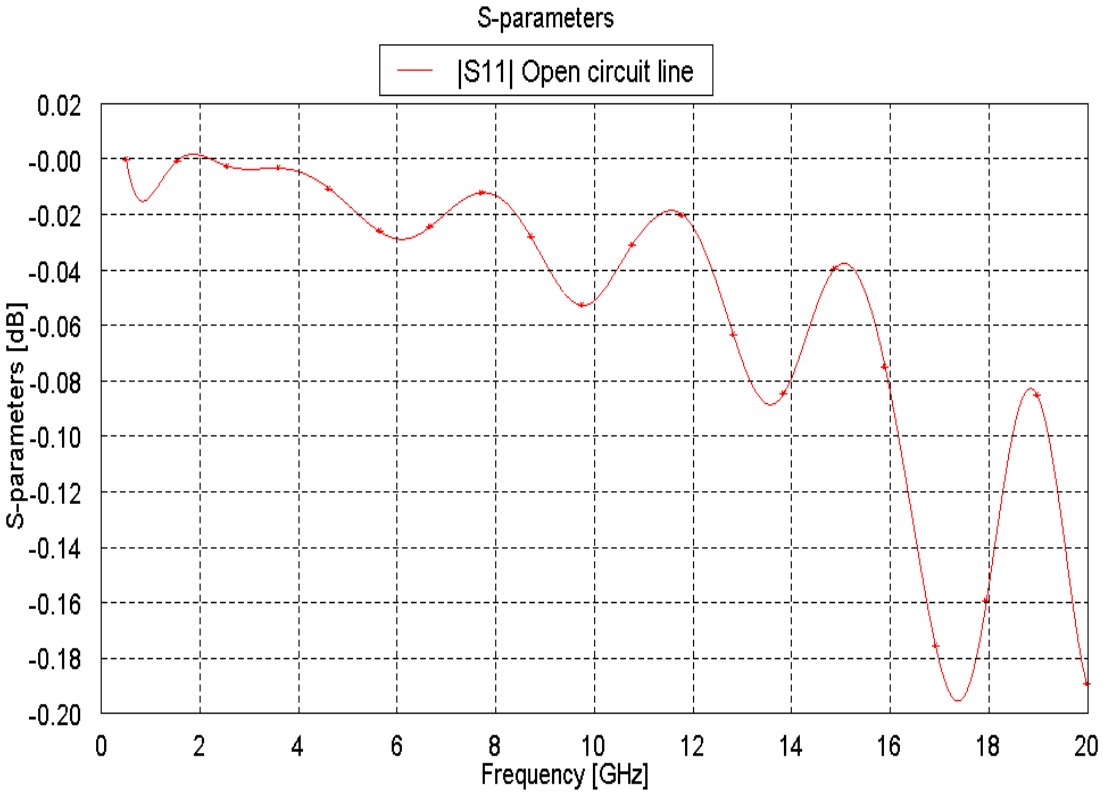

Figure 2.14: Reflection coefficients for open circuit line

Figure 2.14 shows that the full reflection of the signal from load to the source port is achieved when the load is open circuit

Chapter 3

Crosstalk problem between microstrip lines

3.1 Introduction

The layout digital device and bundle of chip is oriented to use high frequency, high density, high speed and low voltage process, this leads to the interconnection of multiple lines in printed circuit board (PCB). The process of high speed will make more problems like noise to the signal transmitted by multiple lines and this effect on the signal integrity (SI) is decisive operator in the layout of high speed PCB [11].

3.2 Crosstalk or Coupling

The crosstalk is a phenomenon which occurs in the coupled transmission lines (microstrip lines or striplines) and is the source of noise because some signals are not absorbed by the load or the antenna. In other words, there is a reflected signal from the load, which is not absorbed by load and it will radiate as radiation pattern and affect the other line or lines.

Crosstalk problem have two important types, far-end and near-end crosstalk (FEXT & NEXT) forward and backward respectively. FEXT has more complex problem than NEXT and it has a direct effect on the signal integrity at the load side [11] which is greater than NEXT [1]. The voltage of the far-end crosstalk is motivated as a result of variation between coupled capacitive and inductive rate to multiple microstrip lines $\frac{C_m}{C_s}$ & $\frac{L_m}{L_s}$ where C_m=C_{21}, L_m= L_{21} which are mutual capacitance and

inductance respectively ; $C_s = \sqrt{C_{11}\,C_{22}}$ and $L_s = \sqrt{L_{11}L_{22}}$ and self-capacitance and inductance respectively. Where the total inductance and the total capacitance are:

$$L = \begin{bmatrix} L_{11} & L_{12} = L_m \\ L_{21} = L_m & L_{22} \end{bmatrix} nH/m \tag{3.1}$$

$$C = \begin{bmatrix} C_{10} + C_m & -C_{12} = -C_m \\ -C_{21} = -C_m & C_{20} + C_m \end{bmatrix} = \begin{bmatrix} C_{11} & -C_{12} = -C_m \\ -C_{21} = -C_m & C_{22} \end{bmatrix} pF/m \tag{3.2}$$

The voltage at the far-end and near-end are related to C_m , C_s , L_m and L_s be given by [11] as follow equations.

For the FEXT voltage at port 4, far from source port is:

$$V_{FEXT}(t) = \frac{1}{2}\left(\frac{C_m}{C_s} - \frac{L_m}{L_s}\right) * T_D * \frac{dV_{in}(t-T_D)}{dt} \tag{3.3}$$

Let $K_a = \frac{C_m}{C_s}$, $K_b = \frac{L_m}{L_s}$

$$V_{FEXT}(t) = \frac{1}{2}(K_a - K_b) * T_D * \frac{dV_{in}(t-T_D)}{dt} \tag{3.4}$$

and for the port 3 which is close to port 1, in other words, near-end has voltage called near-end crosstalk voltage as shown in Equation 3.5 given by [1].

$$V_{NEXT} = \frac{1}{4}(K_a + K_b)[V_{in}(t) - V_{in}(t - T_D)] \tag{3.5}$$

It is clear that K_a must be equal to K_b for zero V_{FEXT} . In this thesis, we carried out a study to reduce the V_{FEXT} i.e. to achieve $K_a \approx K_{\boldsymbol{b}}$. Where T_D the propagation time is over the transmission line and $\frac{dV_{in}(t-T_D)}{dt}$ is changing for the applied voltage at the aggressor line as the ratio of time. The crosstalk in the double microstrip line is due to the mutual inductance and the mutual capacitance between the lines which are given by following equations [1]:

$$v = L_m * \frac{d_i}{d_t} \tag{3.5}$$

$$i = C_m * \frac{d_V}{d_t} \tag{3.6}$$

Where *v*, and *i* represent voltage and current drop respectively in the victim trace, $\frac{d_i}{d_t}$ is the time varying current and $\frac{d_v}{d_t}$ time varying voltage in the feed line. (L_m) and (C_m) are mutual capacitance and inductance. Equation (3.5) indicates the voltage in the victim line due to the changing current in the feed line, while Equation (3.6) shows the current in the victim line due to the changing voltage in the main line. Figure 3.1 shows equivalent circuit for two microstrip lines and also show inductive and capacitive coupling between lines.

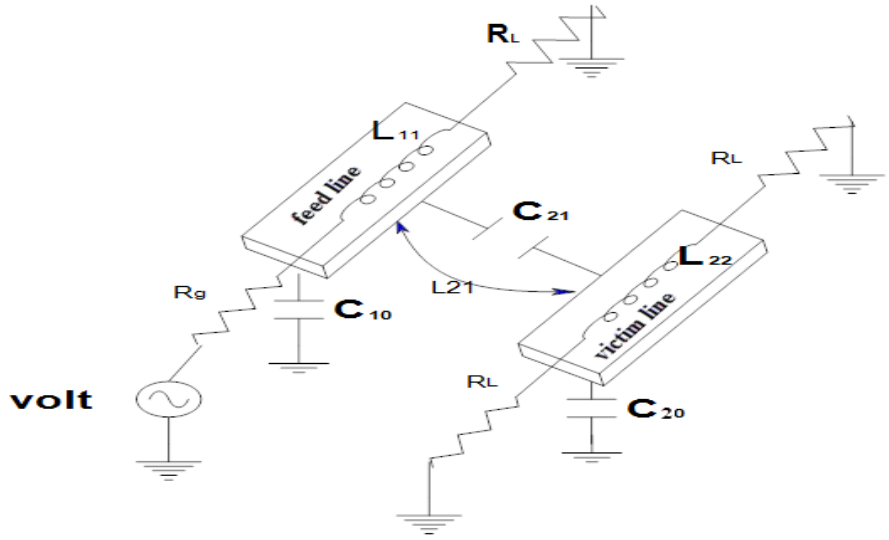

Figure 3.1: Equivalent circuit for two microstrip line [1]

The FEXT problem can be reduced by:

1) Changing the space between lines by using *3W* spacing rule.
2) Changing the length of lines.
3) Using rectangular shape resonator RSR.
4) Connect grounded via fence to guard trace.
5) Using Rectangular Trace.
6) Changing the dielectric constant.
7) Using RVG between microstrip lines.
8) Using CVG between microstrip lines.

3.2.1 Simulation of a Microstrip line by FEKO 5.5 Simulator

Consider a microstrip line like the one in Figure 3.2 which has characteristic impedance Z_o and is matched to the load impedance equal to Z_o (matched load). For the MSL dimensions of length *L*=50mm, width w= 0.33mm placed on the substrate having the thickness *H*=0.2mm with dielectric constant ε_{r1} = 4.2. The simulation was repeated by using coat substrate which is used to protect the metal strips from rust

and corrosion. The coat layer is a dielectric layer with thickness of $H_c = 0.02\text{mm}$ and dielectric constant ε_{rc}=4.1. This layer has direct impact on signal propagation of microstrip lines [12]. The reflection coefficient S_{11} is measured by using FEKO software and it is represented in Figure 3.3.

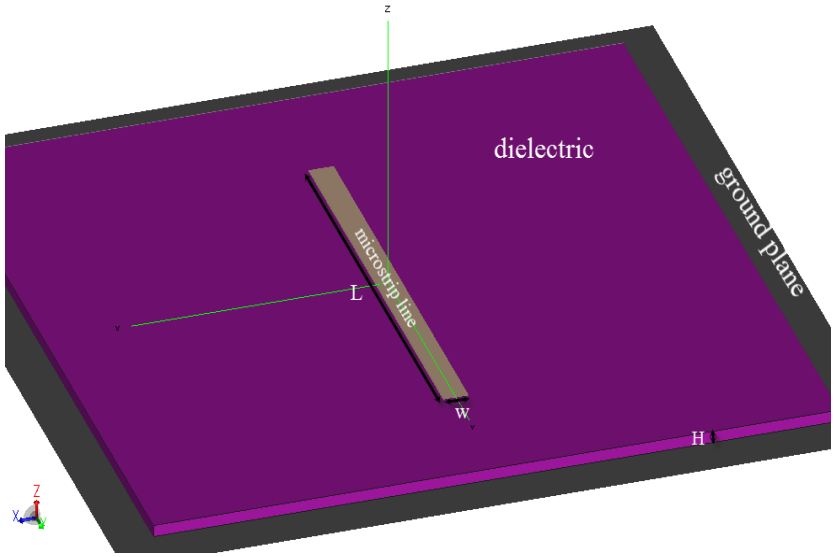

Figure 3.2: Top view microstrip line stricture

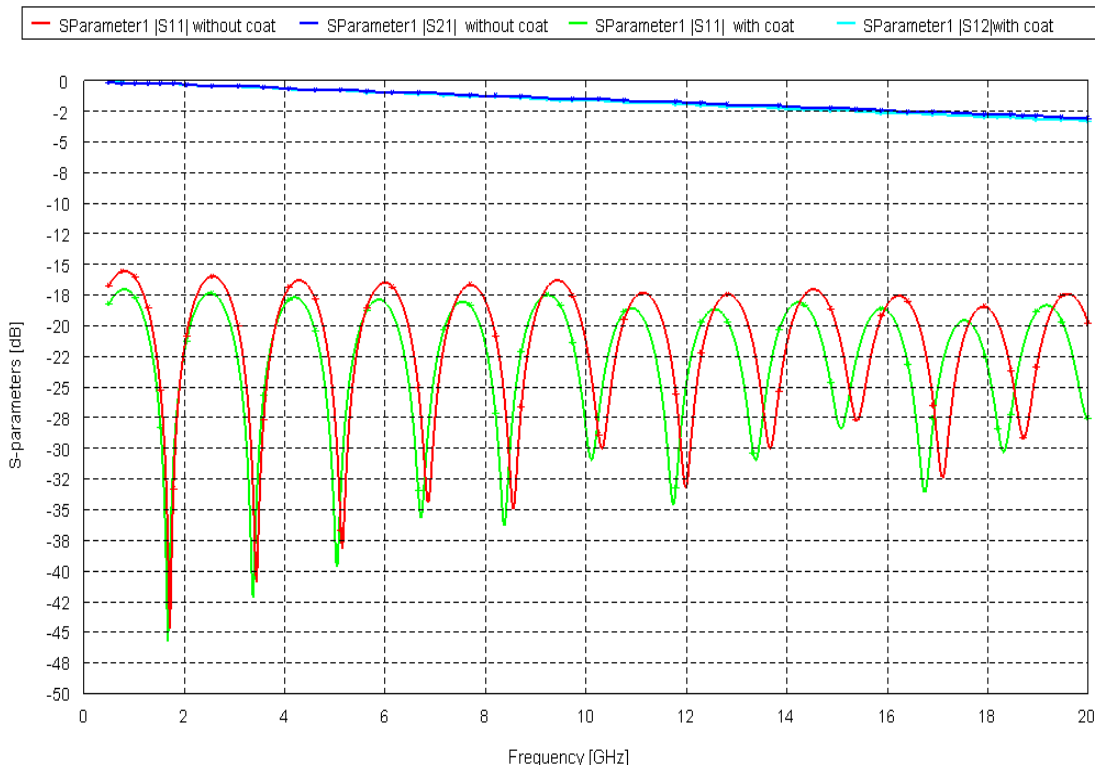

Figure 3.3: S_{11} and S_{21} for one microstrip line

Figure 3.3 shows the reflection coefficient S_{11} and transmission coefficient S_{21} for the range of frequency from 500MHz to 20GHz, for coated and non-coated microstrip line.

3.2.2 Crosstalk between two microstrip lines

When there are multiple lines, there exists an interference known as crosstalk between the lines. The two line system simulation can be consider to demonstrate the reflection coefficient and crosstalk between two lines where the first line is the feed line and the second line which is not excited is called the dead line (victim line) as presented by Figure 3.4. The dimensions and substrate properties are summarized in Table 3.1. Both lines are matched to the load impedance Z_o equal to the characteristic impedance. The victim line beside the feed line has effects on the field and reduces the reflection coefficient S_{11} by 10 dB as it can be observed from Figure 3.5. The victim line that absorbs the part of the signal is known as "coupling".

Table 3.1: Dimensions of microstrip lines

W	$\boldsymbol{H_c}$	*H*	*L*	*S*	$\boldsymbol{\varepsilon_{r1}}$	$\boldsymbol{\varepsilon_{r2}}$
0.33mm	0.02mm	0.2mm	50mm	*N*W*	4.2	4.1

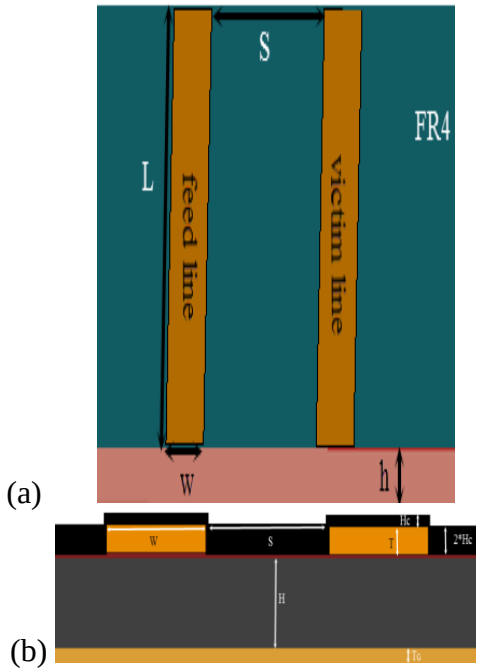

Figure 3.4: (a) Top view of the lines without coating (b) side view with Coating [1]

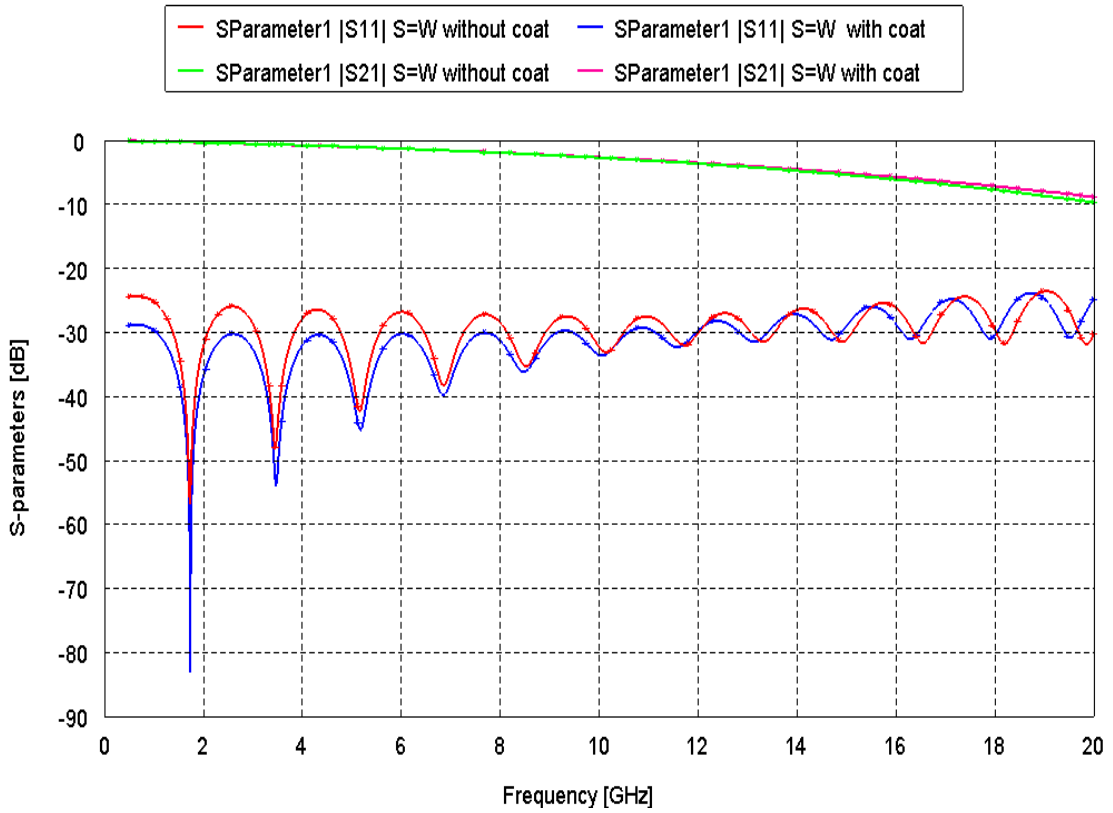

Figure 3.5: S_{11} and S_{21}two microstrip line

Note that the reflection coefficient S_{11} is reduced when the coat is added, because the coat absorbs some of the reflected signal [1].

When another line is placed parallel to the feed line, part of reflected signal from feed line will be absorb by neighboring line and if this signal goes forward it makes Far-End crosstalk (*FEXT*) and if it is goes backward it produces Near-End crosstalk S_{31} (*NEXT*). The forward coupler signal or scattering parameters S_{41} (*FEXT*), S_{21}(direct coupled) and each of reflection coefficient $S_{11}$and NEXT S_{31} are nearly zero because all signal at first moved toward load. The coupling equations are shown below [1]:

$$|S_{21}| = \left|cos[\frac{(\Delta\beta)L}{2}]\right| \tag{3.6}$$

$$\text{Or } |S_{21}| = 20\, log\, \frac{V_2}{V_1} \tag{3.7}$$

$$|S_{41}| = \left|sin[\frac{(\Delta\beta)L}{2}]\right| \tag{3.8}$$

$$\text{Or } |S_{41}| = 20\, log\, \frac{V_4}{V_1} \tag{3.9}$$

Where $\Delta\beta = \beta_e - \beta_o$

β_e and β_o are even and odd mode propagation constant respectively.

Scattering parameters for the backword coupling are direct couple S_{21}, *NEXT* S_{31} and S_{41}. But the refflection coefficient S_{11} and $S_{41}$are zero.

$$S_{21} = \frac{\sqrt{1+D^2}}{\sqrt{1-D^2}cos\theta + jsin\theta} \tag{3.10}$$

$$S_{31} = \frac{jDsin\theta}{\sqrt{1-D^2}cos\theta+jsin\theta} \tag{3.11}$$

$$\text{Or } |S_{31}| = 20\log\frac{V_3}{V_1} \tag{3.12}$$

Where θ is the phase coupling or electrical length of the coupling microstrip lines where if the length of the coupled line increases, the lead to the phase of signal will increase as shown in equation from [1]:

$$\theta = \beta L = w\sqrt{\mu\varepsilon}L = \frac{2\pi fL}{u} \tag{3.13}$$

And the coupling parametar is:

$$D = \frac{Z_{0e}-Z_{0o}}{Z_{0e}+Z_{0o}} \tag{3.14}$$

Where L is the physical coupling length of the line, V_2 is the direct coupling voltage or reflected voltage from port 2, V_4 is the Far-End crosstalk voltage, V_1 is the input voltage (source voltage) and V_3 is near-end crosstalk voltage; $Z_{0e}$and Z_{0o} are even and odd mode charecterstic impedances respectively of the coupled lines where the characteristic impedance of line $Z_0 = \sqrt{Z_{0e} * Z_{0o}}$. From above equations, note that S_{41} is inversely related with S_{21}; when direct couple increases the forward couple decreases and vice versa [1] as shown in Figure 3.6; and note that the phase shift between direct couple and *FEXT* is 90° in as shown by Figure 3.7.

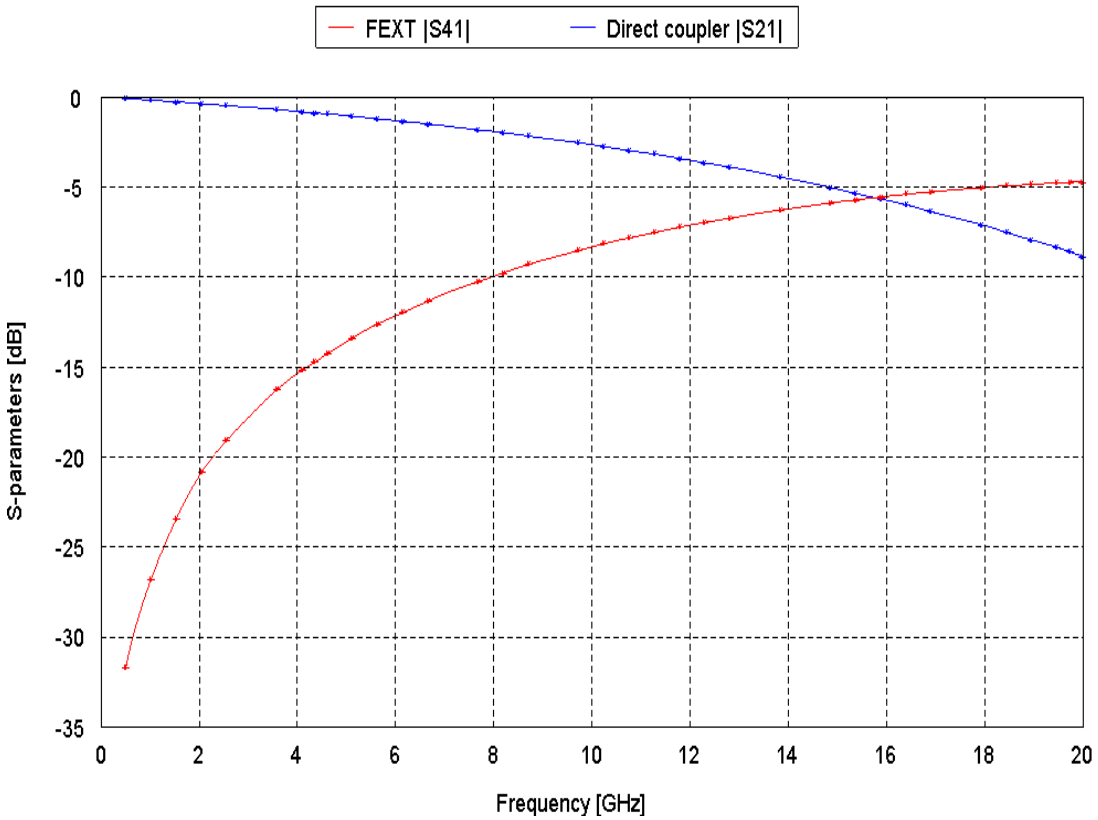

Figure 3.6: Comparison between the diract coupling and Far-End coupling for $S=W$

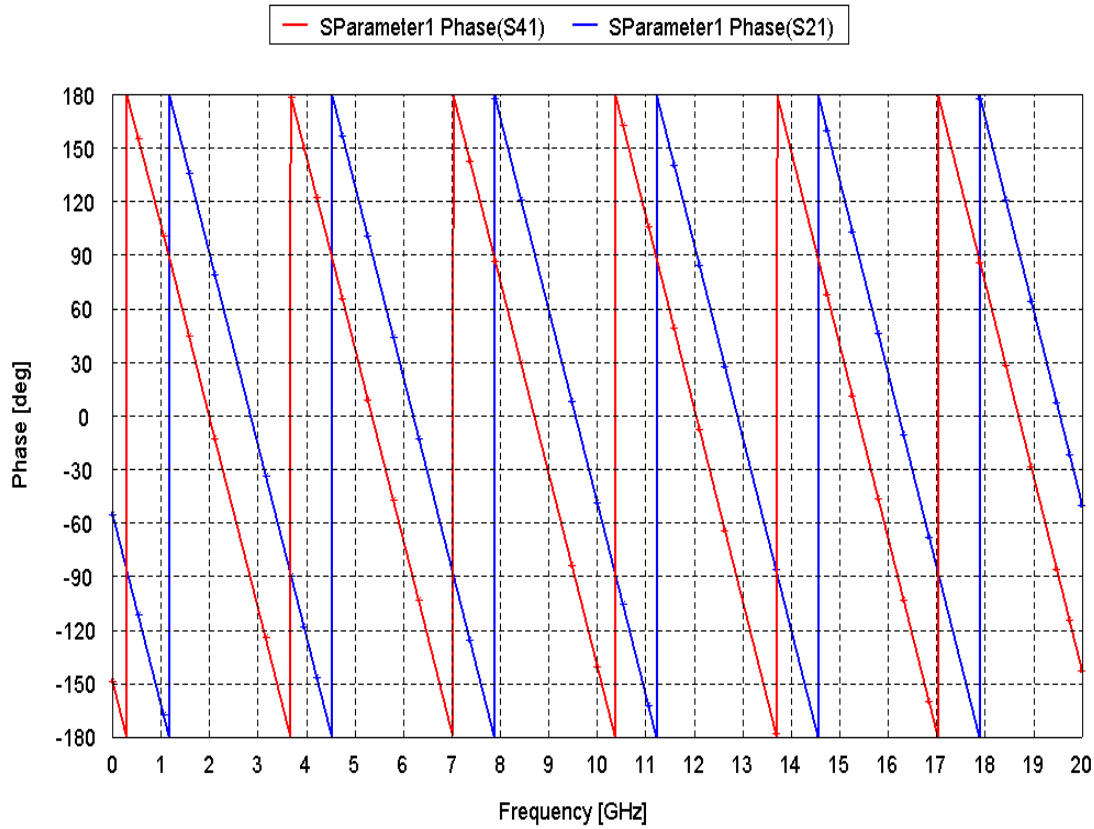

Figure 3.7: Comparison of the Phase of S_{41} and Phase of S_{21} for $S=W$

3.2.3 Simulation Results

3.2.3.1 Changing the Space between Lines by Using *3W* Rule

Mbairi et al., worked to analyze and reduce the crosstalk between microstrip lines by using *3W* rule (spacing rule). They simulated the coated microstrip lines by using HFSS software, at high frequency (up to 20 GHz) as shown in the Figure 3.8 with dimensions tabulated by Table 3.2.

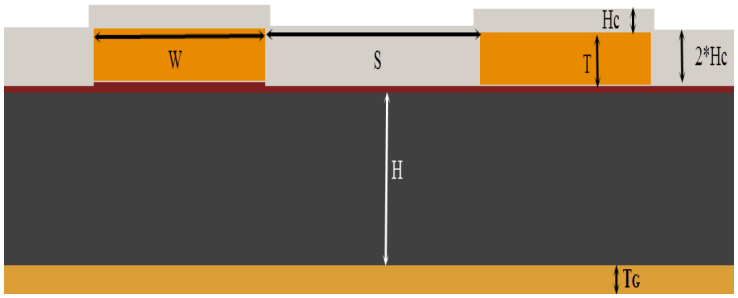

Figure 3.8: Cross section of the coupled coated lines

Table 3.2: Dimension of the coating microstrip line design [1]

H	ε_{r1}	ε_{r2}	W	W_2	S	T	T_G	H_c	L
0.2*mm*	4.2	4.1	0.33*mm*	0.305*mm*	*N*W*	0.05*mm*	0.018*mm*	0.02*mm*	50*mm*

This rule discusses, the relationship between the spacing of the microstrip lines and the crosstalk (FEXT and NEXT). The Far-End and Near-End crosstalk results are shown by Figures 3.9 and 3.10 respactively [1].

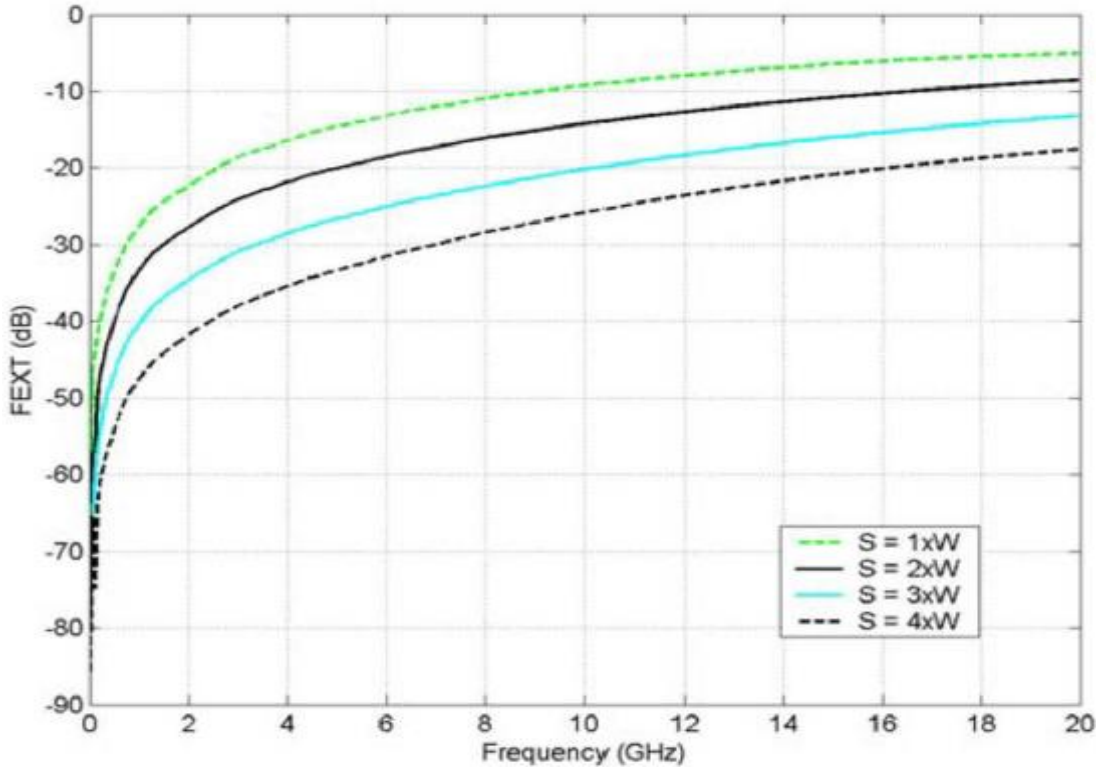

Figure 3.9: Simulation of FEXT [1]

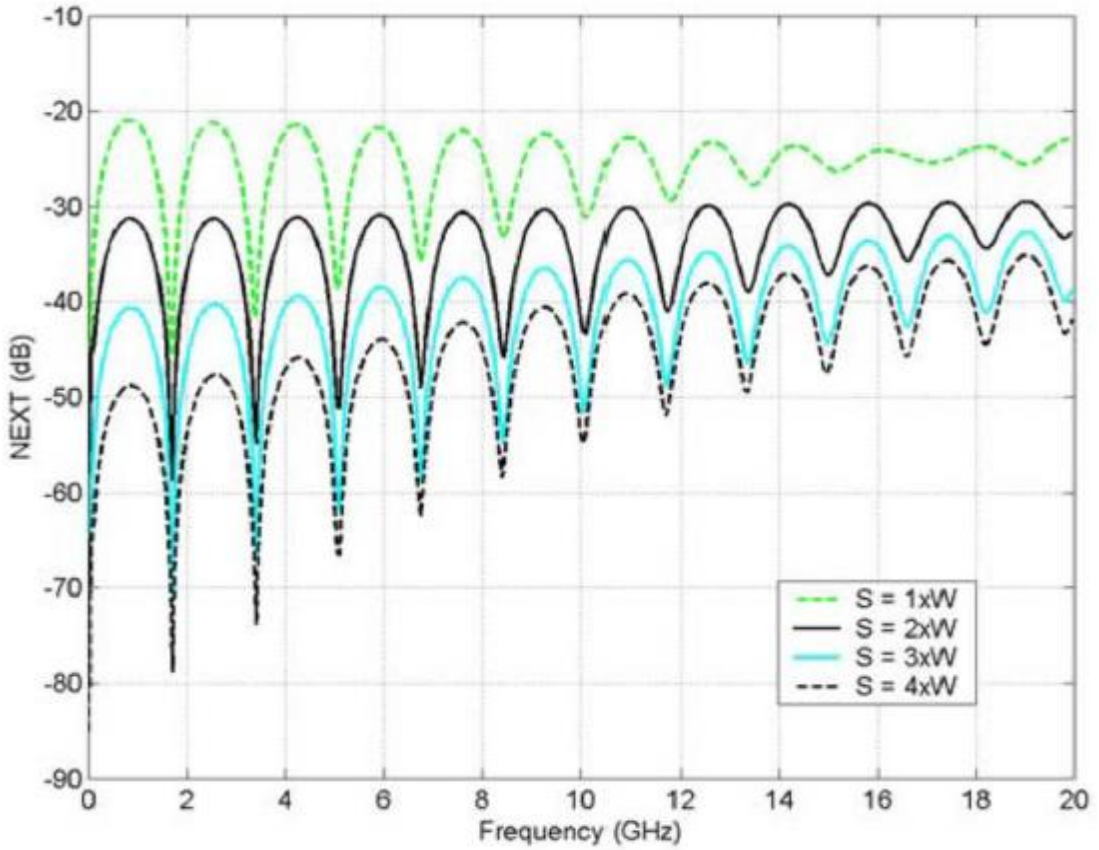

Figure 3.10: NEXT simulation [1]

The same simulation has been carried out by using FEKO software for validation. The results are demonstrated by Figures 3.11 and 3.12.

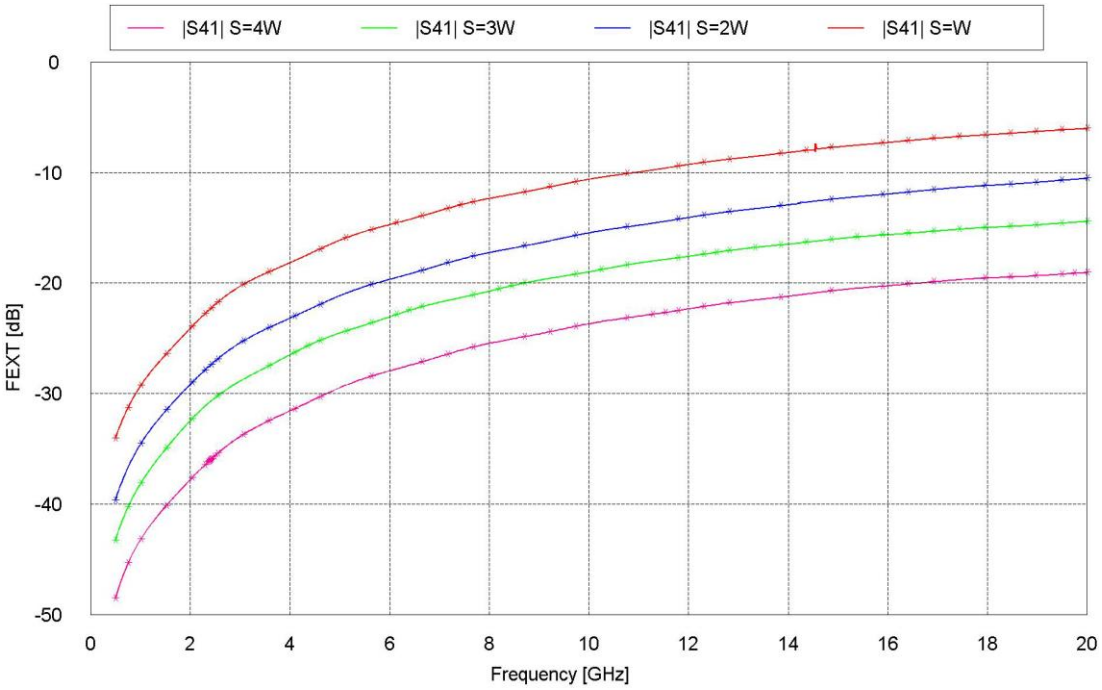

Figure 3.11: Simulated FEXT for the coated microstrip lines by FEKO

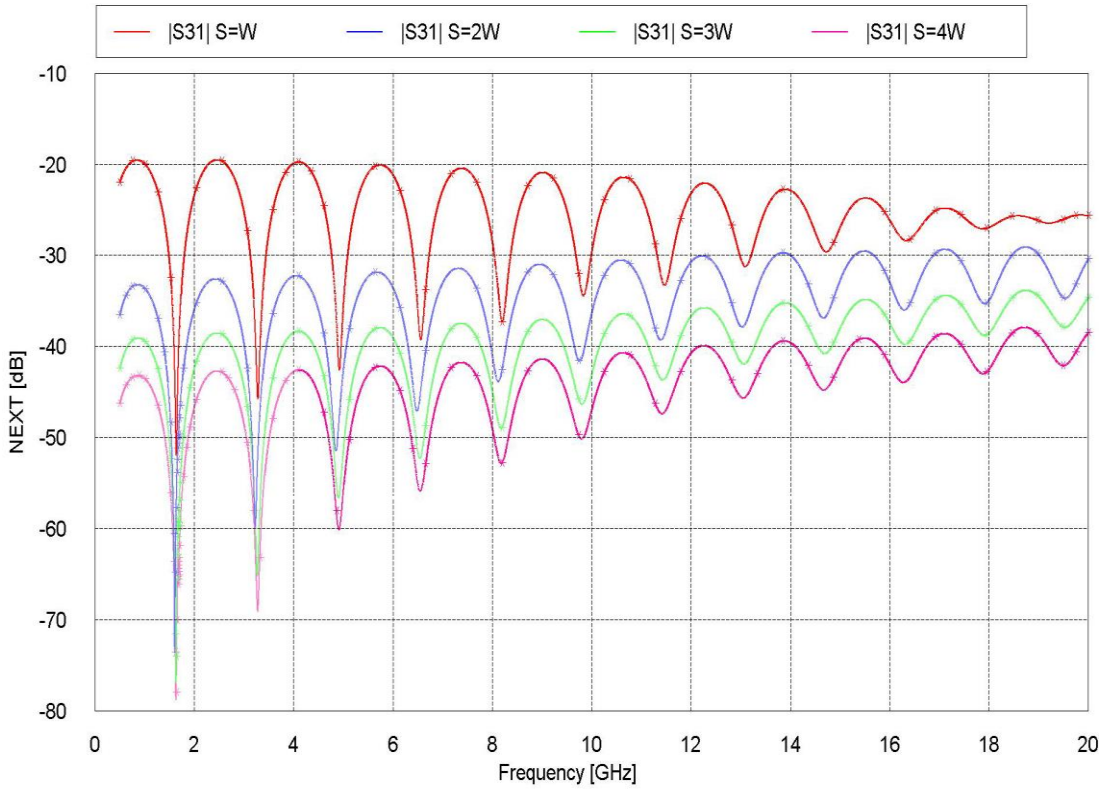

Figure 3.12: NEXT simulation for the coated microstrip lines by FEKO

Comparing the reference [1] and FEKO results studied here, we can see a good agreement. It can be concluded that, the *3W* spacing rule works and the coupling between the microstrip lines reduces with the increase in the separation distance.

Also we added the top view field diagrams of the parallel microstrip lines, by Figures 3.13 and 3.14 to illustrate the electromagnatic field distripution after the excitation.

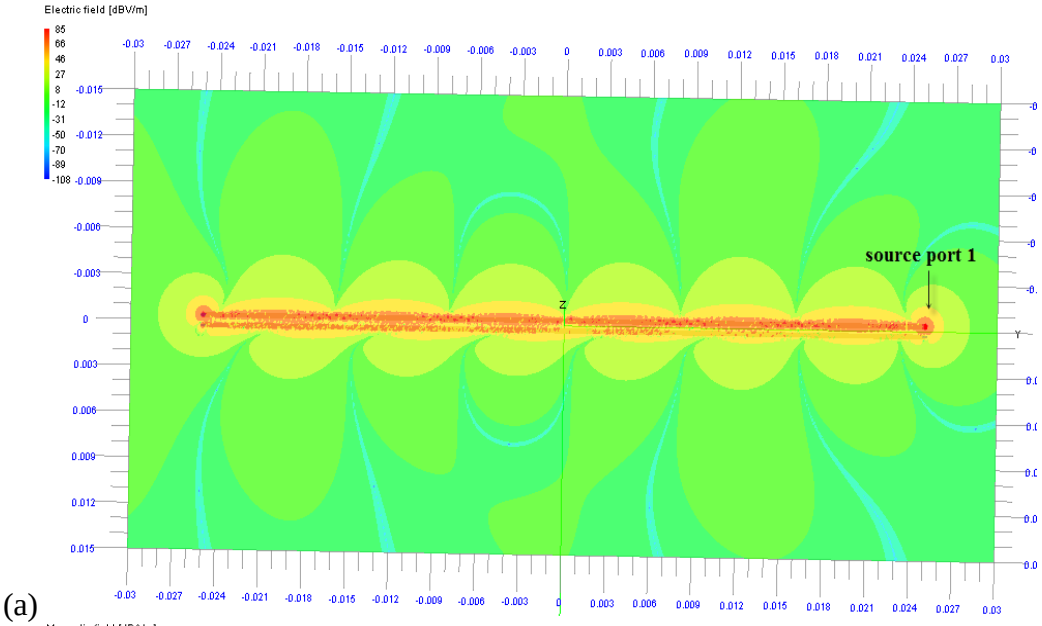

(a)

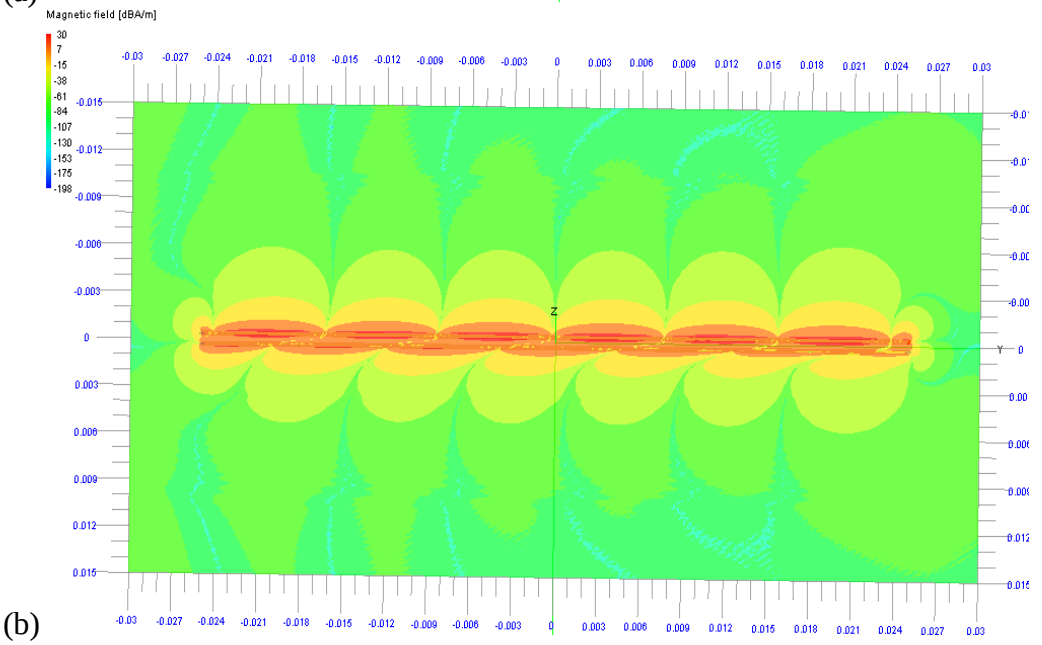

(b)

Figure 3.13: Electromagnetic field when $S=W$ (a) Electric field coupled (b) Magnetic field coupled

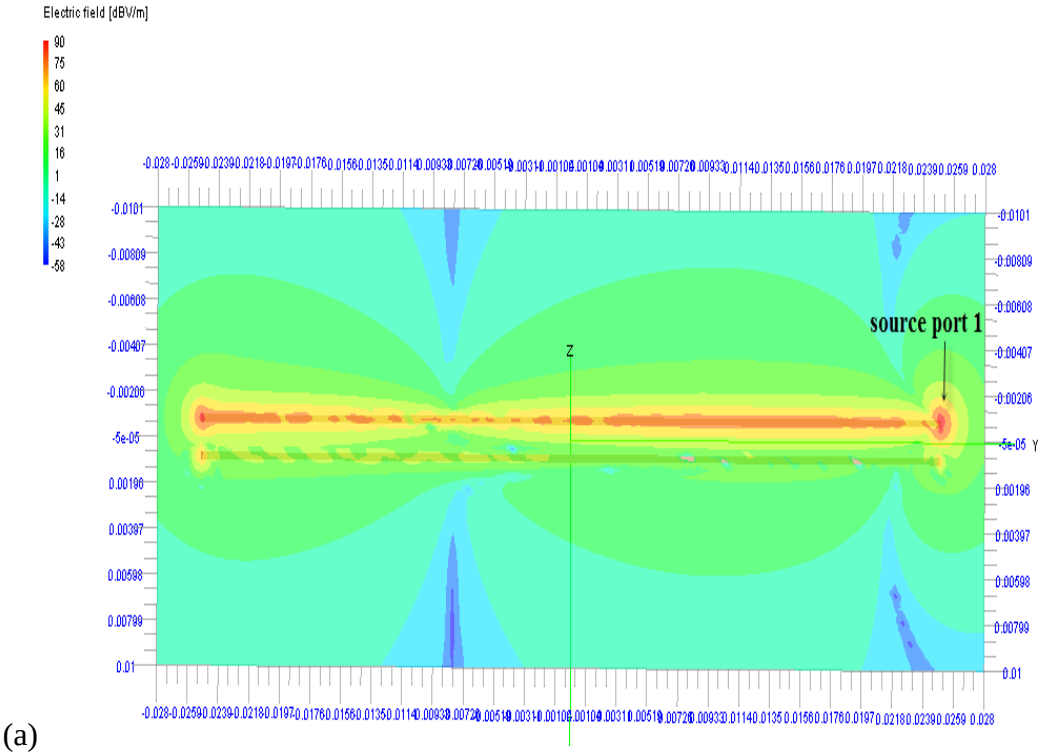

(a)

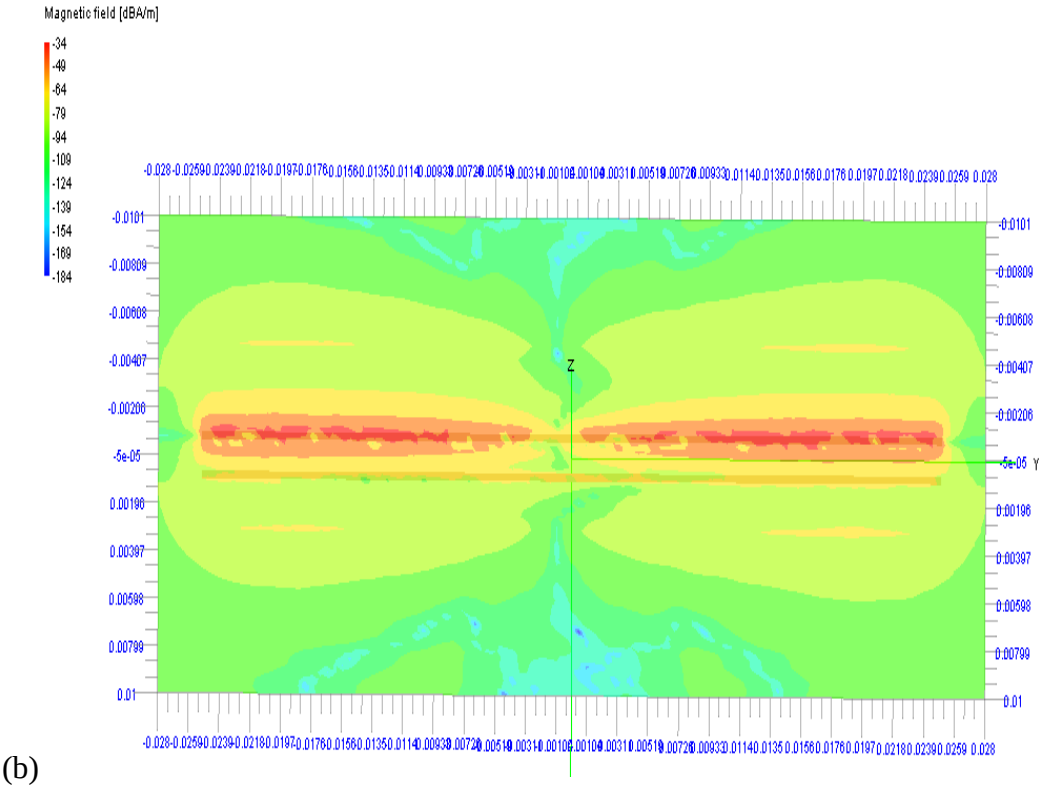

(b)

Figure 3.14: Electromagnetic field coupled when S=4W (a) Electric field (b) Magnetic field

From the figures above it can be observed that, the coapling is much more reduced when S= 4W compared with S=W.

3.2.3.2 Changing the Length of the Microstrip Lines

Surahmat et al., studied the crosstalk in parallel microstrip lines like the lines in the Figure 3.15 by changing the line length. They simulated this work by using 3*D* simulator [2].

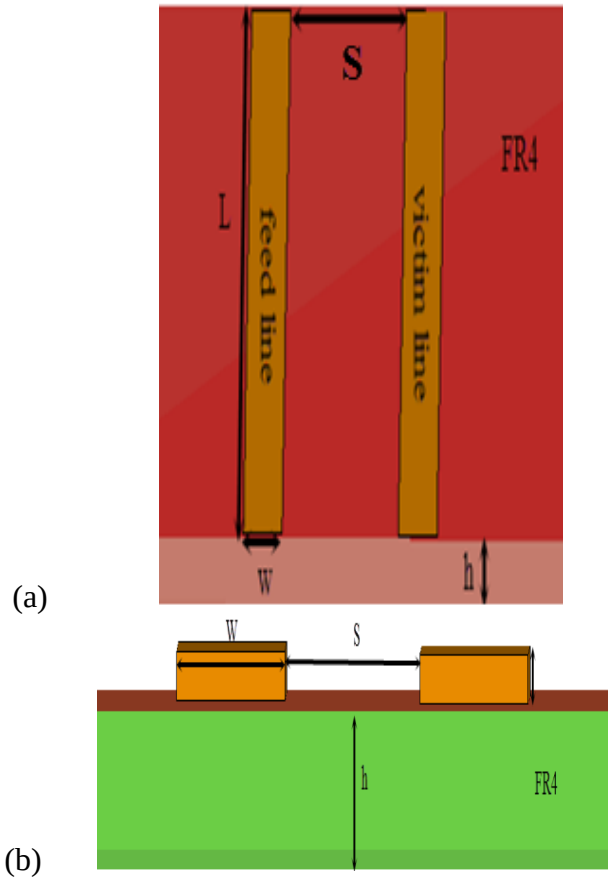

Figure 3.15: Microstrip lines (a) Tope view (b) Side view [9]

The result configuration for parallel microstrip lines related with the frequency is given by Figure 3.16 [2]. They used different lines lengths and they observed that the crosstalk was decreased slightly [9] when the length of the line decreased from 200mm to 50mm. The spacing between lines was kept constant 5mm and the width of lines is 2mm; the relative permittivity of the substrate was 4.3 and the thickness *h* 1.6mm. According to these results and the results simulated by FEKO 5.5 (Figure 3.17) it can be seen that they are closely matching.

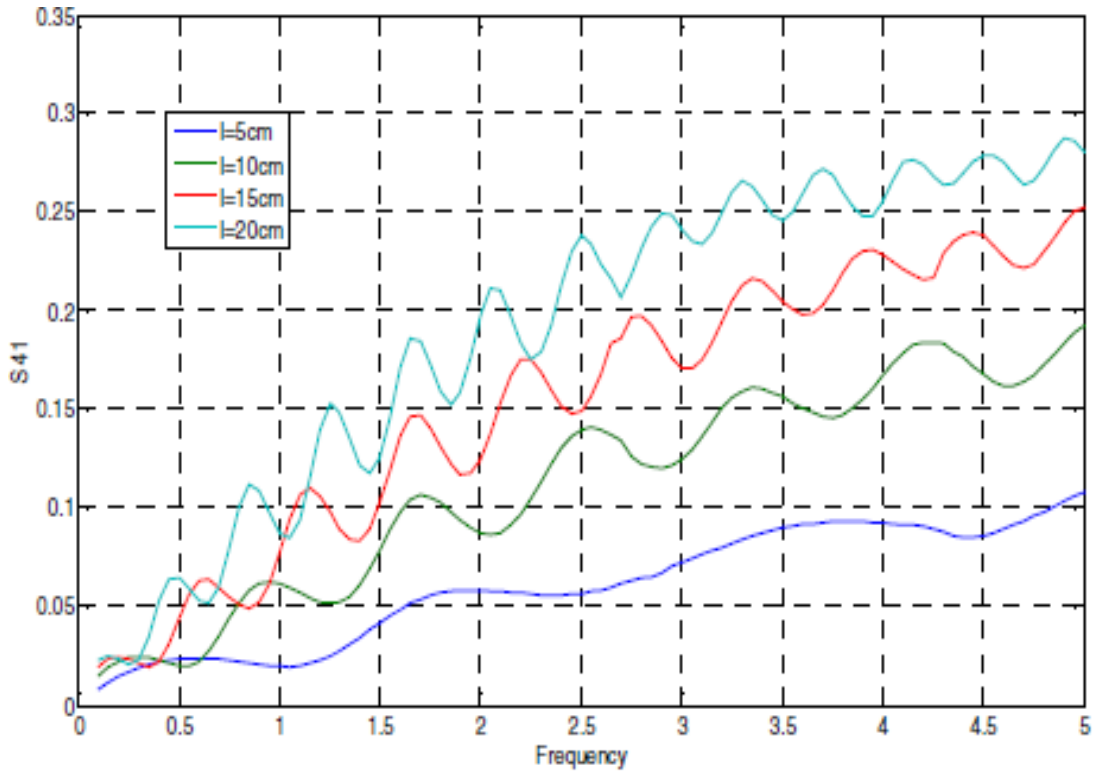

Figure 3.16: Effect of changing length of lines on the FEXT [2]

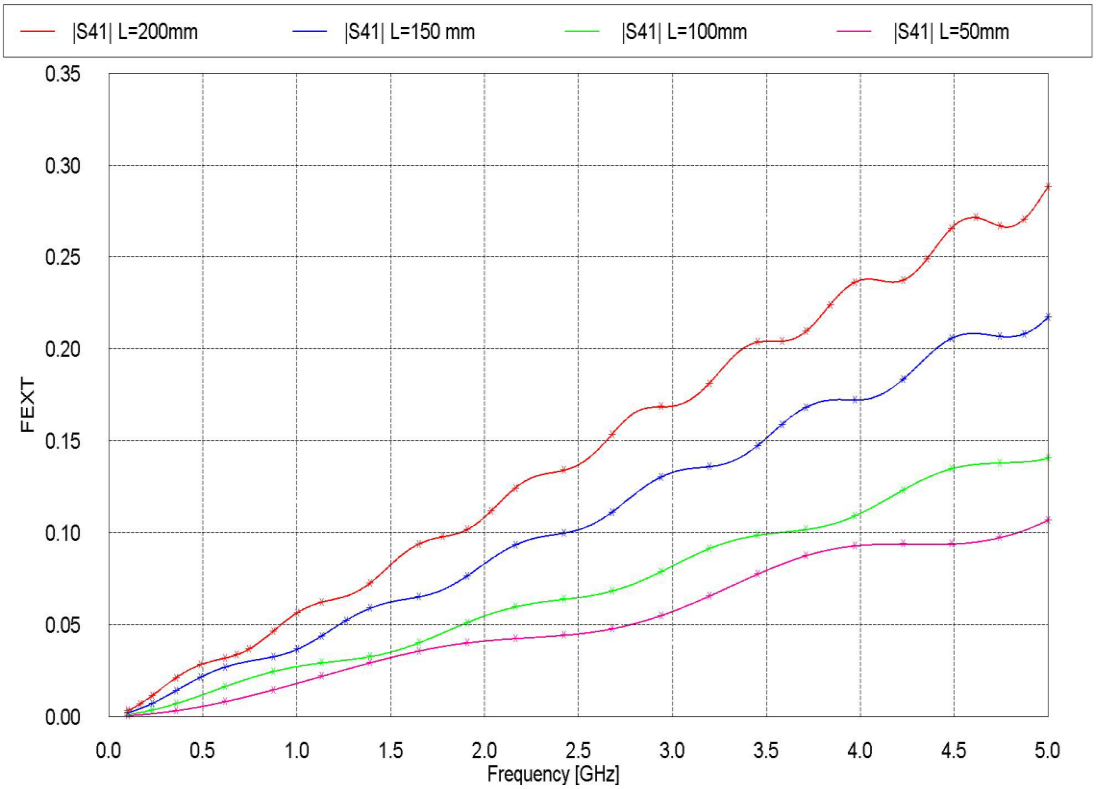

Figure 3.17: FEKO Simulation FEXT results for different line lengths

3.2.3.3 Using a Rectangular Shaped Resonator RSR

Ding-Bing et al., worked together in frequency domains by using HFSS simulator to analyse and reduce Far-End crosstalk between microstrip lines in three methods 3W rule, Serpentan gard trace with shorting via and rectangular shape resonantors RSR as shown in Figure 3.18 with the dimensions shown in Table 3.3 [3].

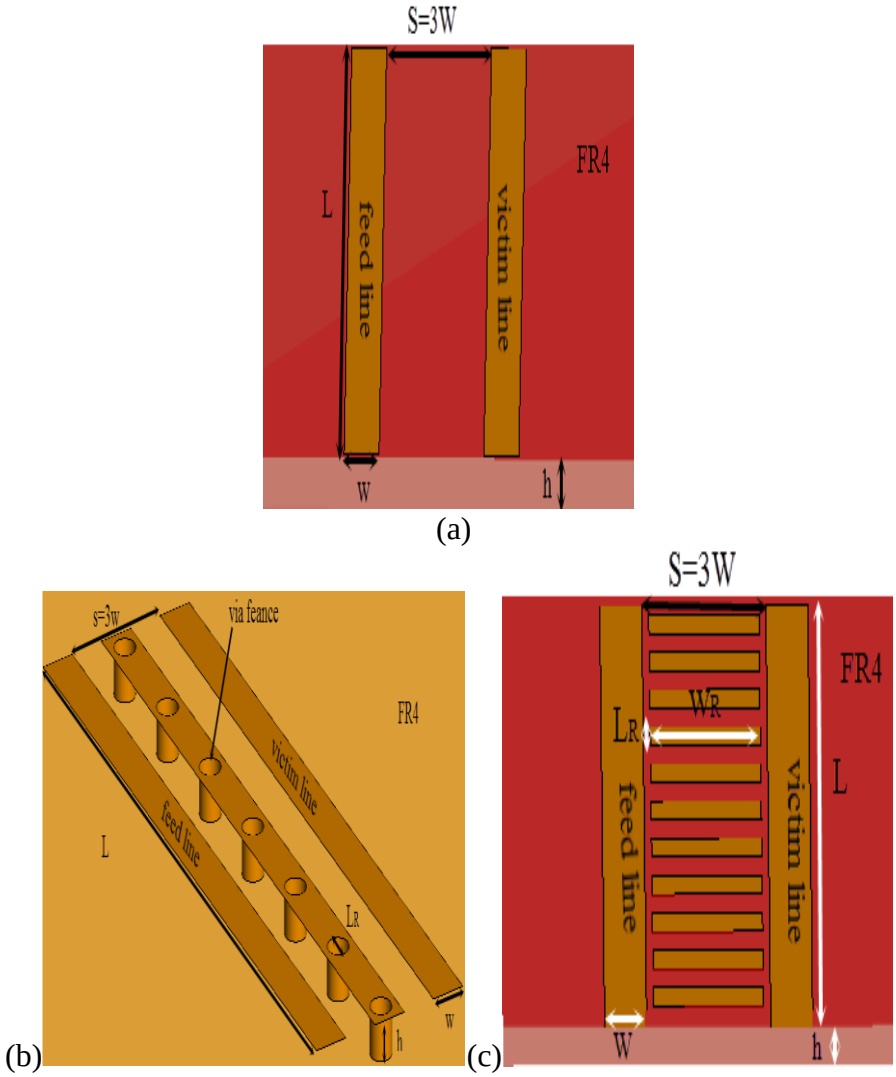

Figure 3.18: (a) 3*W* rule (b) Shorting via (c) RSR construction [3]

Table 3.3: Dimension of the microstrip lines in [3]

W	H	ε_r	L_R	W_R	T	L_R	S	L	ΔS
3*mm*	1.6*mm*	4.4	8*mm*	1*mm*	0.035*mm*	1*mm*	3**W*	50*mm*	7.8*mm*

FEXT comparison was made for each method and found out that the crosstalk was reduced by 7dB for RSR compared to 3*W* spacing rule results and 3dB compared with utilized shorting-via guard trace as shown in Figure 3.19. Also the simulation results by FEKO 5.5 are nearly matching with [3] as shown in Figure 3.20. We will use this design to enhance the FEXT and NEXT in the next section.

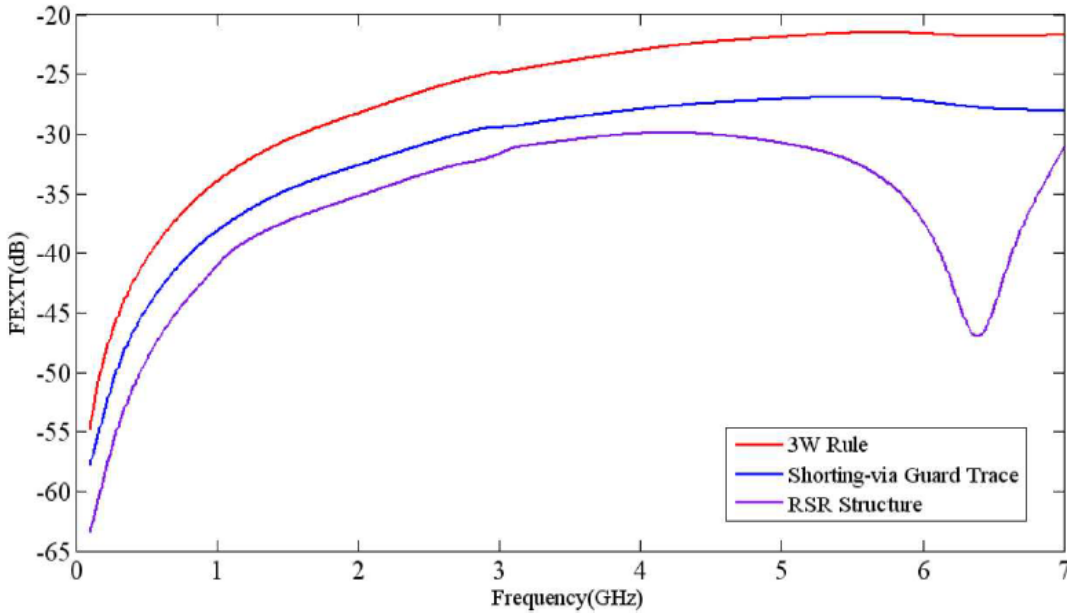

Figure 3.19: FEXT simulations to compare among RSR, 3*W* rules and shorting via[3]

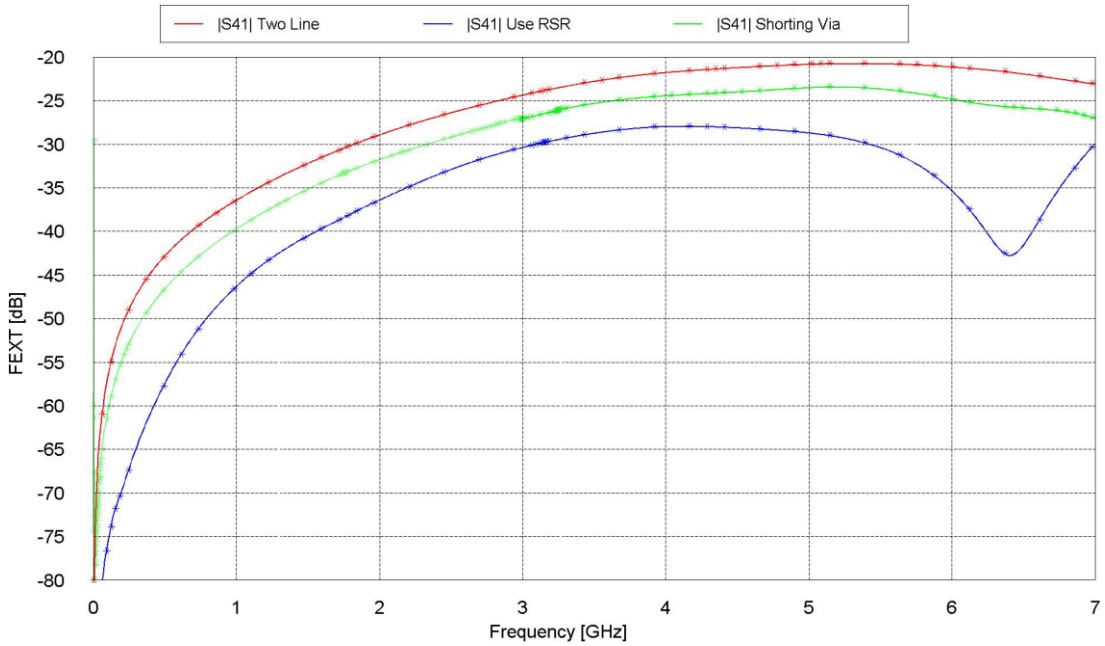

Figure 3.20: FEXT simulation by FEKO

3.2.3.4 Connecting Grounded Via Fences to the Guard Trace

Ponchak et al., worked to analyze and reduce the coupling problem between microstrip lines in dense RF bundles. They simulated their work by 3*D* FEM electromagnetic simulator to realize the crosstalk for the two line conductors and via fences between them as shown in Figure 3.21. They used metal filled via hole fences in them design with the dimensions shown in Table 3.4.

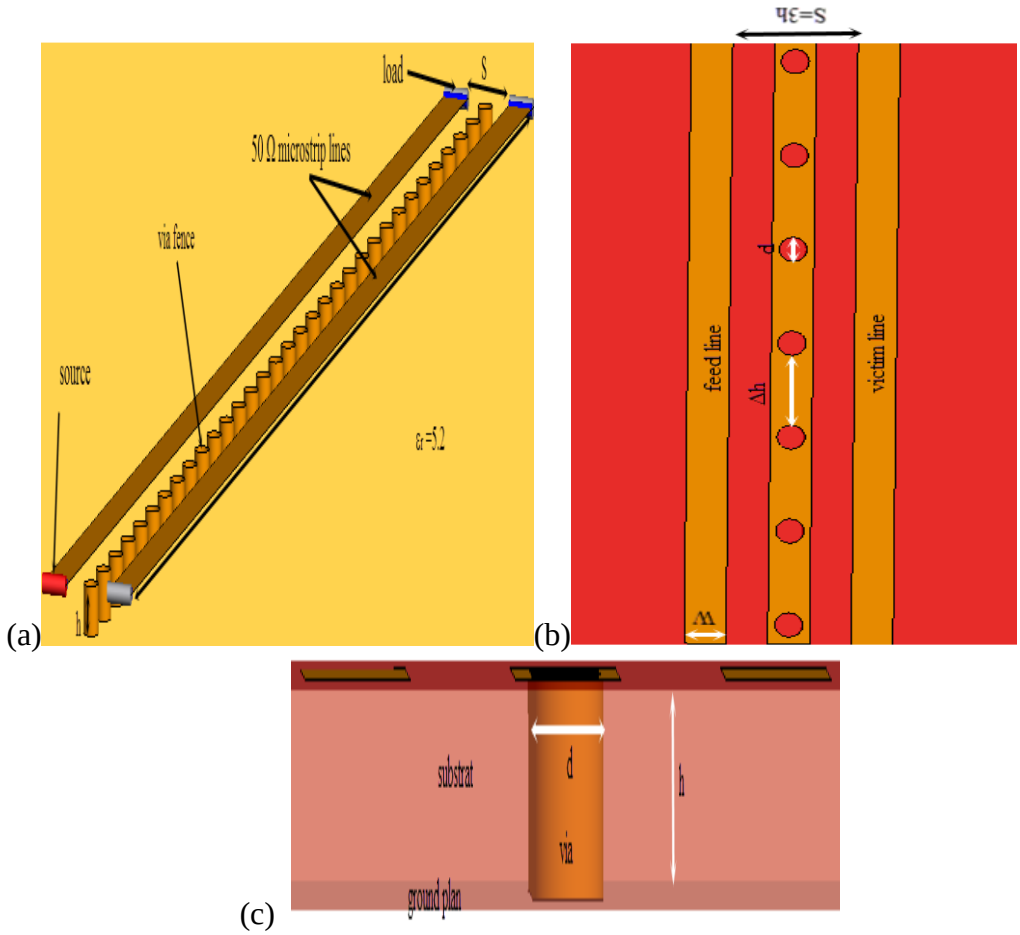

Figure 3.21: Microstrip lines structure with via (a) via without connection to metal (b) via connected to metal (b) Side view

Table 3.4: Dimensions of the coupled microstrip lines [4]

W	*S*	D_v	*H*	ε_r	Δh	ΔS	*tan* δ	*L*
0.414mm	2Δ*S*+W	0.25mm	0.25mm	5.2	0.4	0.25mm	0.0002	22mm,

They noted that, the results show that the via fences did not reduce the coupling but when they connected via fences with the metal conductor, the coupling was reduced by 8dB. The FEKO 5.5 simulator was used to compare the results with the previous work [4], and a good agreement was found between them as shown in the Figures 3.22 and 3.23.

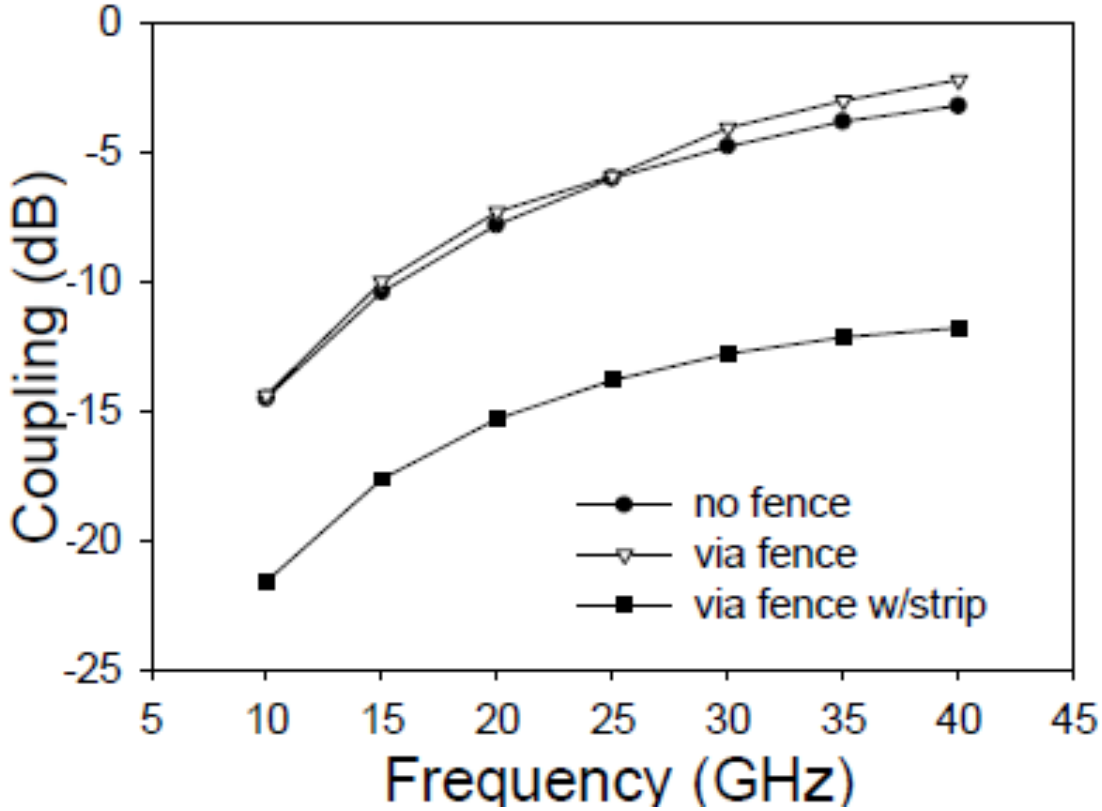

Figure 3.22: Coupling between microstrip lines (FEXTS_{41}) [4]

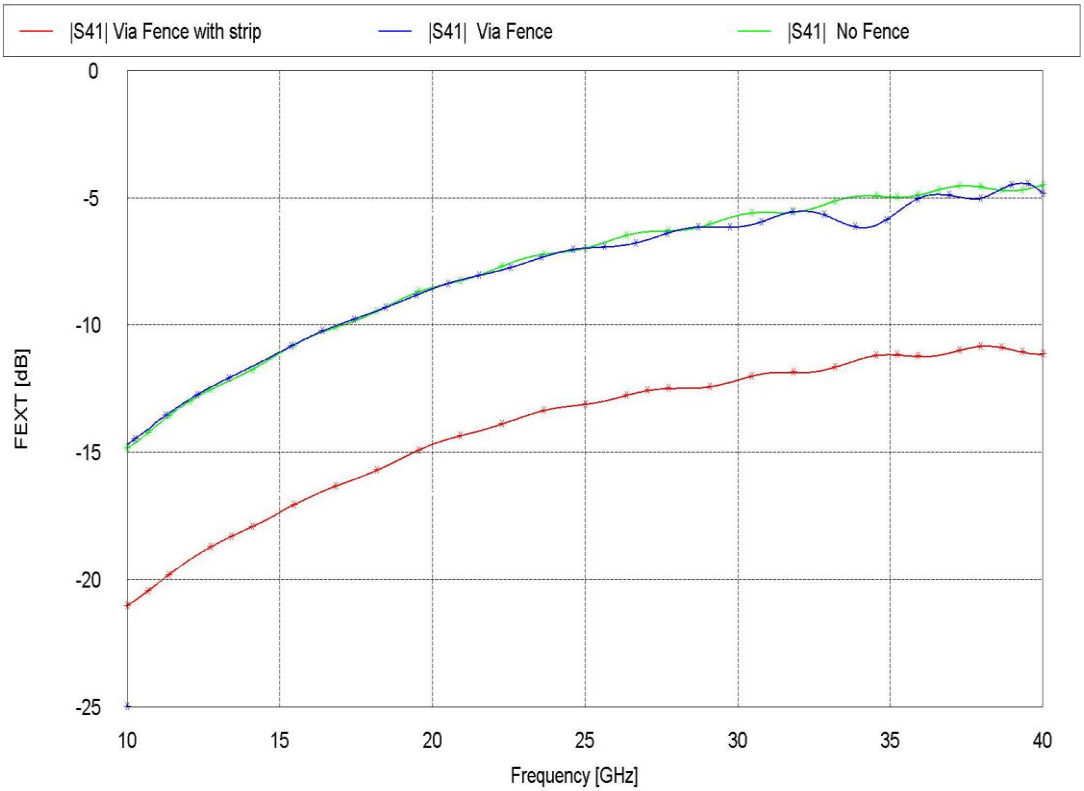

Figure 3.23: FEXT as a function of frequency by FEKO

It can be seen that this method is very effective in reducing the crosstalk between double lines compared to the via fences placed in the middle of microstrip lines [4]. Note that the via diameter must be the same with the width of the trace so as to conserve the signal integrity within the bandwidth of interest [13].

The electromagnetic coupled problem between two microstrip lines where there is no via fences between them, is shown in Figure 3.24.

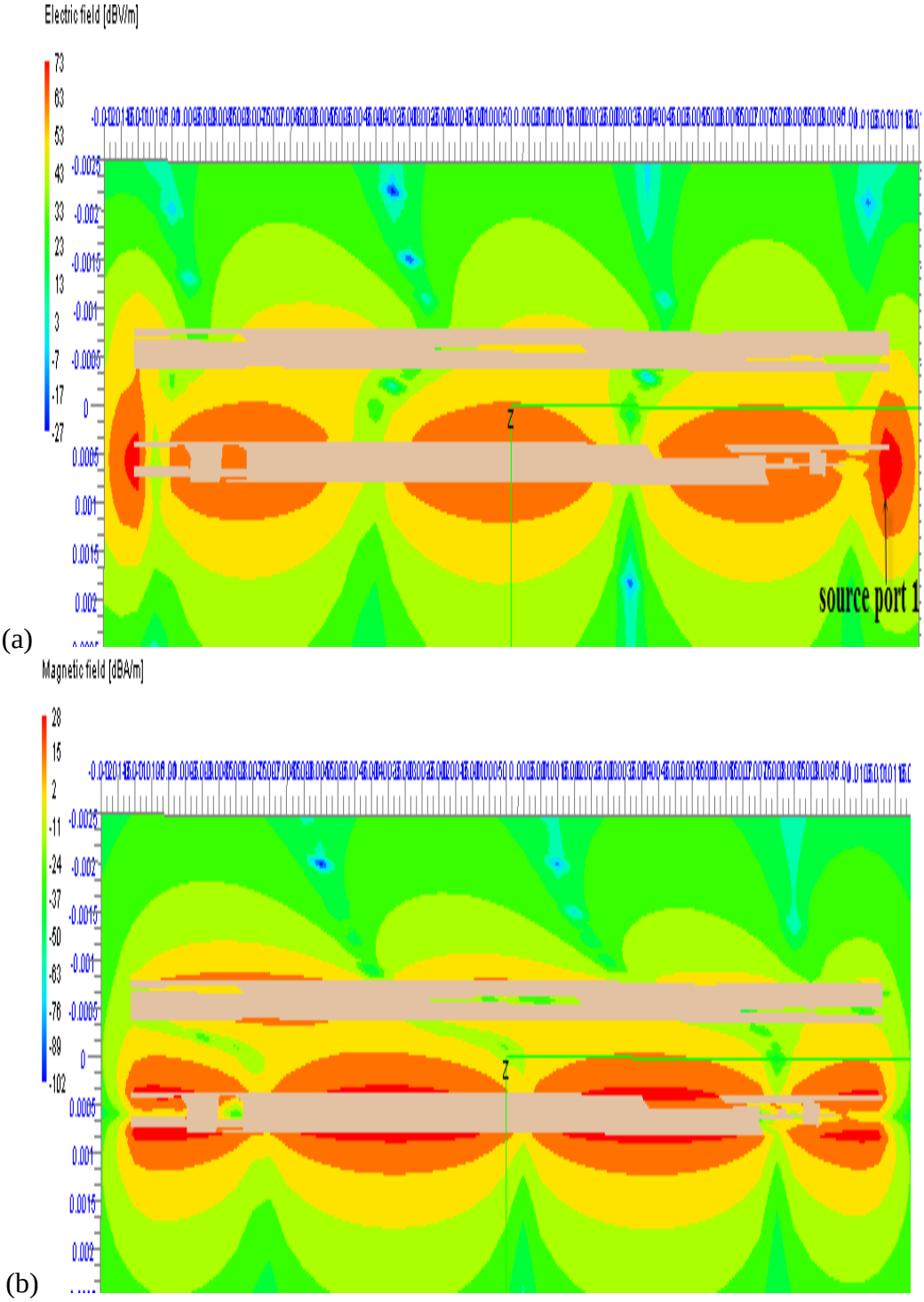

(a)

(b)

Figure 3.24: Electromagnetic coupling between double lines (a) Electric field (b) Magnetic field

The electromagnetic coupled field between microstrip lines, when there are via fences between them is shown in Figure 3.25.

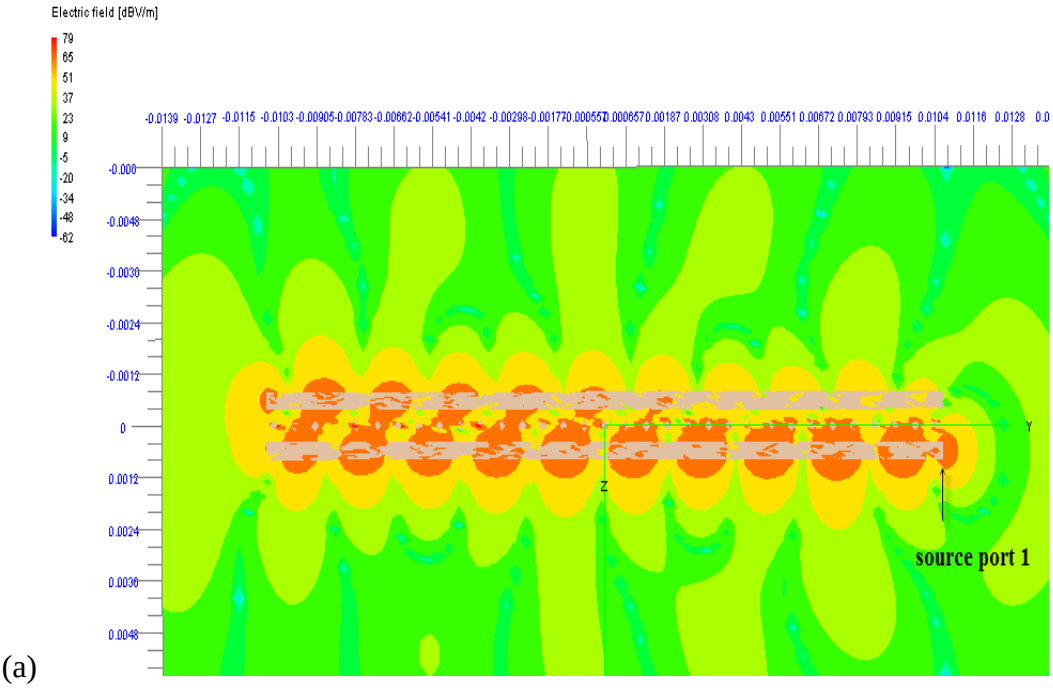

(a)

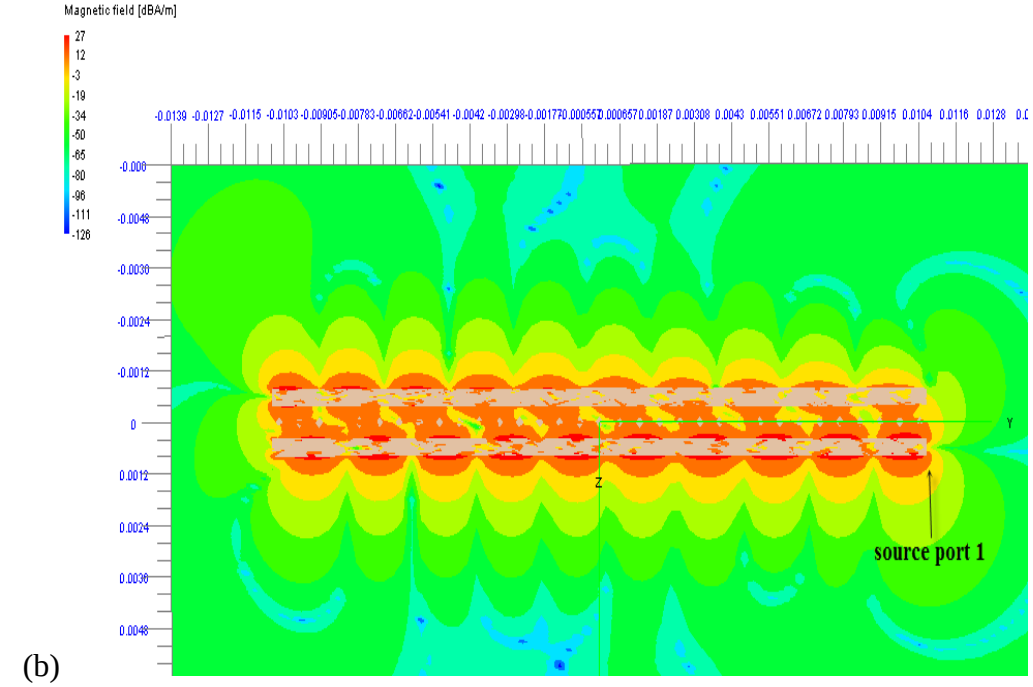

(b)

Figure 3.25: Electromagnetic coupled use via fences (a) Electric field (b) Magnetic field

The electromagnetic coupled field is shown by Figure 3.26, when there are via fences connected by the guard trace between double microstrip lines.

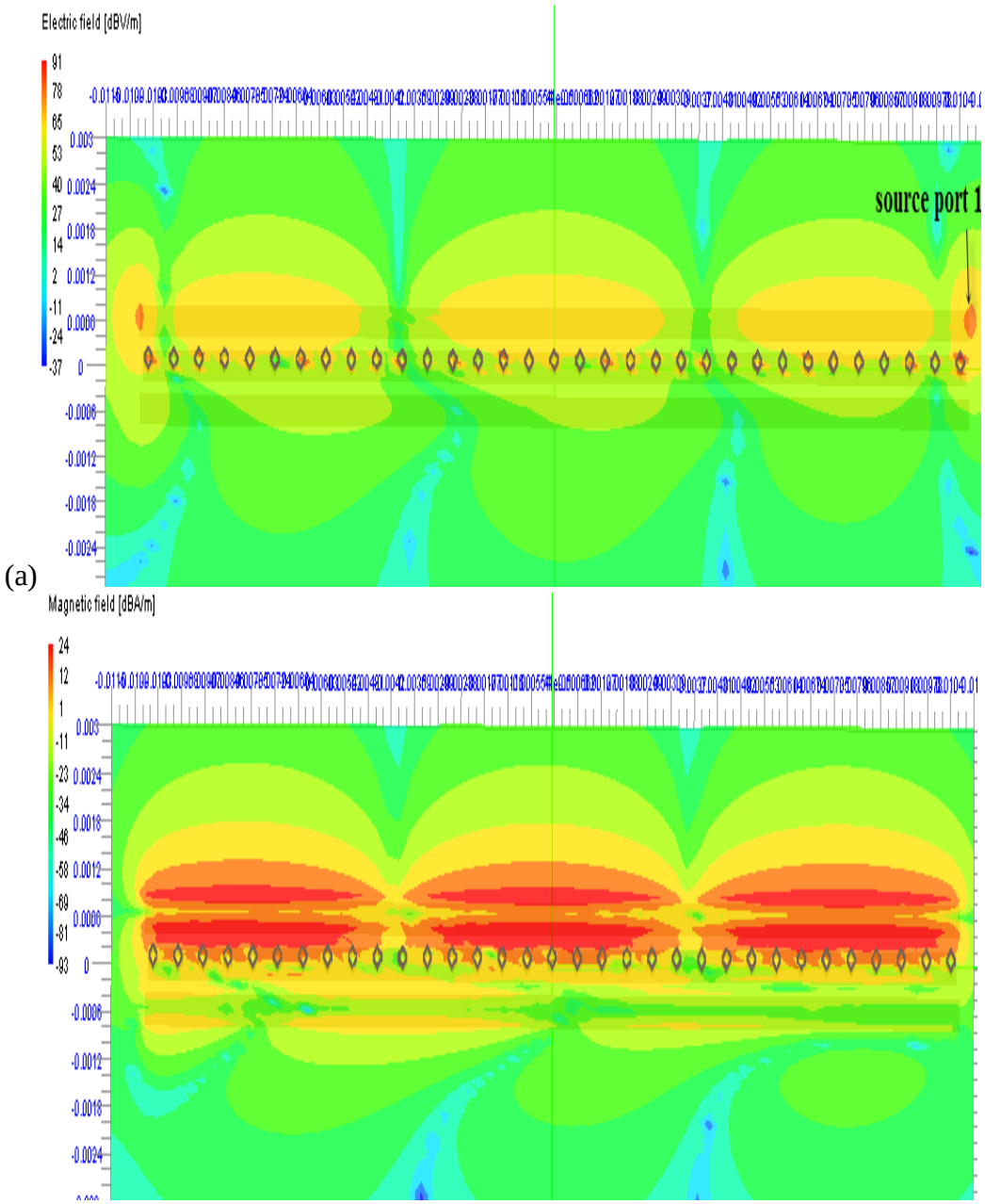

Figure 3.26: Electromagnatic field use guard trace and via (a) Electric field (b) Magnetic field

We note from the figures above that for the electromagnetic coupling field between the double microstrip lines is reduced when via fences are connected by a guard trace.

Also for the coated microstrip lines with 63 via fences having the dimensions shown in the Table 3.5; the direct coupled S_{21} and the crosstalk (FEXT S_{41} and NEXT S_{31})

result comparing with 3W spacing rule are shown in Figures 3.27, 3.28 and 3.29 respectively.

Table 3.5: Dimensions of Microstrip lines with via fences

W	S	$\boldsymbol{D_v}$	H, H_c	$\boldsymbol{\varepsilon_{r1}}$, $\boldsymbol{\varepsilon_{r2}}$	$\boldsymbol{\Delta h}$	$tan\ \boldsymbol{\delta}$	L
0.396mm	*3W*	*W*	*0.2mm, 0.02mm*	*4.2, 4.1*	*1.1855mm*	*0.0002*	*50mm*

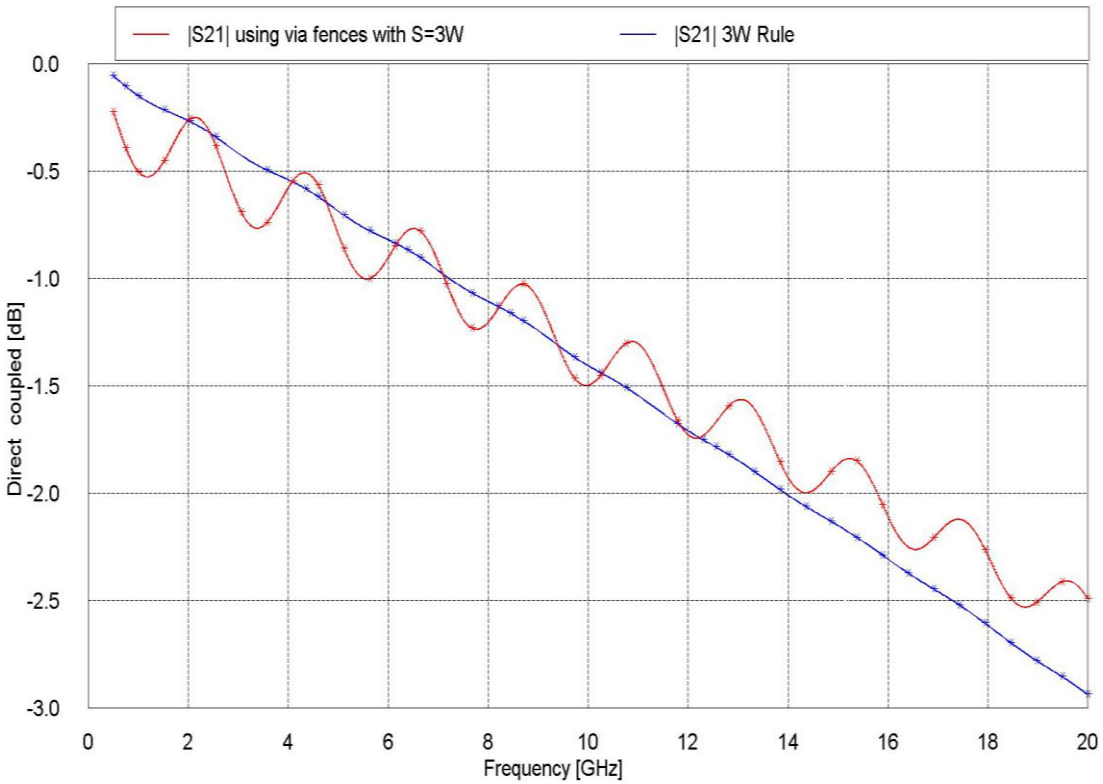

Figure 3.27: Comparison of the direct coupling between using via fences and 3*W* rule

FEXT S_{41} is shown in Figure 2.28:

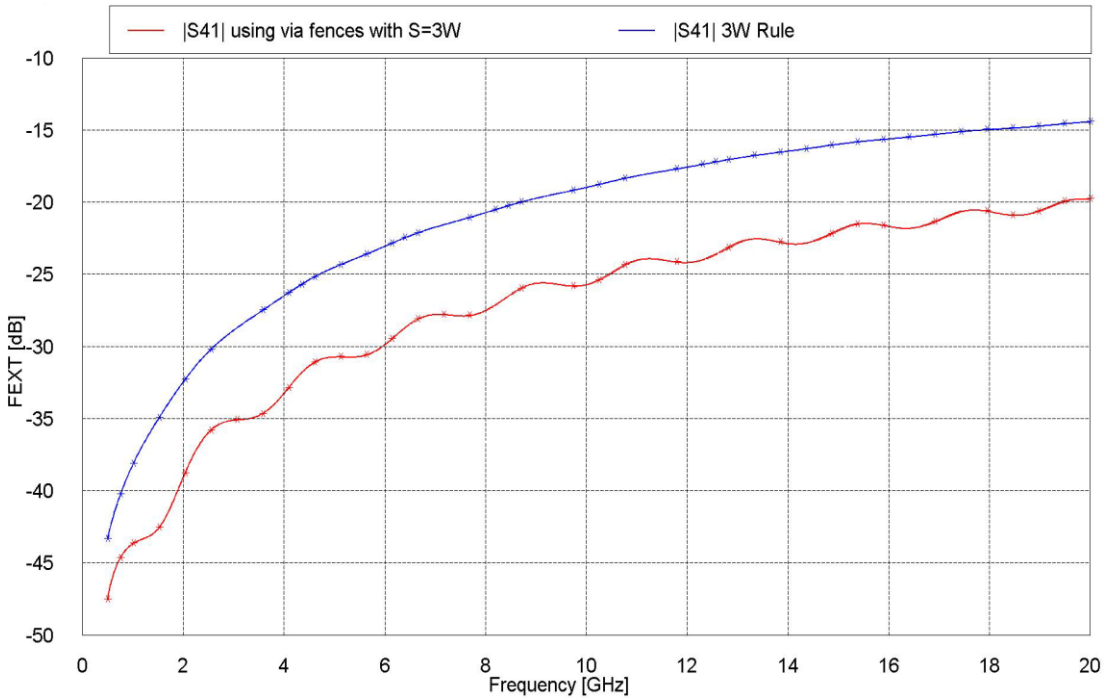

Figure 3.28: Compare the FEXT between using via fences and 3W rule

NEXT S_{41} is shown in Figure 2.29:

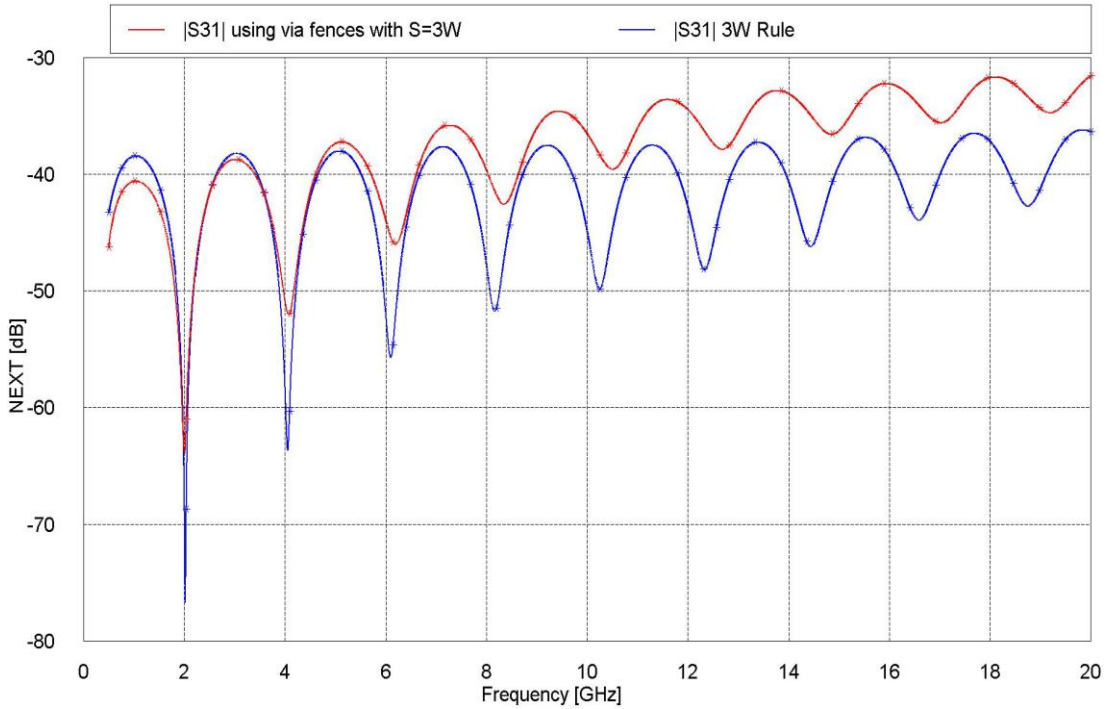

Figure 3.29: Compare the NEXT between using via fences and 3*W* rule

3.2.3.5 Using rectangular Trace

In this section, a rectangular trace is used between the lines to reduce the crosstalk. The trace is connected with the ground plane as shown by Figure 3.30. This kind of trace has low cost and the results are reasonably good compared with via fences. Simulations have been carried out with the dimensions shown in Table 3.6 below. The lines have characteristic impedance of 50Ω matched to the load impedance.

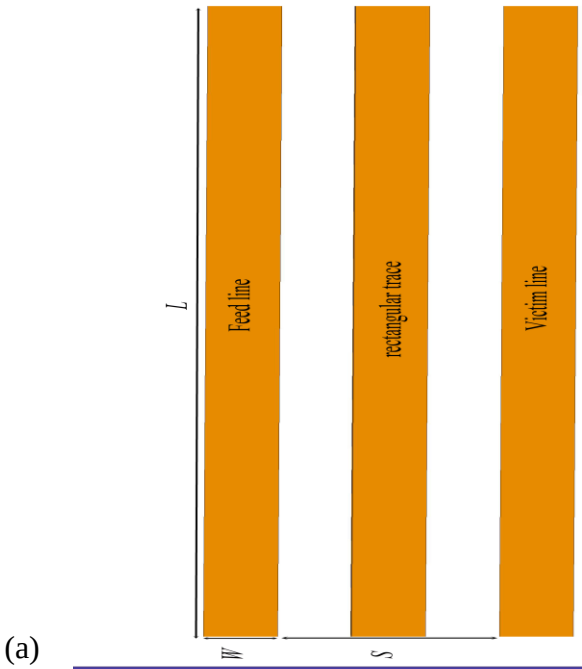

Figure 3.30: Double microstrip lines with rectangular Trace (a) Tope view (b) Side view

Table 3.6: Dimensions of microstrip line with the Design

W	H, H_c	L	S	W_R	$\varepsilon_{r1}, \varepsilon_{r2}$
0.588mm	*0.2mm, 0.02mm*	*50mm.15mm*	*3W*	*0.396mm*	*4.2, 4.1*

From the results it observed that is FEXT is less, compared with the previous methods (3W spacing rule and with use via fences) by 7dB and 1dB respectively as shown in the Figures 3.31, 3.32 and 3.33 which demonstrate direct coupling, crosstalk (FEXT) and (NEXT) between lines respectively.

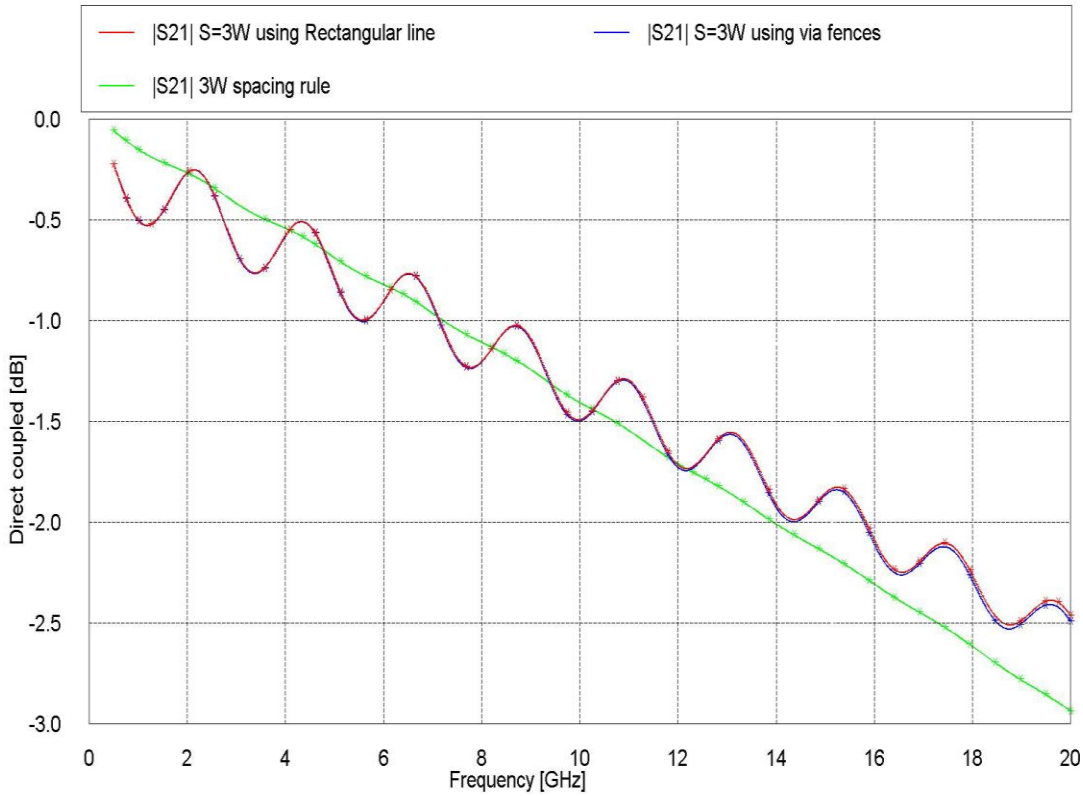

Figure 3.31: Comparison of the direct coupling S_{21} for rectangular trace, use via fences and with 3W rule, with S=3W

FEXT S_{41} when the rectangular trace was used with the spacing is 3*W*:

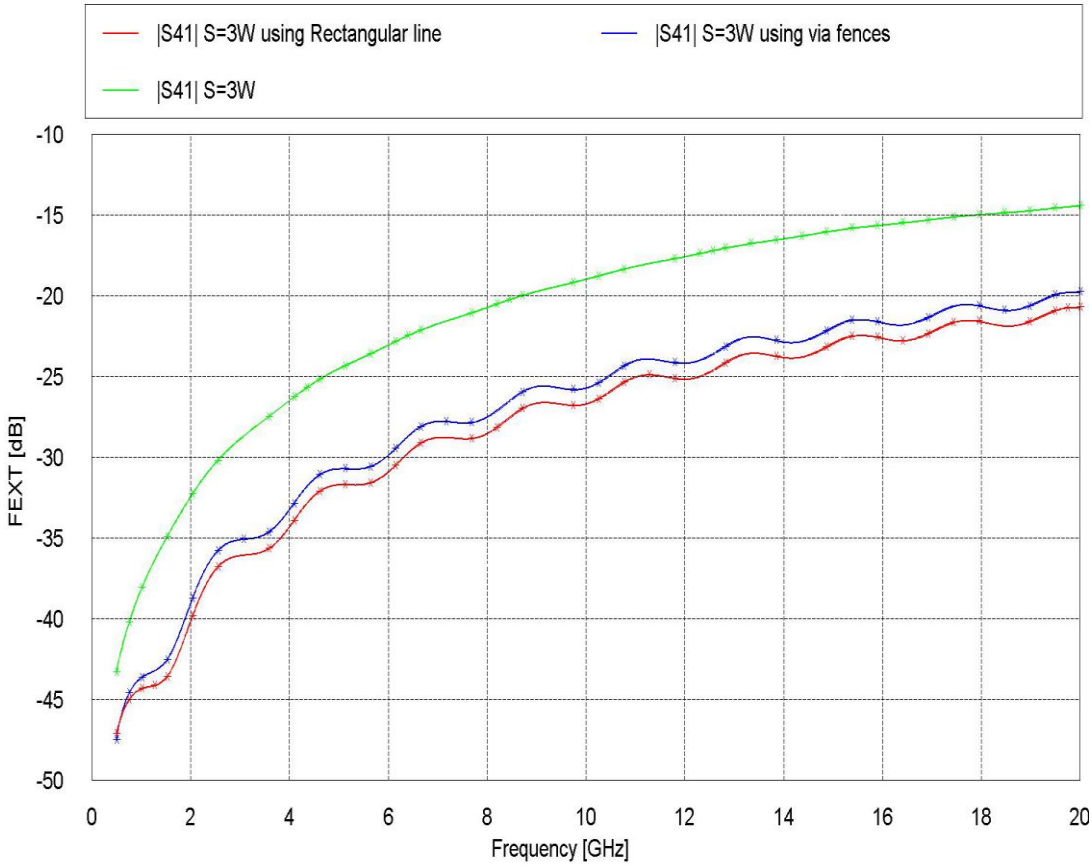

Figure 3.32: Description of FEXT among use rectangular trace, use via fences and with 3*W* rule, with *S*=3*W*

We note that from the results above, the amount of crosstalk FEXT in new dimensions is less than the old dimensions which are (*S*=4*W*, *W*=0.396*mm* placed on substrate has same thickness and $\varepsilon_{r1}$and ε_{r2} are 4.2*mm*, 4.1 respectively) by nearly 10dB.

NEXT S_{31} when the rectangular trace was used with the spacing is 3*W*:

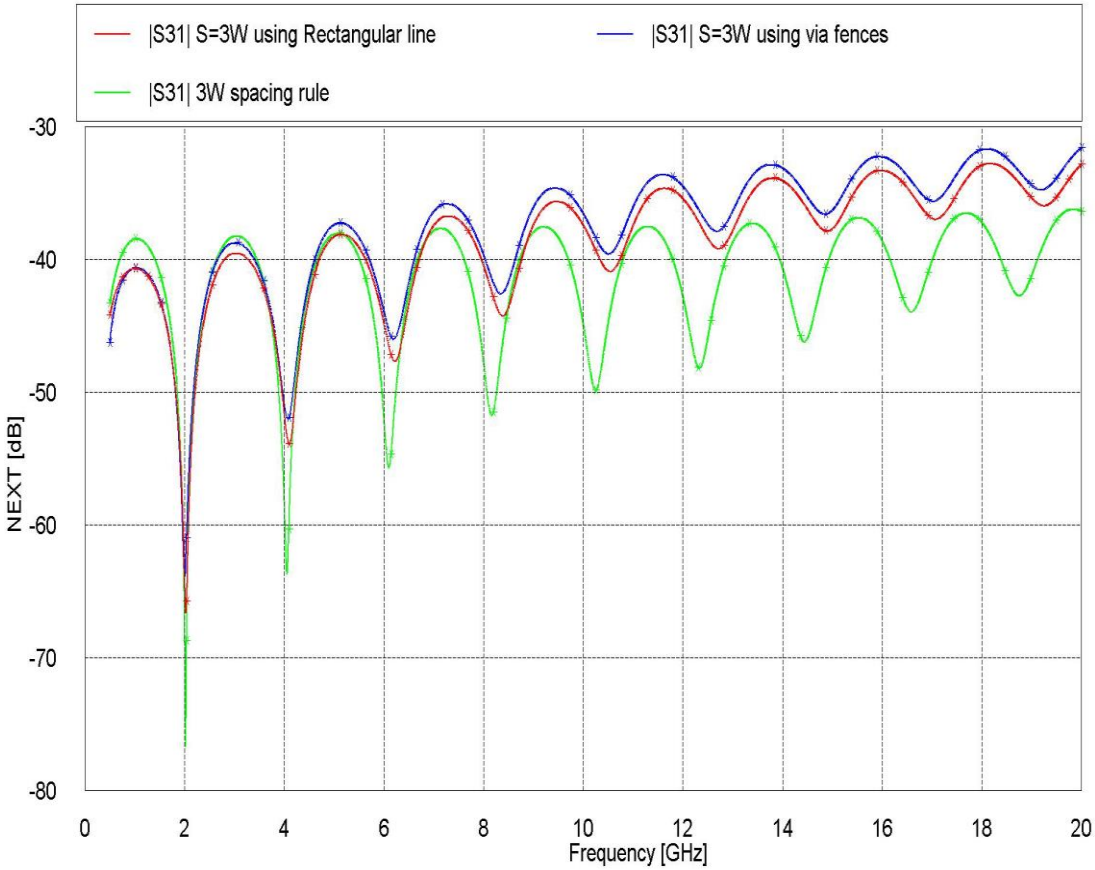

Figure 3.33: NEXT for rectangular trace, use via fences and with 3*W* rule, with *S*=3*W*

By effecting change in the length of the lines when used via fence connected by metal conductor and when replace it by rectangular trace with 15mm for each technique shown in Figures 3.34 and 3.35 and comparing this results with the result obtained when the length was 50mm, with range of frequency from 1GHz to 20GHz.

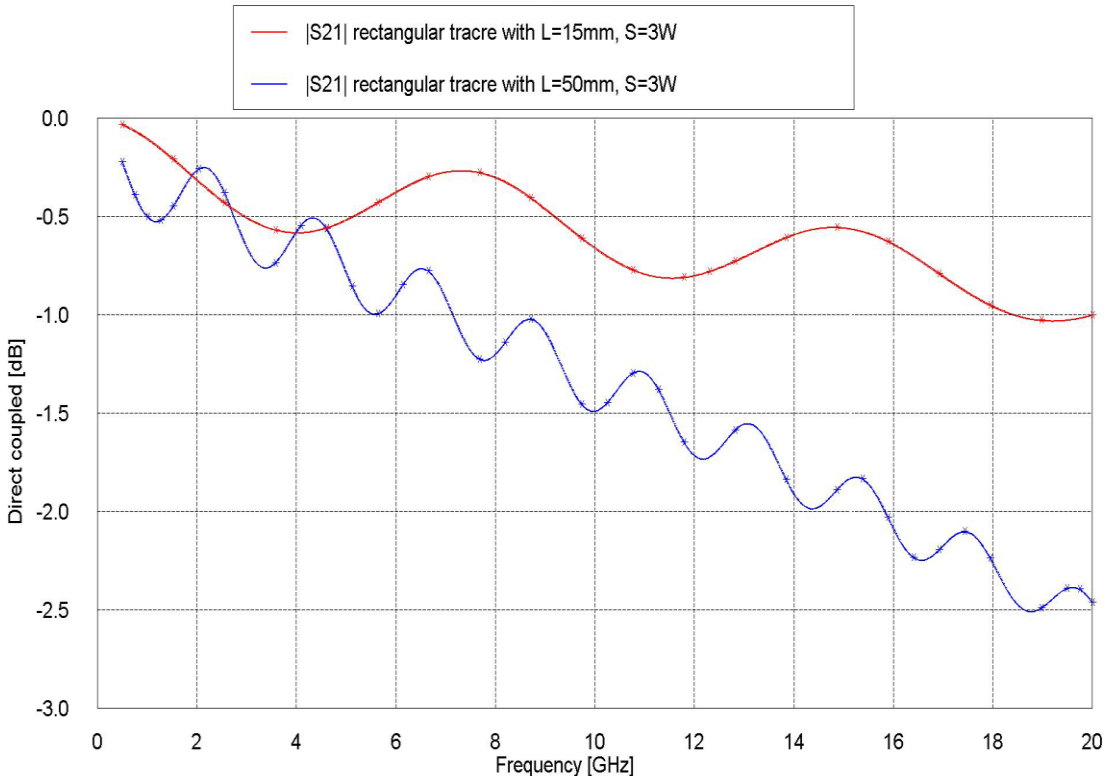

Figure 3.34: Direct coupling for two different lengths 15*mm* and 50*mm*

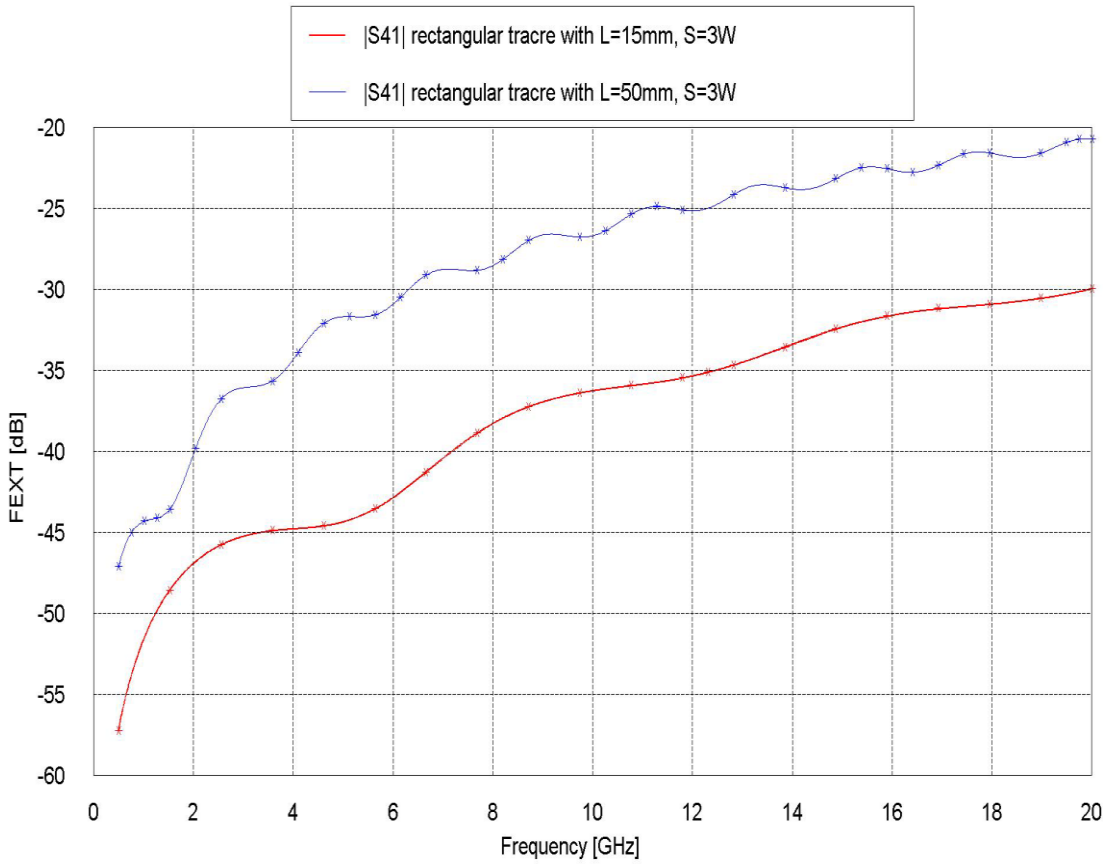

Figure 3.35: FEXT for two different lengths 15*mm* and 50*mm*

The electromagnetic field when the rectangular trace was used between microstrip lines shown in Figure 3.36 at frequency 10GHz

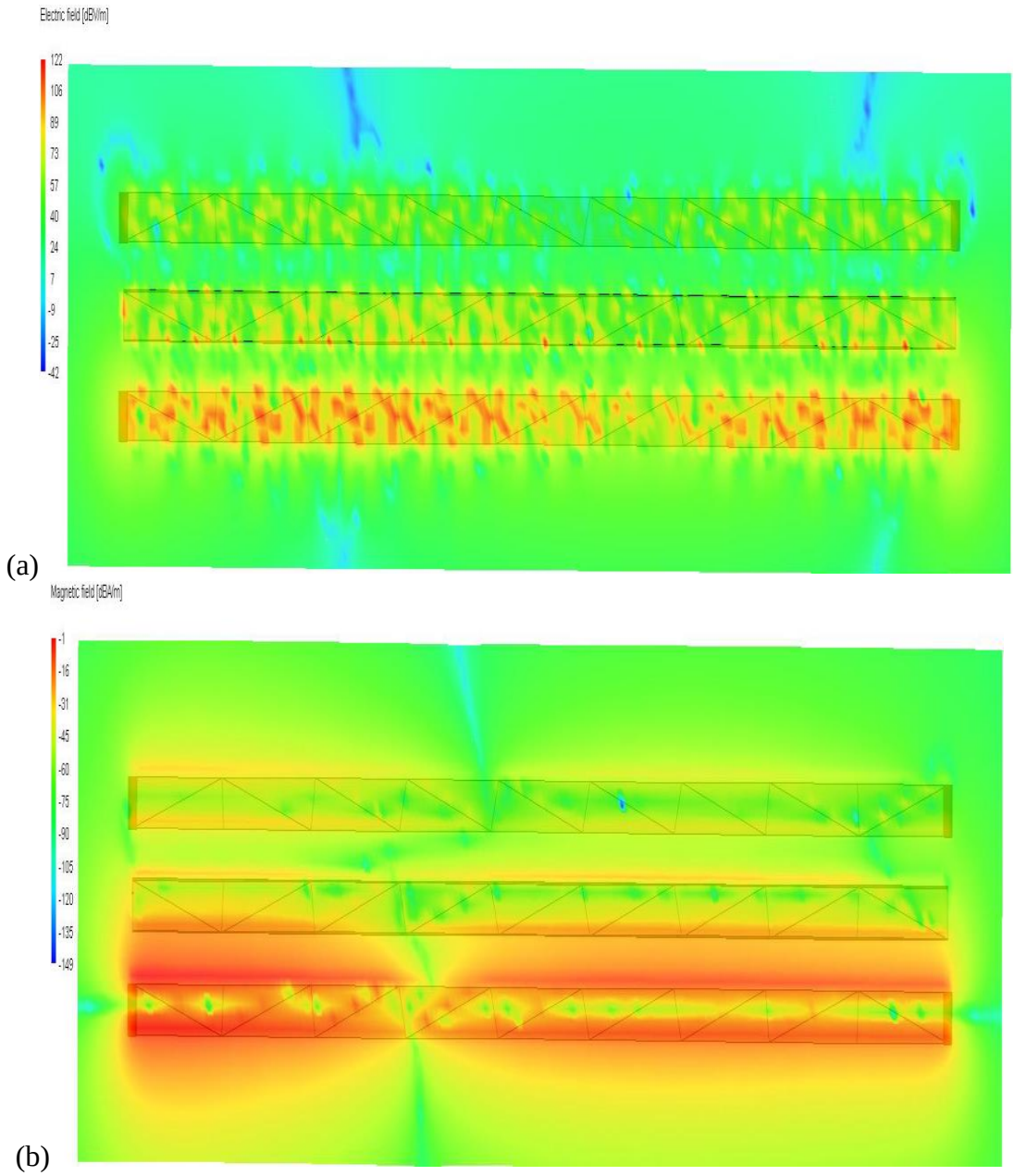

Figure 3.36: The electromagnetic field of the double microstrip lines with rectangular trace (a) Electric field (b) Magnetic field

3. 2.3.6 Changing the Dielectric Constant

In this work the crosstalk study has been carried out, when the value of the dielectric constant is 2.2, 3, 4.2 or 6.15, for the constant width having a characteristic impedance of 50Ω. For the length of line L=50mm and spacing equal to the width of the lines, Figures 3.37, 3.38 and 3.39 show the effect of the dielectric constant on direct coupling S_{21}, NEXT S_{31}, and FEXT S_{41} respectively as a function of frequency, for coated microstrip lines.

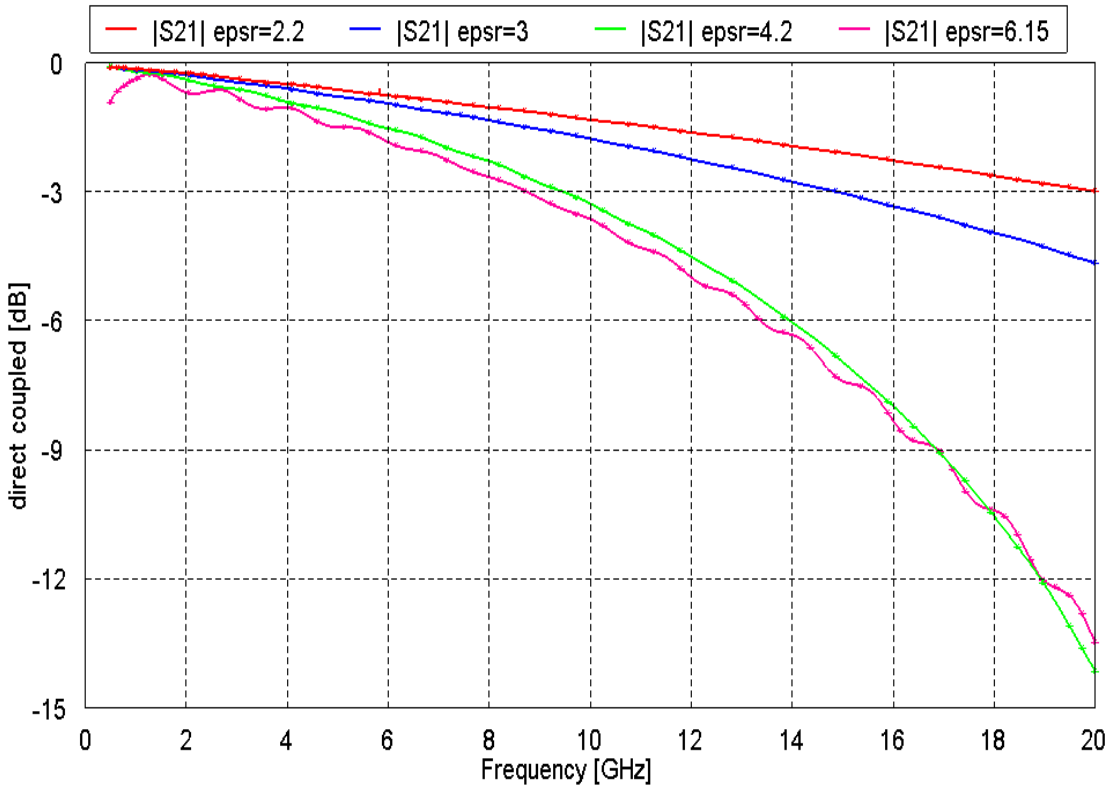

Figure 3.37: Direct coupling S_{21} for different dielectric constants

$S_{21,}$ reduces when the dielectric constant increases.

FEXT S_{41} is shown in Figure 2.38:

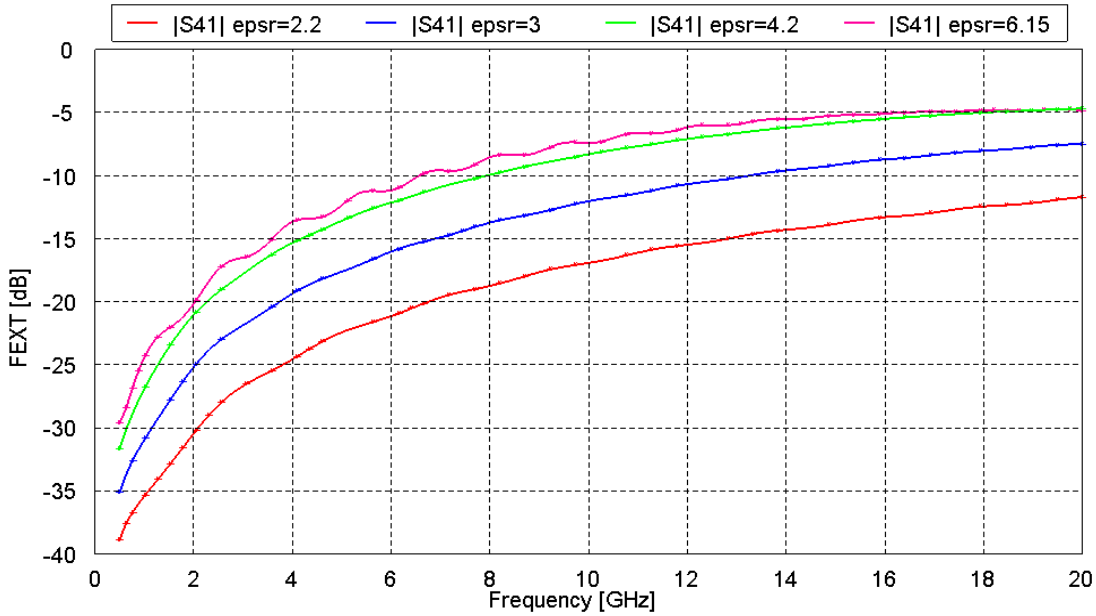

Figure 3.38: Simulated FEXT for different dielectric constants

The figure shows that S_{41} increases as the dielectric constant increases.

NEXT S_{31} is shown in Figure 3.39:

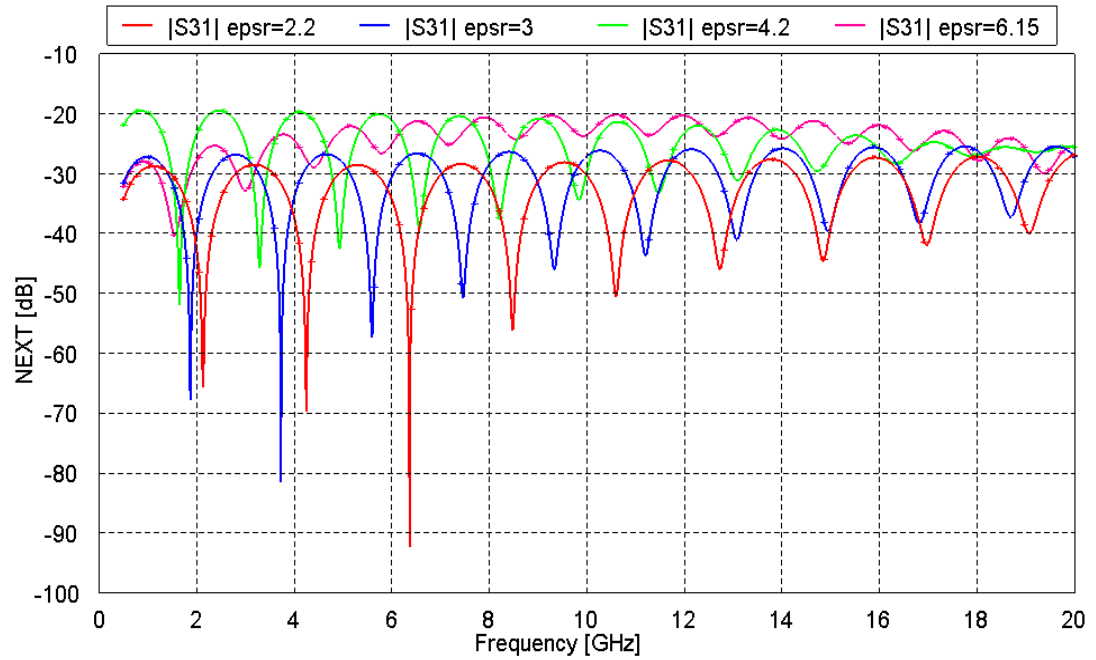

Figure 3.39: Simulated NEXT for different dielectric constants

Figures above shows that the cross crosstalk is less for the low values of the permittivity [14].

3.2.3.7 Using RVG

Rectangular shapes and via fences are connected by guard trace between microstrip lines as shown in Figure 3.40. In this method the spacing between the microstrip lines is smaller and it utilizes 31 RSR. All dimensions are presented in Table 3.7. The number of the via fences are equal to 32, having diameters *d* and it is connected to the guard trace, having same length and width of the microstrip lines.

Table 3.7: Design Parameters of RVG design

W	H	L	W_R	S_R, SV	L_R	Dv	$\varepsilon_{r1}, \varepsilon_{r2}$	S
0.396mm	*0.2mm*	*50mm ,15mm*	*1mm*	*1.5mm, 1.613mm*	*0.1mm*	*0.2mm*	*4.2, 4.1*	*3W*

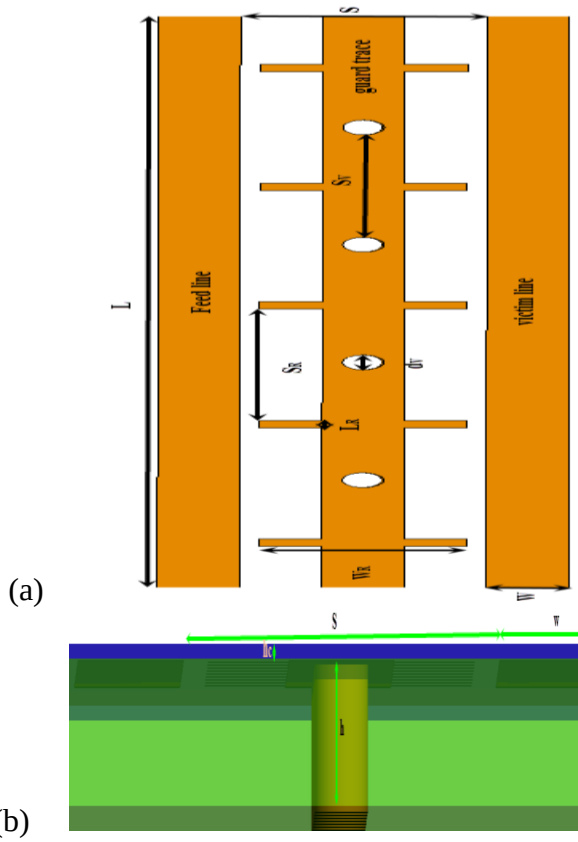

(a)

(b)

Figure 3.40: Double microstrip lines with RVG (a) Top view (b) Side view

It can be observed from Figures 3.41, 3.42 and 3.43 that using RVG with spacing 3*W*, leads to an increase in the direct couple S_{21}. For this reason the crosstalk (FEXT an NEXT) between microstrip lines decreased by 4dB, compared with the same structure with spacing *S*=4*W*.

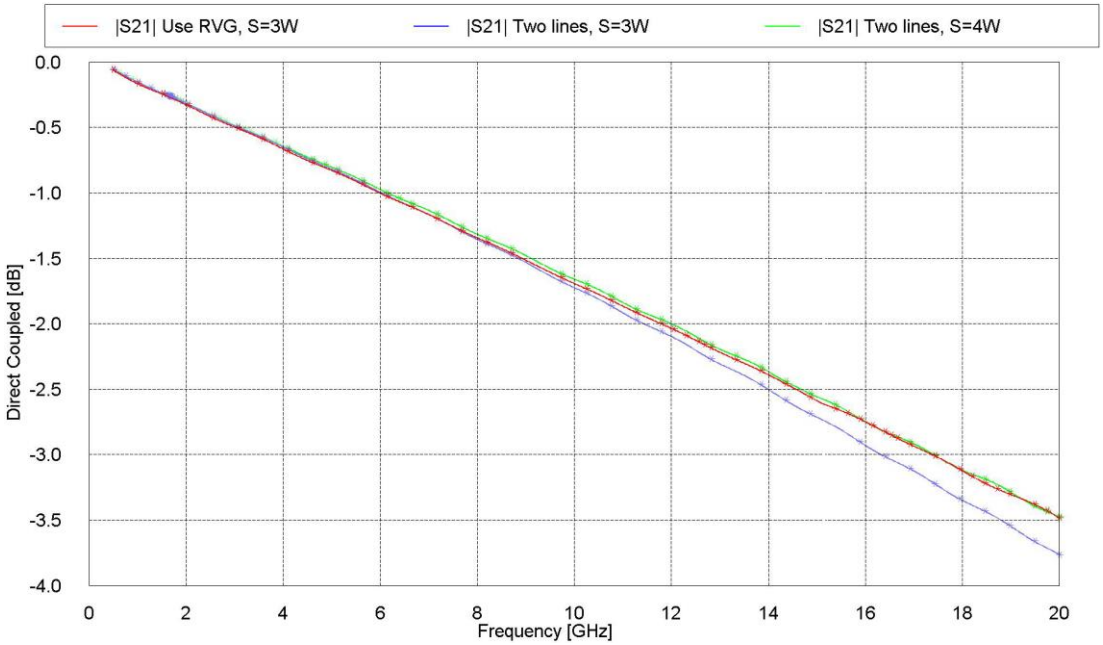

Figure 3.41: Comparison the direct couple S_{21} between use RVG and 3*W* rule

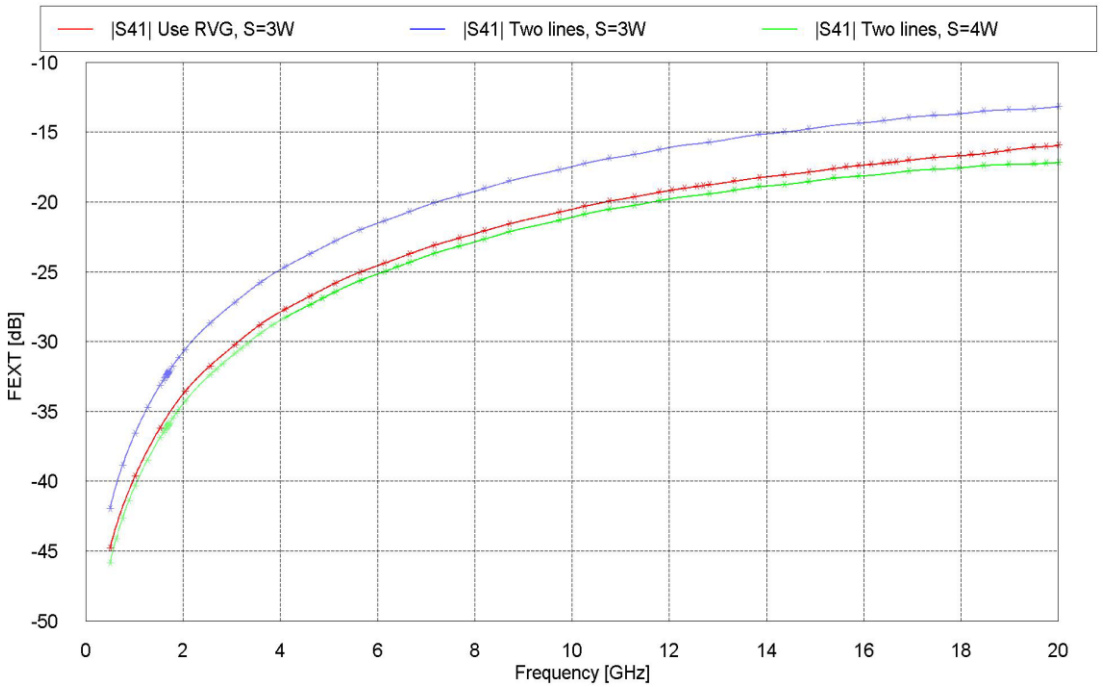

Figure 3.42: Comparison of FEXT between RVG and 3*W* rule

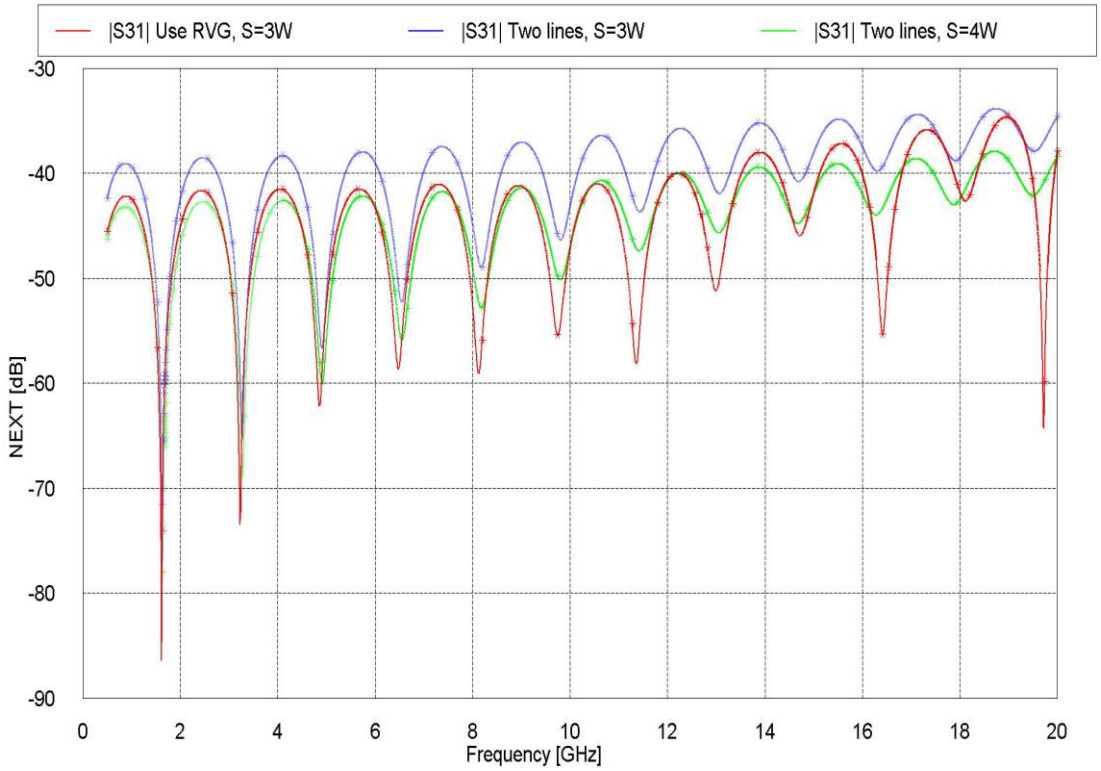

Figure 3.43: Comparison of NEXT between RVG and 3*W* rule

Figures 3.44 and 3.45 show the comparison of the results for two lengths of microstrip lines (50*mm* and 15*mm*) for RVG design.

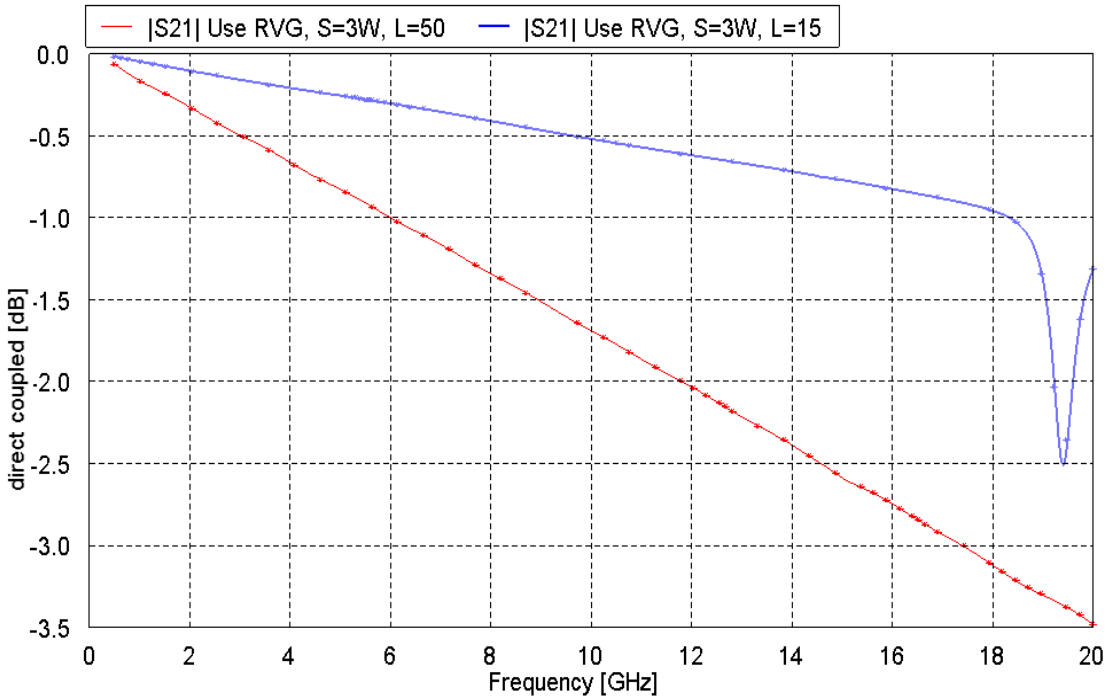

Figure 3.44: Direct couple S_{21} for two different line lengths

It can be observed from Figure 3.44 that, the direct coupling reduces as the length of the line increases. On the other hand, Figure 3.45 demonstrates that as the line length increases the FEXT increases.

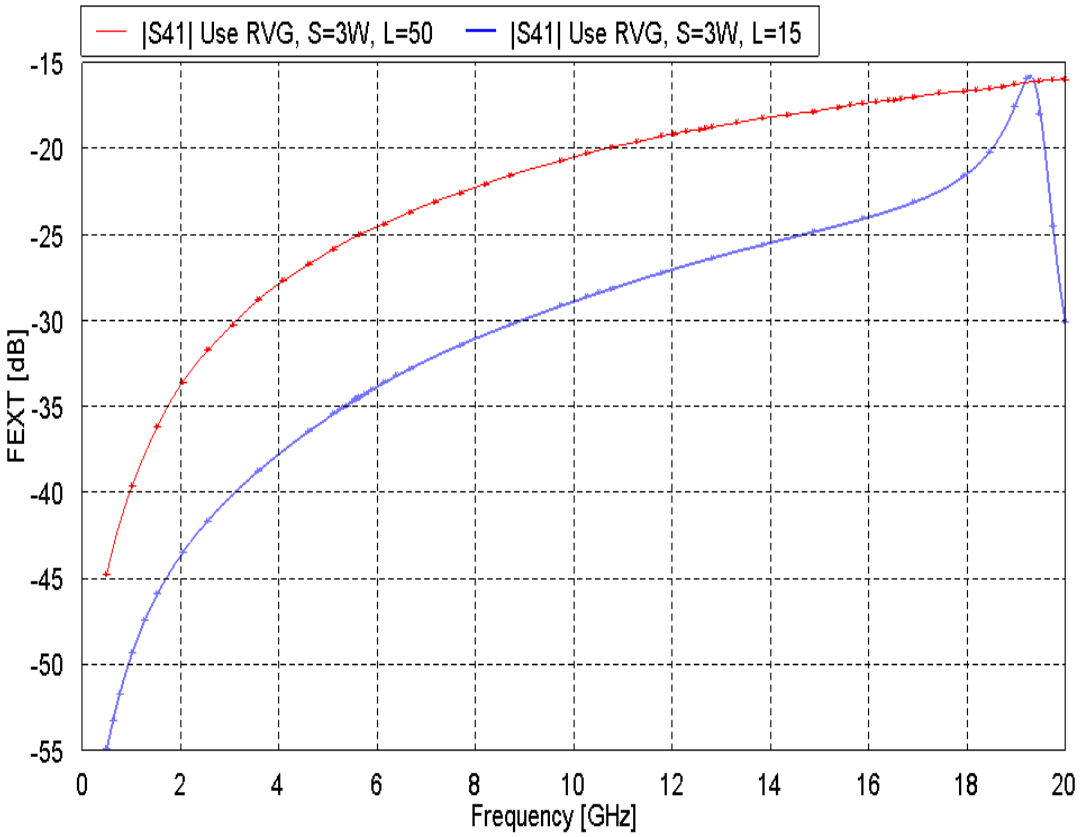

Figure 3.45: FEXT for two different line lengths

The electromagnetic field coupled between lines can be seen by Figure 3.46, when the RVG structure was used at frequency 10GHz.

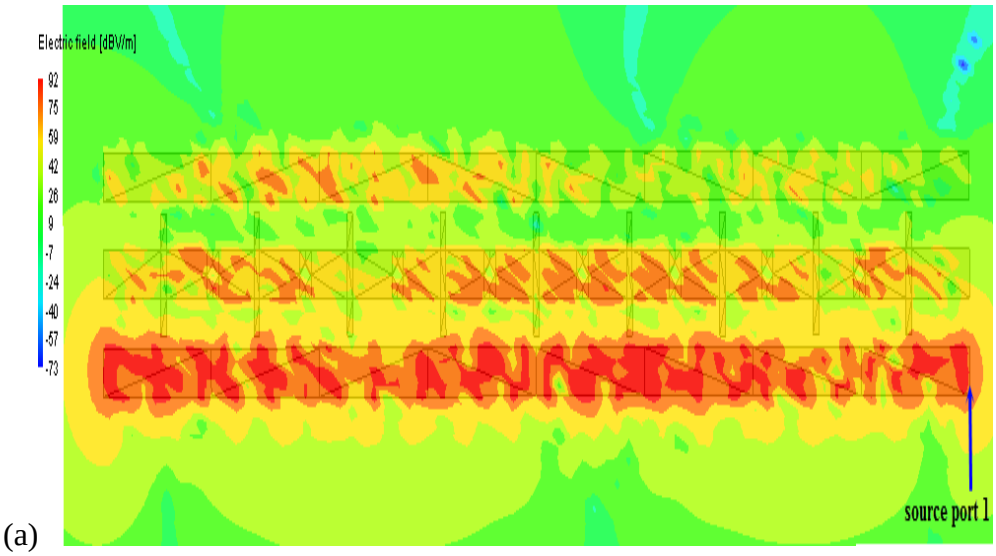

(a)

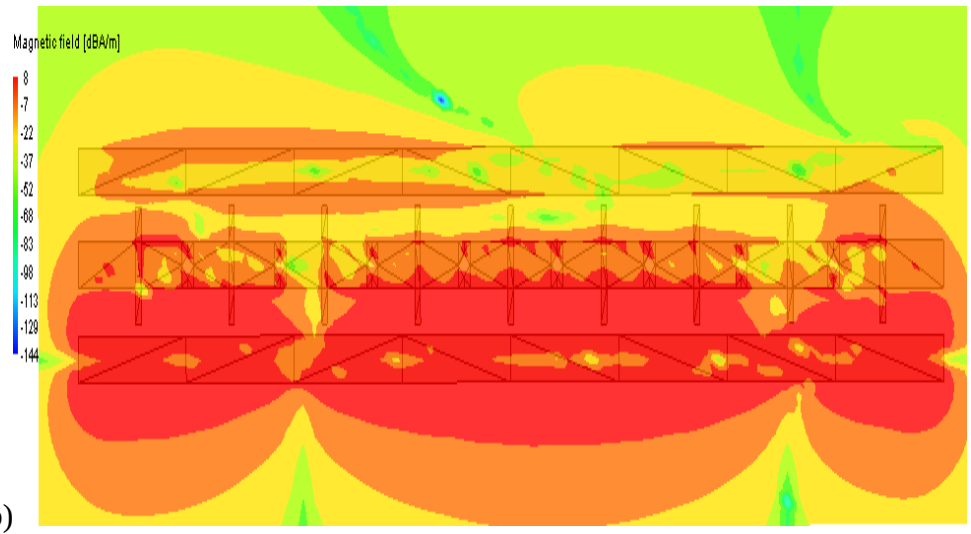

(b)

Figure 3.46: Electromagnetic field at 10 GHz for length15mm (a) Electric field (b) Magnetic field

3.2.3.8 Using CVG Between Microstrip Lines

This method is suggested to reduce the crosstalk by having less space between the microstrip lines. Cross Shape Resonators (CSR) were used with via fences connected by Guard Trace CVG as shown in Figure 3.47. The dimensions for this design are

explained in the Table 3.8. Also this method is one of the best methods to solve spacing problem to reduce crosstalk.

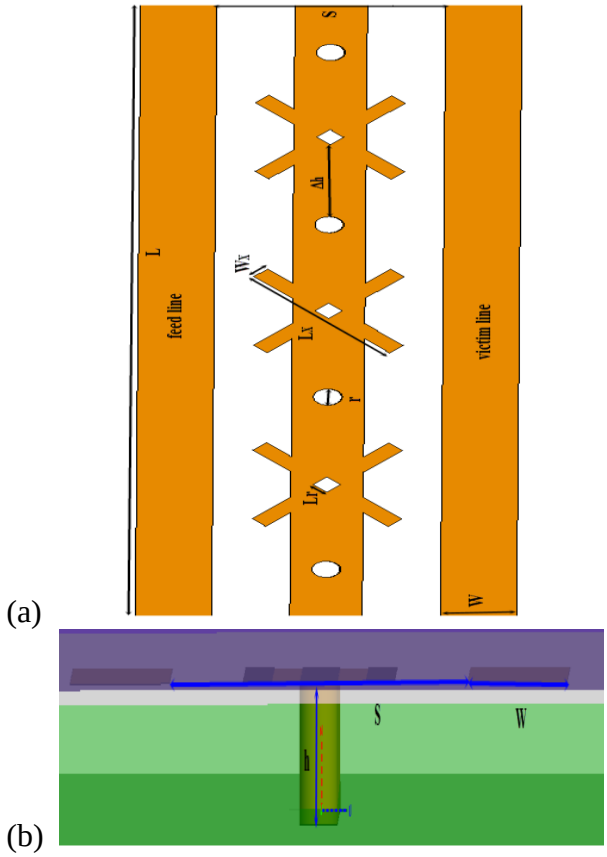

Figure 3.47: CVG structure (a) Top view (b) Side view for double microstrip lines

Table 3.8: Dimensions of CVG design

W	$\boldsymbol{W_X}$	L	$\boldsymbol{L_X}$	$\boldsymbol{L_r}$	h, $\boldsymbol{h_c}$	S	R	$\boldsymbol{\varepsilon_{r1}}$, $\boldsymbol{\varepsilon_{r2}}$	$\boldsymbol{\Delta h}$
0.396mm	*0.1mm*	*50mm, 15mm*	*1mm*	*0.1mm*	*0.2mm ,0.02mm*	3*W*	*0.15mm*	*4.2, 4.1*	*0.62mm*

In the Figures 3.48, 3.49 and 3.50 we will discuss the effect of using CVG between microstrip lines. We note that the new method reduces the FEXT 4dB compared with 3*W* spacing rule, and when the spacing in each design is 3*W* it is nearly the same with spacing 4*W*. Also it has Upswing in NEXT, known length of traces 50*mm*.

When length of traces is 15*mm*, XT is less compared to 50*mm*. FEXT is 8dB less for the shorter length as indicated in Figure 3.51 and the direct coupled indicated in Figures 3.52.

In the Figures 3.48, 3.49 and 3.50 discuss the effect of using CVG between microstrip lines compared with 3*W* and 4*W*.

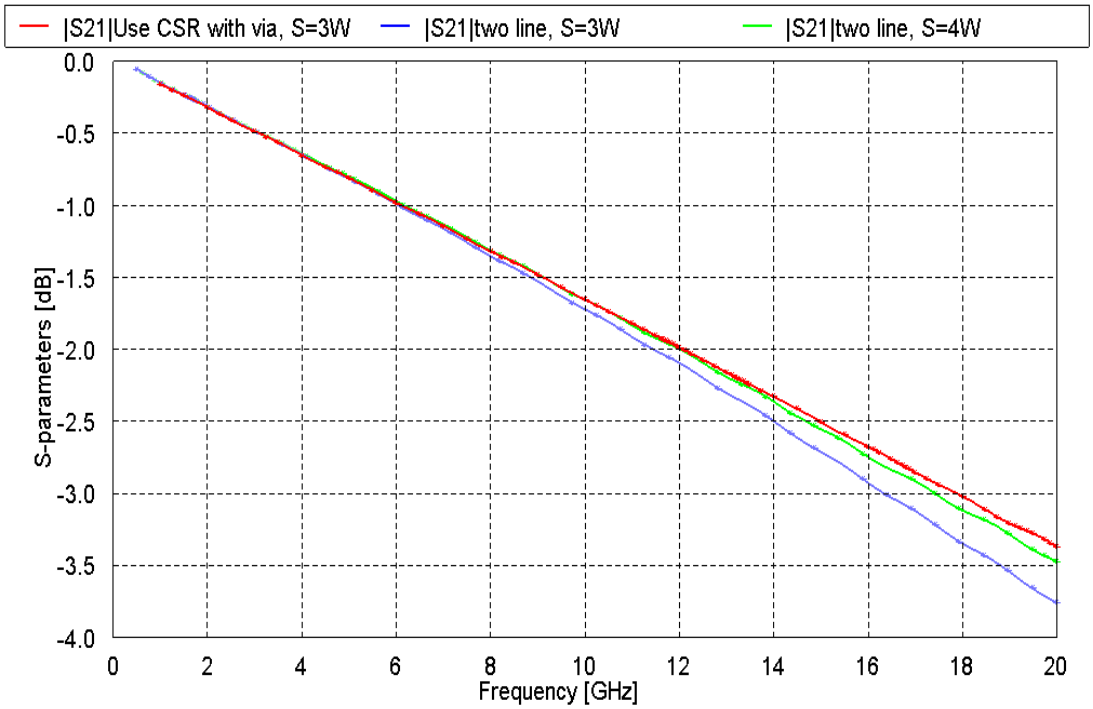

Figure 3.48: Direct couple S_{21} for CVG and 3*W*, 4*W*, when *L*=50mm

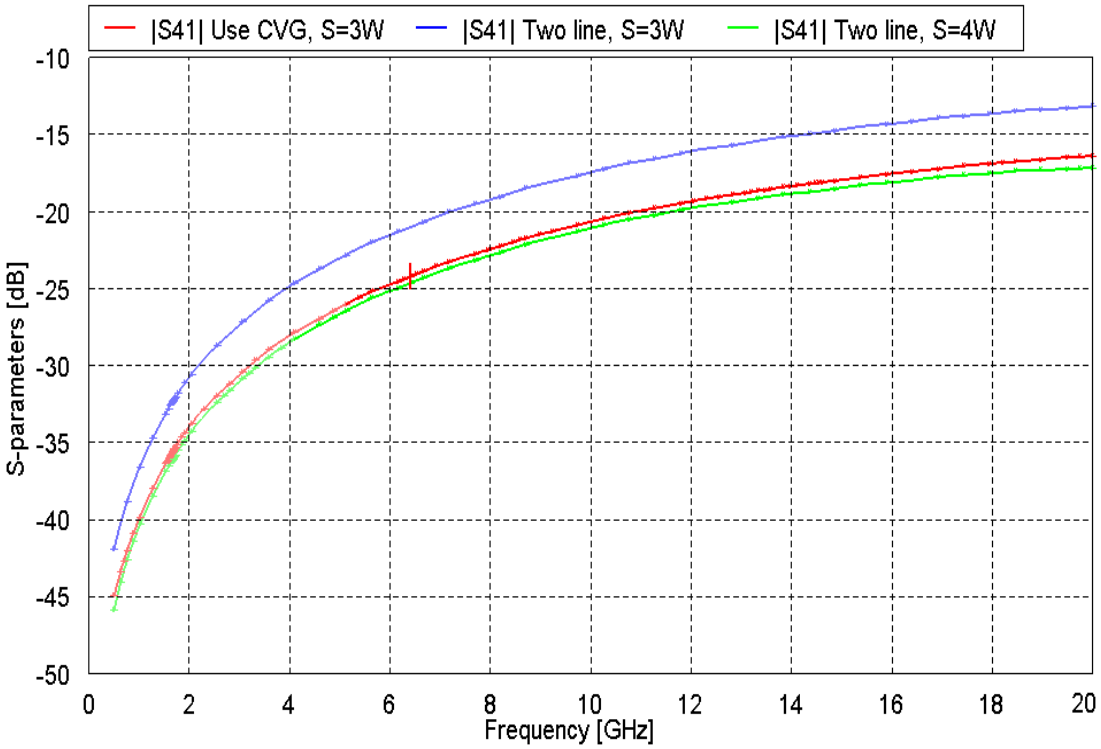

Figure 3.49: FEXT for CVG and 3*W*, 4*W* rule when length 50*mm*

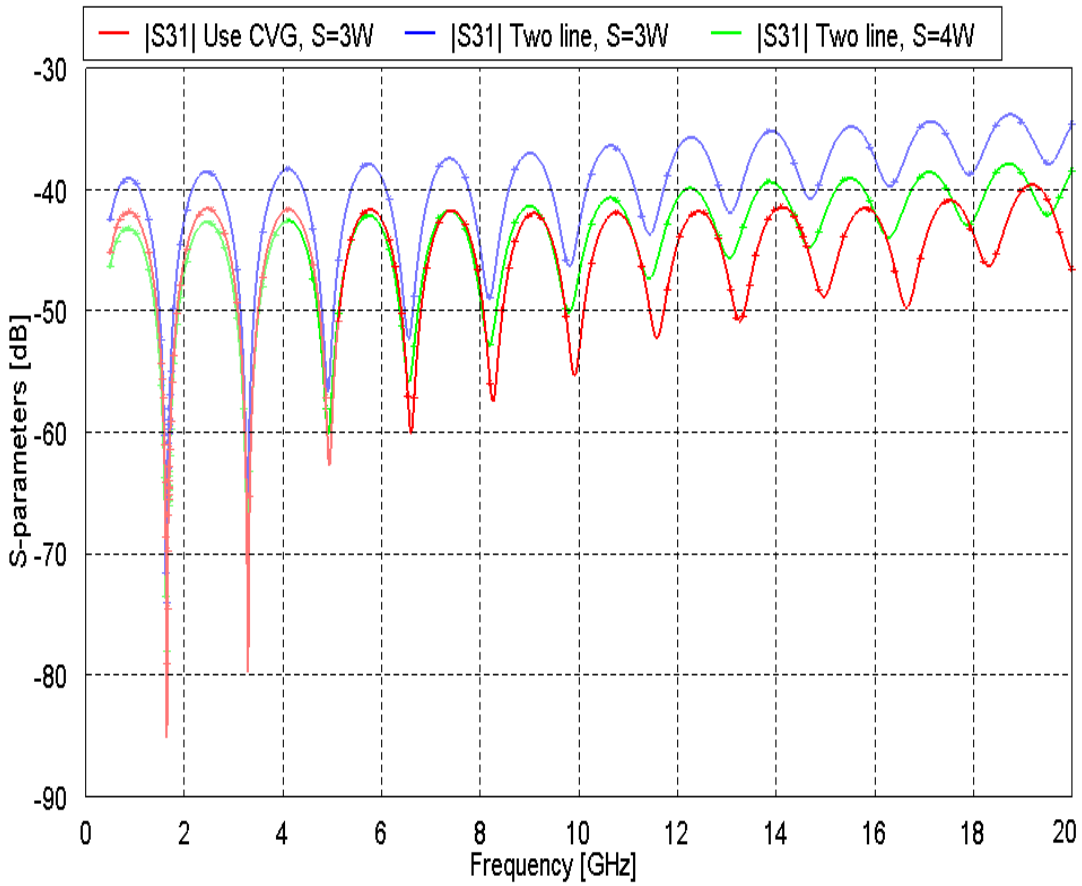

Figure 3.50: NEXT for CVG, 3*W*, *4W* with length 50*mm*

We note that the new method reduces the FEXT by 4dB compared with a 3*W* spacing rule, and it is nearly the same with spacing 4*W*. Also it has Improvement in NEXT, known length of traces 50*mm*. When length of traces is 15*mm*, it gives best result by helping to reduce XT than using 50*mm*. The direct coupled indicated in Figure 3.51 and FEXT is reduced by 8dB as indicated in Figures 3.52.

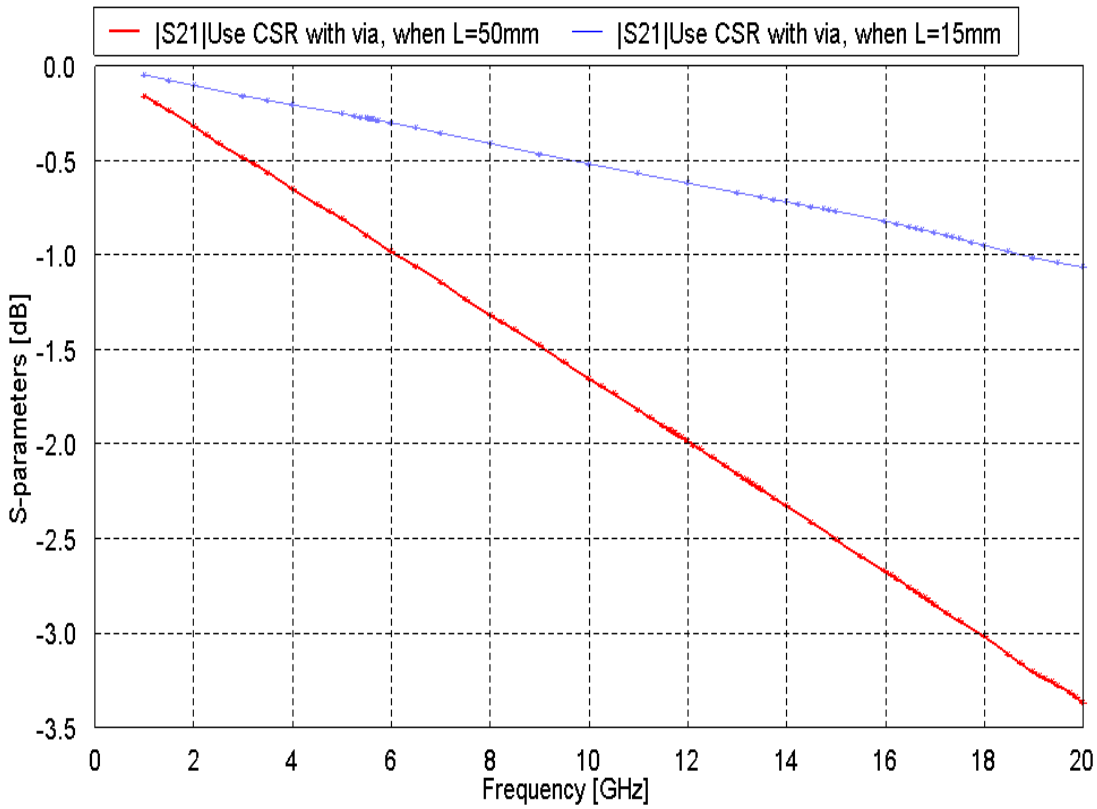

Figure 3.51: CVG results for direct couple when *L*=50*mm* and 15*mm*, *3W*spacing

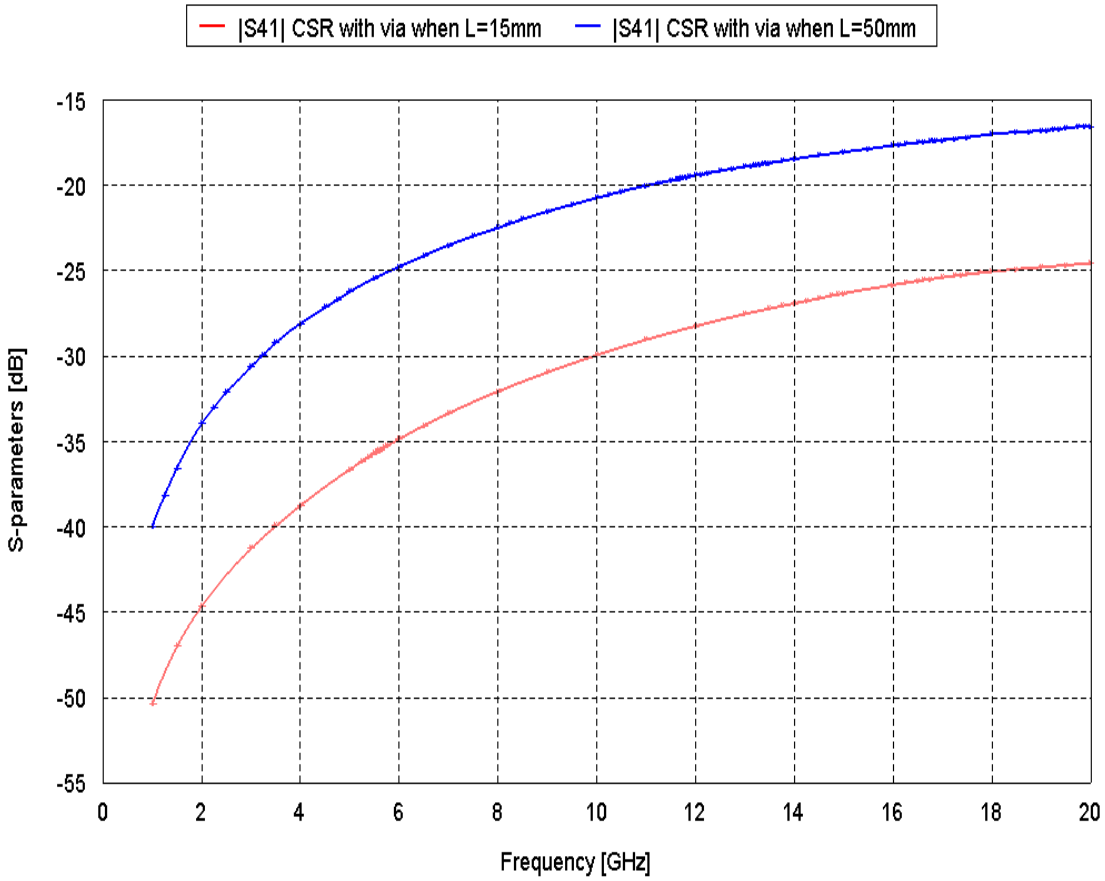

Figure 3.52: Compare CVG results of FEXT when *L*=50*mm* and 15*mm, with 3W* spacing

Figures 3.51 and 3.52 above show the comparison of the result for two lengths of microstrip lines (50*mm* and 15*mm*) when using CVG design.

The electromagnetic coupling between microstrip lines when CVG are used is shown in Figure 3.53 at 10 GHz frequency.

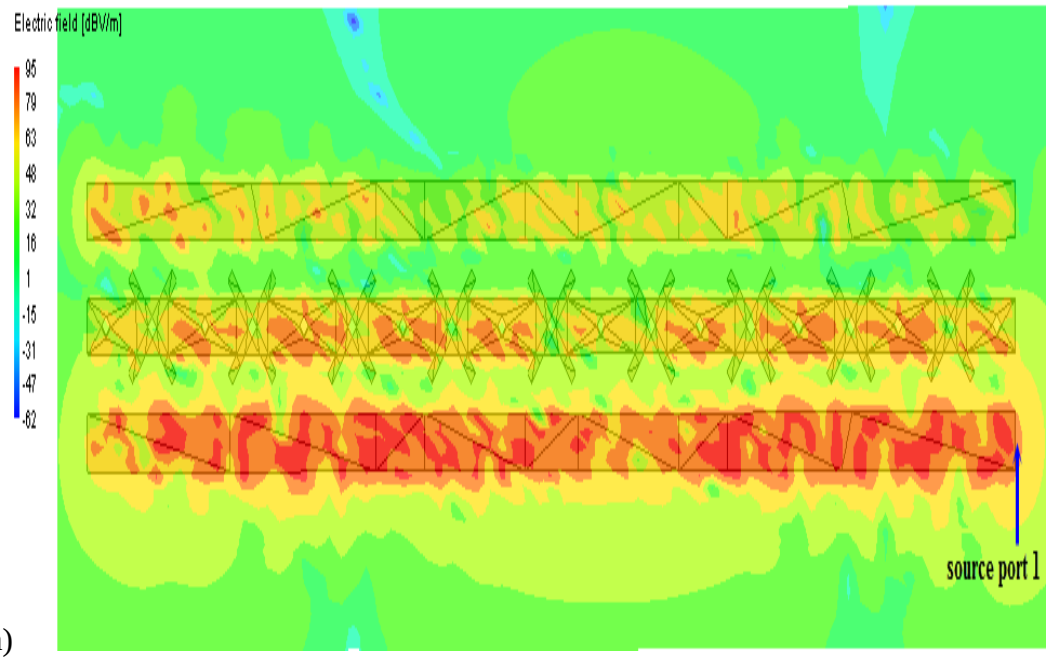

(a)

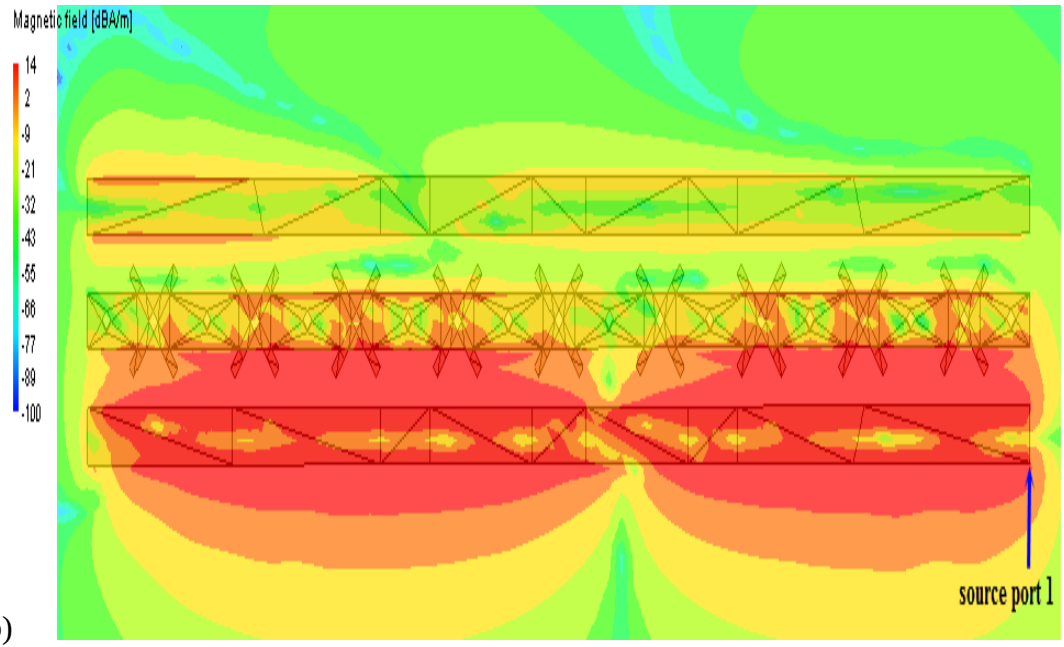

(b)

Figure 3.53: Electromagnetic coupling, *L*=15*mm* (a) Electric field (b) Magnetic field

Figures 3.54, 3.55 and 3.56 shows the results of direct coupling S_{21} at port 2, FEXT S_{41} at port 4 and NEXT S_{31}at port 3 respectively comparing among new methods which are (RVG, CVG and Rectangular trace with line length 15). We note that the result for using CVG is slightly better than using RVG but it is not better than the use of shorting via with smaller relative permittivity.

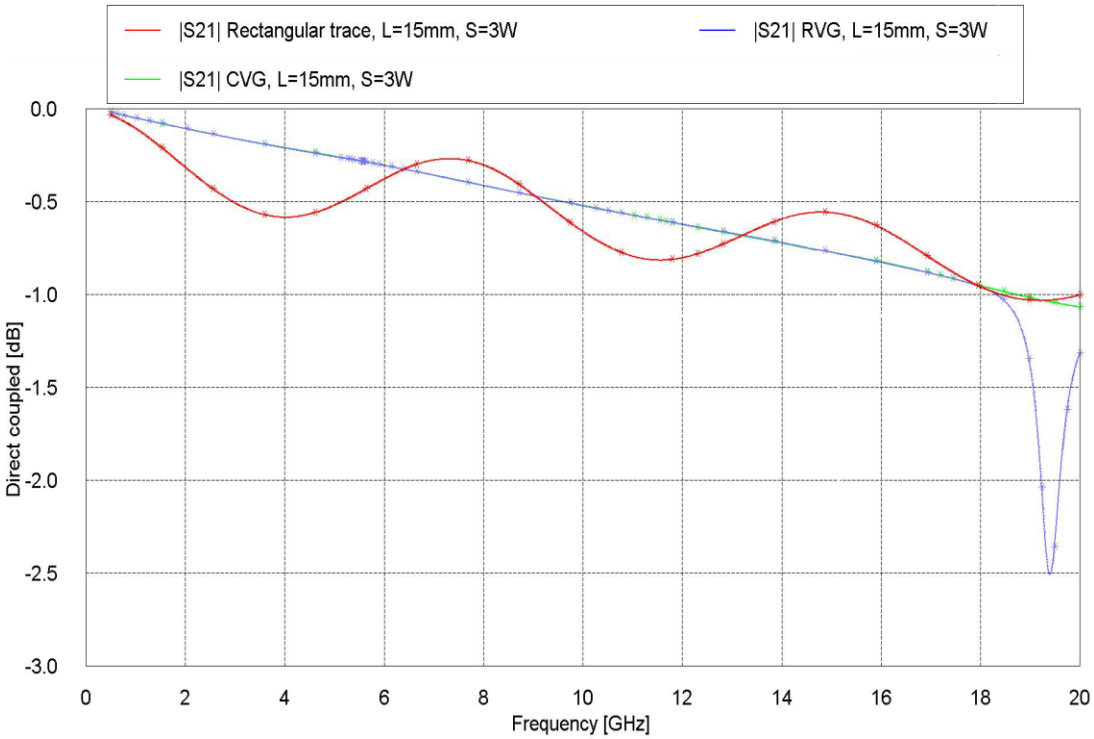

Figure 3.54: Comparing the direct couple among CVG, RVG and use Rectangular trace, when L=15mm

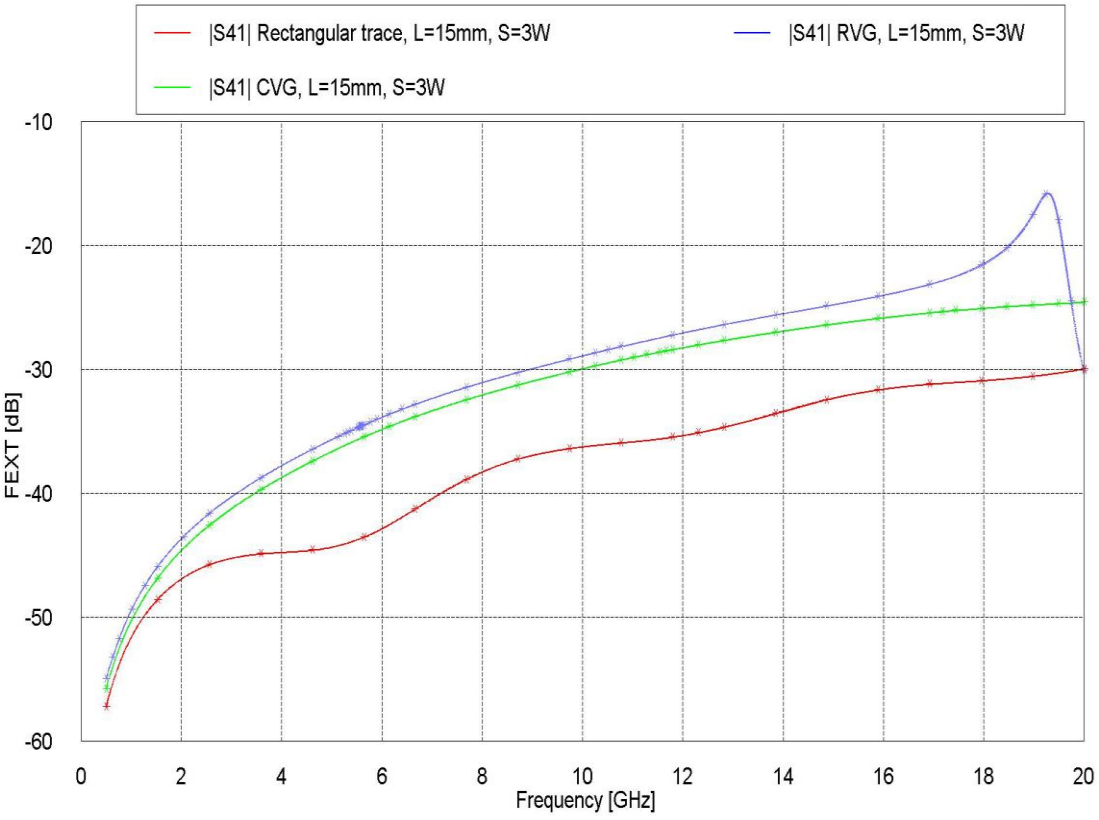

Figure 3.55: Comparing the FEXT among CVG, RVG and use Rectangular trace , when L=15mm

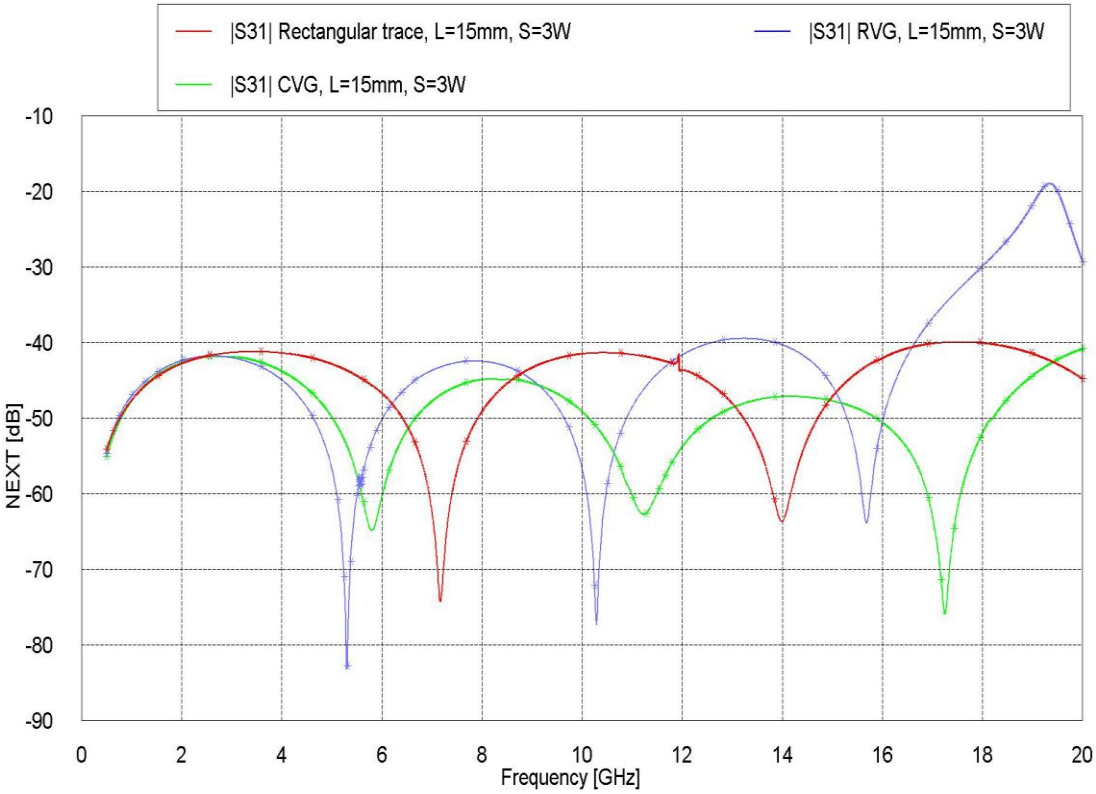

Figure 3.56: Comparing NEXT among CVG, RVG and use Rectangular trace, when L=15mm

Chapter 4

DISCONTINUITY PROBLEM

4.1 Introduction

The discontinuity problem in microstrip lines e.g. step-width, bending, open and short-circuit, series gap, T-junction, cross junction etc. is frequently found in microwave circuit. The performance of circuit is affected by the discontinuity when the frequency increases [7]. In the discontinuity part of microstrip lines, the surface waves are produced. When they are generated they will move and radiate. This leads to coupling with other lines of the circuit and reduce the isolation among the networks. For all reasons above, the surface waves are undesired cases in the transmission lines theory [15].

The discontinuity problem is due to sudden change in the geometry of microstrip lines and the distribution of electric and magnetic fields differ close to the discontinuity part. The changes in distribution of electric field lead to changes in capacitance and the altered magnetic field circulation leads to an alteration in inductance of the microstrip line [15].

The discontinuity effect is undesired but sometimes important to justify other cases of discontinuities. These cases of discontinuities may be intentionally entered into the circuit to perform specific electrical functions such as do stubs on a microstrip line for matching or filtering [10].

To solve the discontinuity problem, we must get rid of the discontinuity part. This is achieved by making gradual change in impedance instead of sudden changes which generates discontinuity in the signal.

4.2 Types of Discontinuities

In this section the two cases of discontinuities will be studied; step-width and bending or right angle bend in microstrip lines.

4.2.1 Step in Width Discontinuity

In this case the sudden variation in the impedance of the TL's occurred, for this reason the discontinuity in the signal will occur. On the other hand, the steps-width in MSL's in lowpass filters and general transformation to achieve matching in transmission line circuit is utilized [16]. Figure 4.1 shows the equivalent circuit of Step-Width MSL's. For removal of discontinuity or reduction, is possible by chamfering the corners [17]. This case makes the impedance of TL's to be gradually changing by ensuring that the width in the transition part between two different width lines doesn't change suddenly but gradually. The chamfered steps are shown in Figure 4.2.

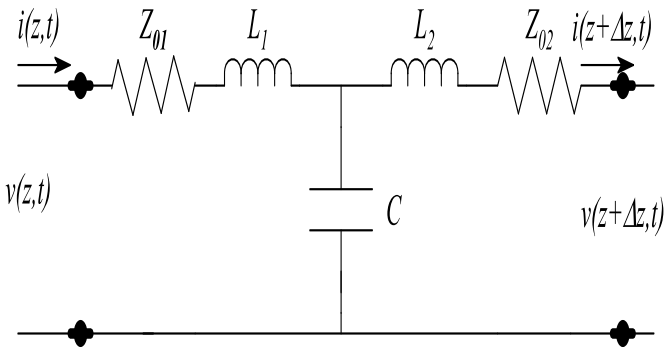

Figure 4.1: The equivalent circuit of the Step in width MSL [10]

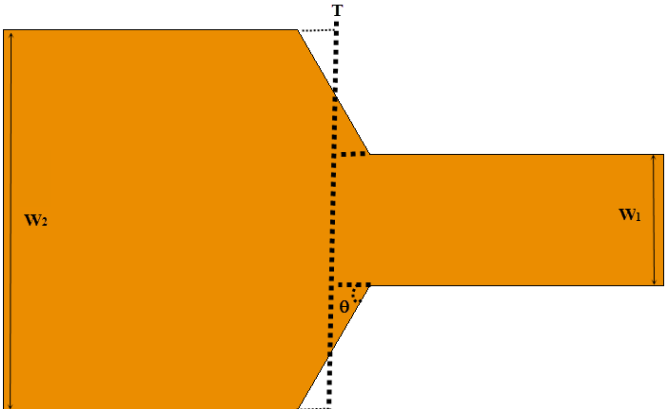

Figure 4.2: Step in width with chamfered step

4.2.2 Right angle bend Discontinuity

Right angle bend is one of the discontinuity cases that consider the discontinuity capacitance caused by increase area of the conductor at the corner of bend line. The equivalent circuit of the bending microstrip line is shown in Figure 4.3. The discontinuity effect on this case and that of step impedance could be eliminated by chamfered corner with specific angle. In the right angle bend the best results achieved when angle is 45° miter as shown in Figure 4.4, it is the distance between indoor corner *M* and outdoor corner *Y* [10] .

In this chapter we will analyze the problem and reduce it.

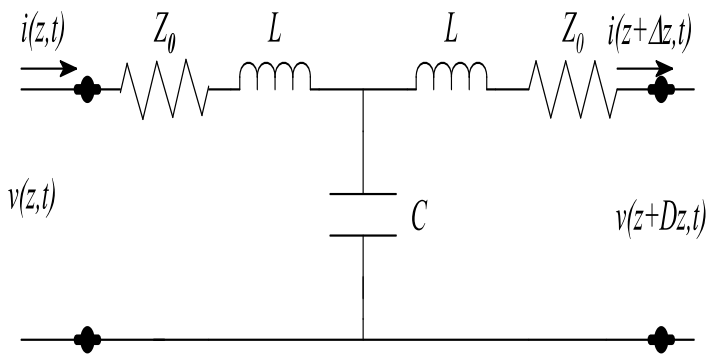

Figure 4.3: Equivalent circuit for bending microstrip line [10]

4.3 Simulation Results

In this section we will analyze the discontinuity in transmission lines and reduce it by using compensated step discontinuities, and by chamfering occasion triangular parts on the wider area of strip, by using FEKO 5.5 simulator.

4.3.1 Right angle bend discontinuity

Jianbo et al., worked together to analyze the discontinuity problem in microstrip lines right angle and step-in-width as shown in Figure 4.4. They used Finite-Difference Time-Domain FDTD method in wide frequency range to study this problem.

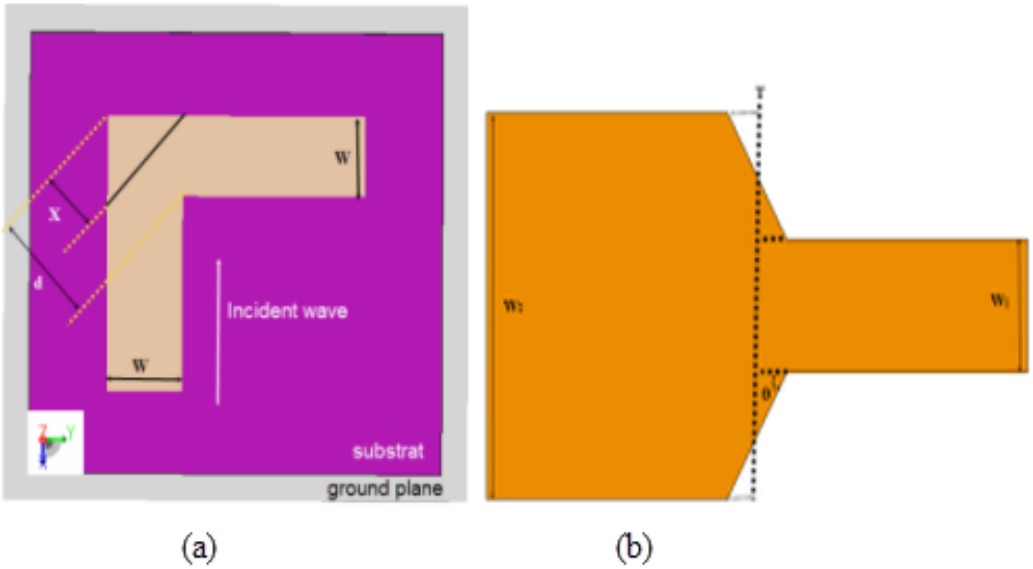

Figure 4.4: Top view of (a) The bending (b) Step-width microstrip lines [7]

The design dimensions of the bending structure consists of width of lines w = 0.12 mm, and the microstrip line put on the substrate have thickness h=0.127mm and 9.9 relative permittivity ε_r. They found out that when the pulse reaches the bend part, the reflection occurs and the pulse has gradual attenuation. They was reduced this problem by chamfering the corner of bending microstrip lines as shown in the Figure 4.5. The comparison was done between results by [7] and results by using FEKO 5.5

simulator as shown in Figures 4.6 and 4.7 which show a good agreement between them.

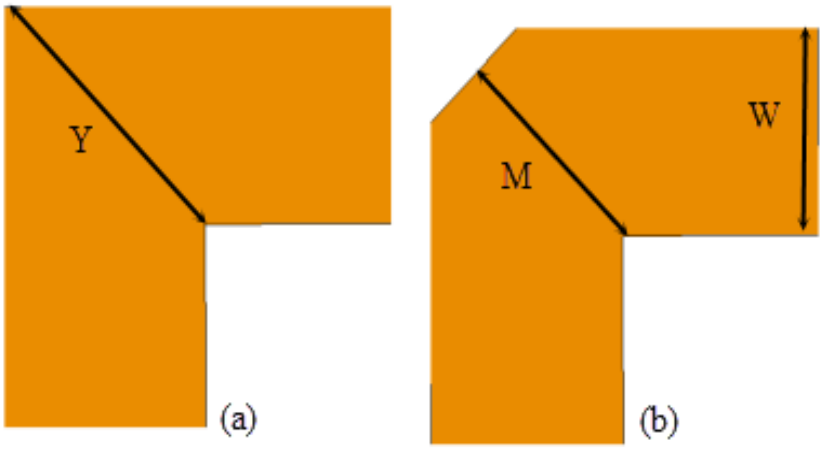

Figure 4.5: Top view structure of the bending (a) without chamfered (b) with chamfered

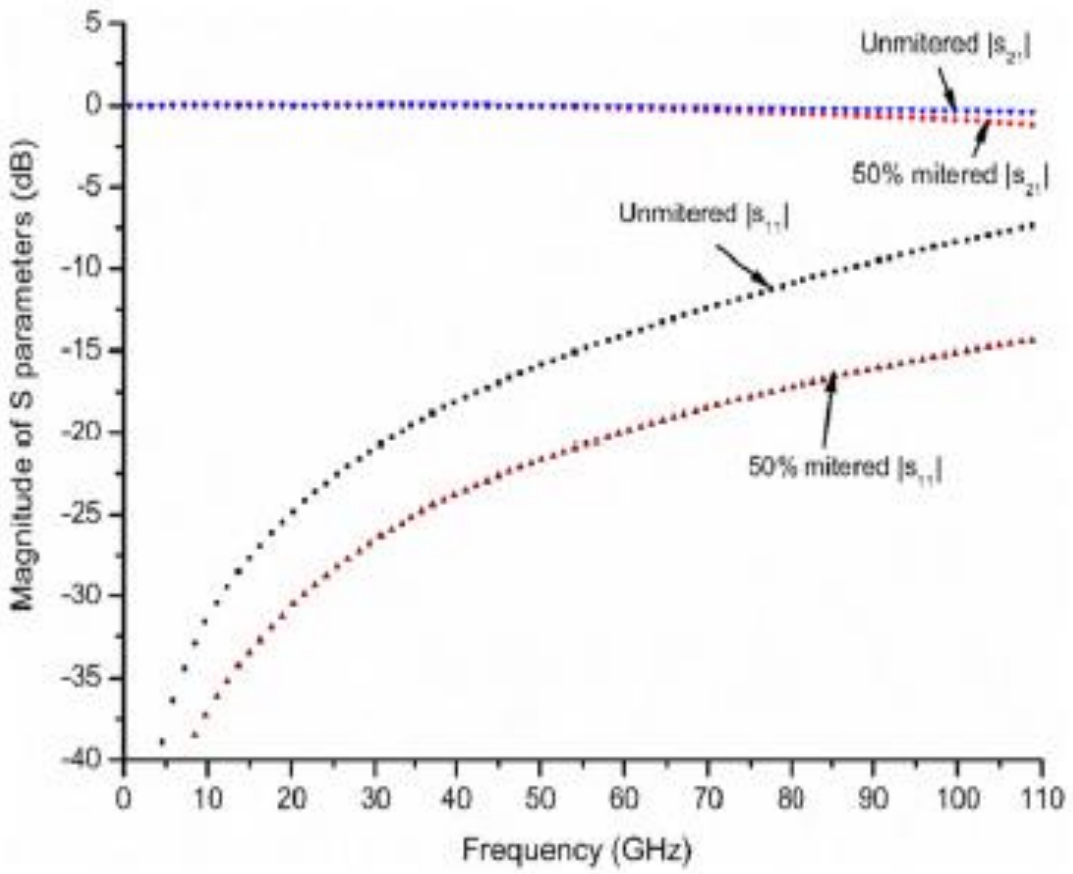

Figure 4.6: Comparing S-parameters between chamfered and non-chamfered line [7]

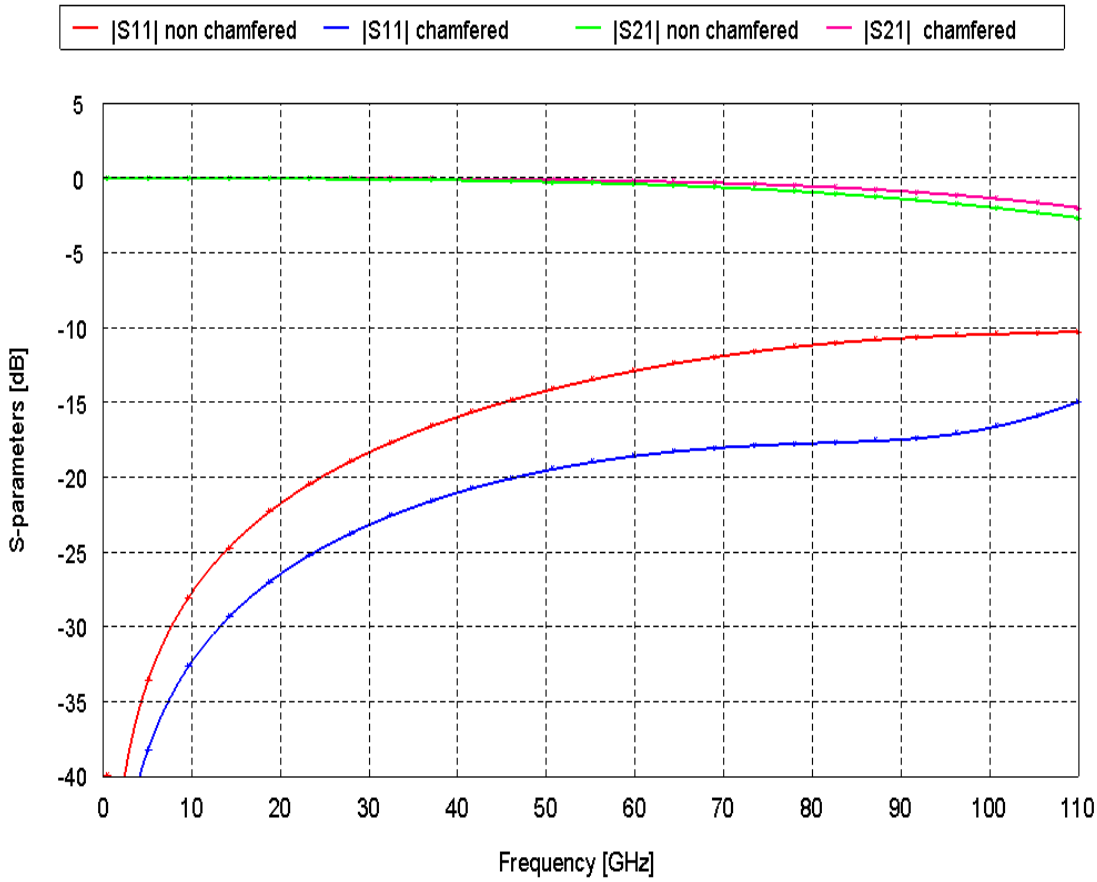

Figure 4.7: Comparing between chamfered and Non-chamfered bend line by FEKO

In those results we observe that the reflection coefficient S_{11} and transmission coefficient S_{21} are improved when chamfer the bend corner by making ratio $\frac{Y-M}{Y}$ equal to 50% than without chamfer.

When the chamfer method was applied by the ratio 70 % from the bend corner, it gives a better result than 50% by 3dB for great bandwidth from 19 to 95 GHz as shown in Figure 4.8.

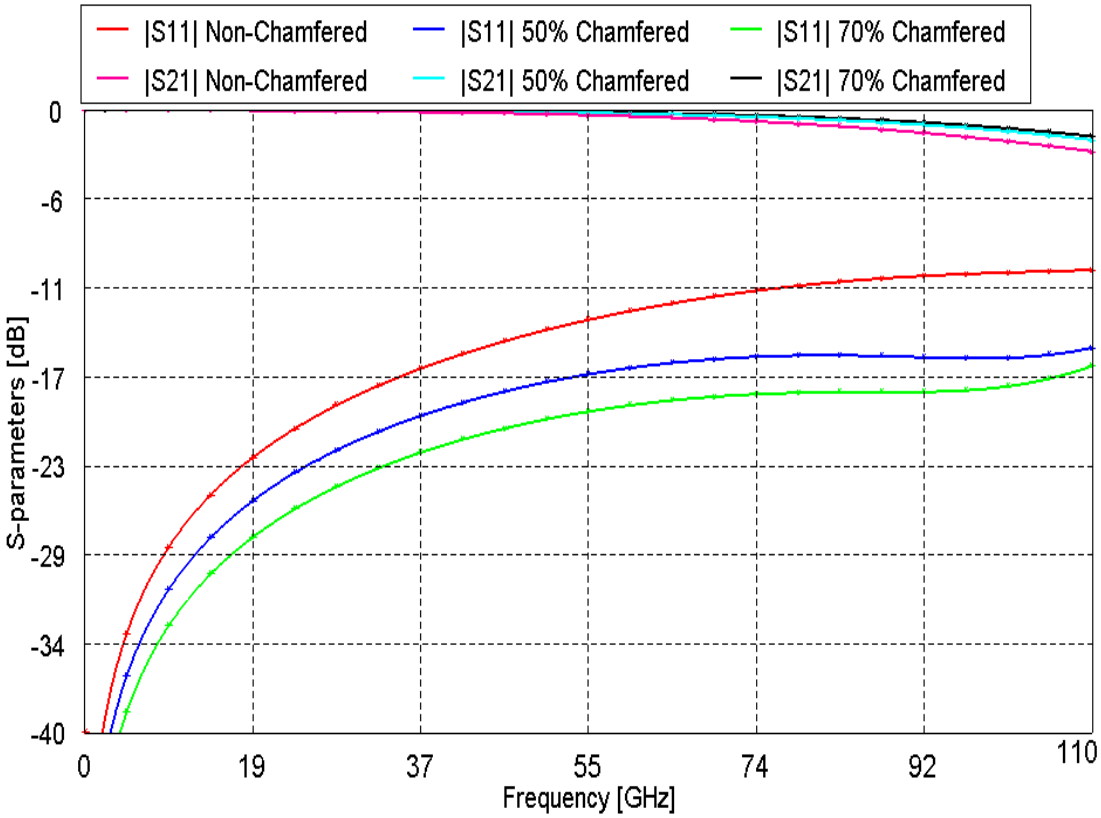

Figure 4.8: Effect of chamfered bend line by 70%

Figure 4.9 shows the electric field at source, bend and load respectively, and the magnetic field is shown in Figure 4.10, when the bend corner in transmission lines is non-chamfered.

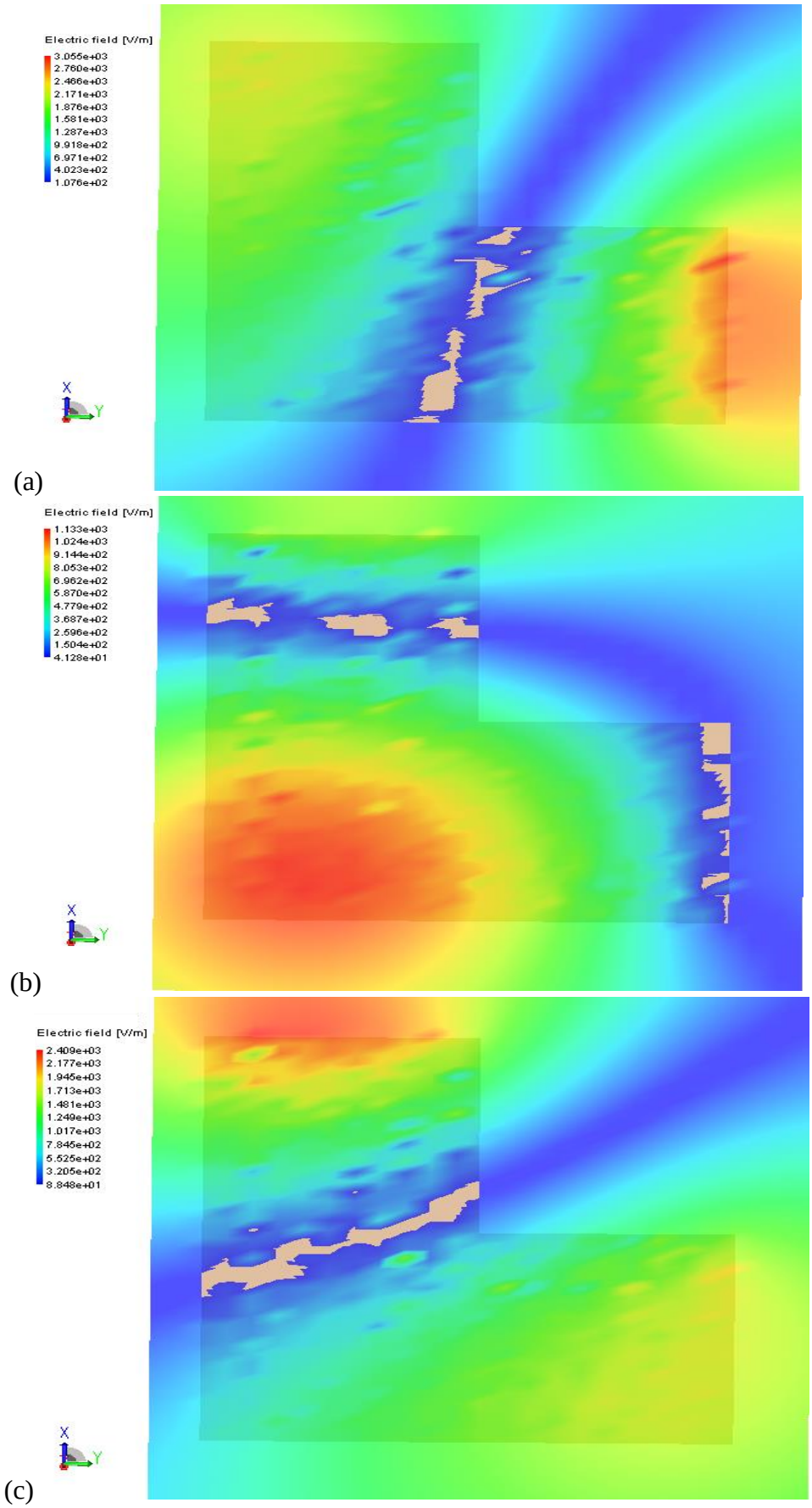

Figure 4.9: Electric field (a) At source (b) At bend (c) At load

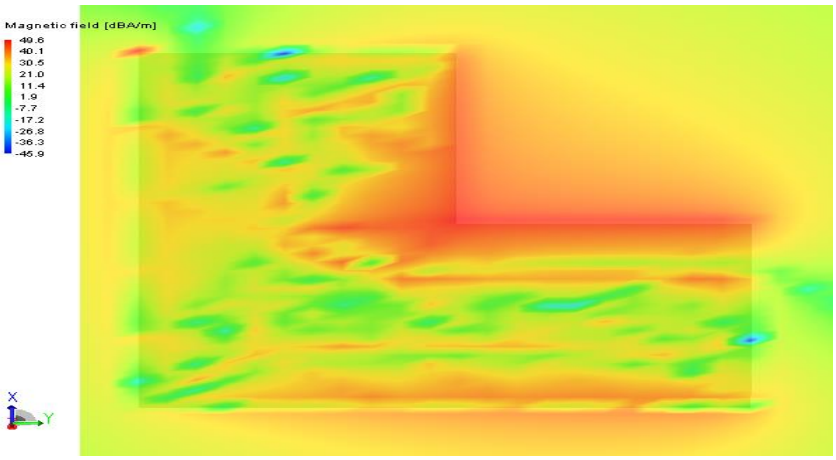

Figure 4.10: Magnetic field, non-chamfered line

Figures 4.11 and 4.12 are show the electric and magnetic field when the corner of the bend lines is chamfered.

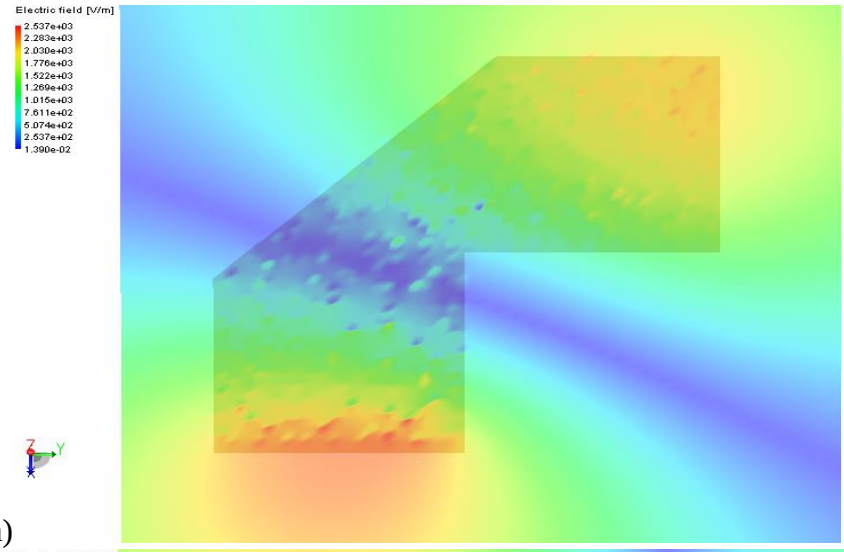

(a)

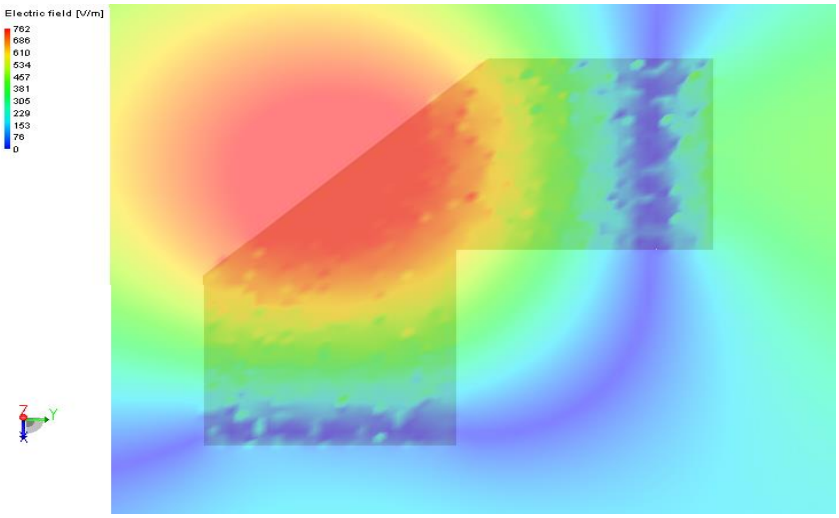

(b)

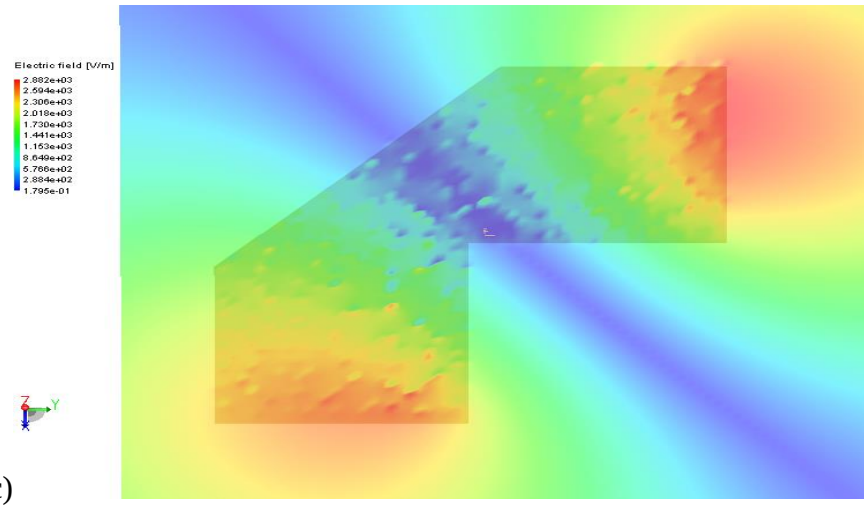

(c)

Figure 4.11: Electric field (a) At source (b) At chamfered bend (c) At load

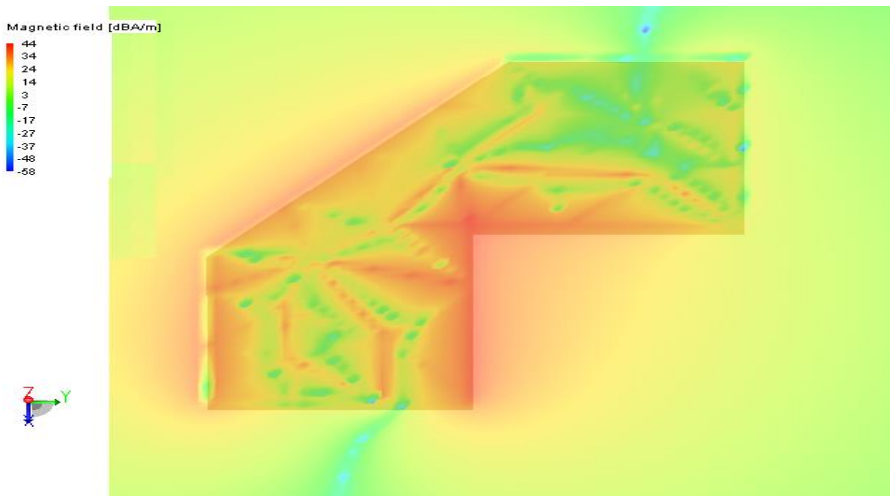

Figure 4.12: Magnetic field, chamfered bend

4.4.2 Step in Width Discontinuity

For the Step-Width the narrow width W_1 with 1.25mm and the wide Step-Width W_2 with 6mm is placed on the substrate having 2.22 as relative permittivity ε_r and thickness h is 0.508mm [7] as shown in the Figure 4.13. The authors found out that when using chamfer it leads to an improvement in the results; when θ decreases from 90, 60 to 45 the reflection coefficient get better. The comparison between the reference [7] and the results by FEKO 5.5 simulator gives closely same as indicated in Figures 4.14 and 4.15.

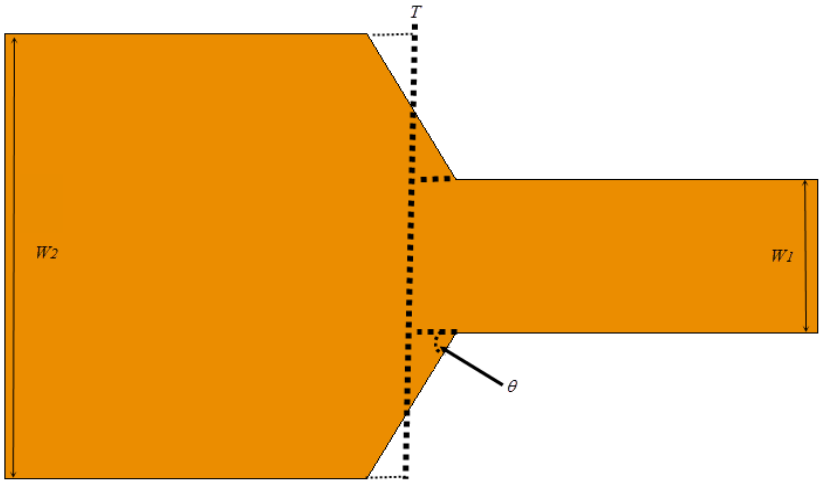

Figure 4.13: Step width structure for different angles

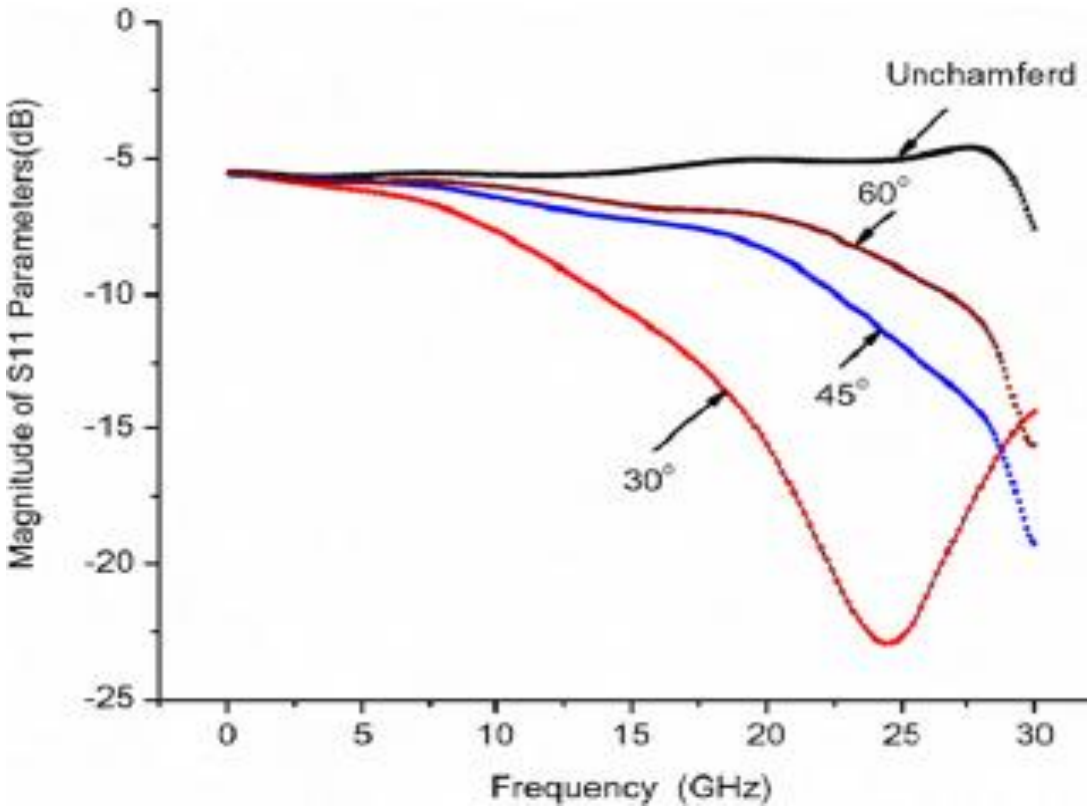

Figure 4.14: Comparsion of the S_{11}between chamfered and non-chamfered line [7]

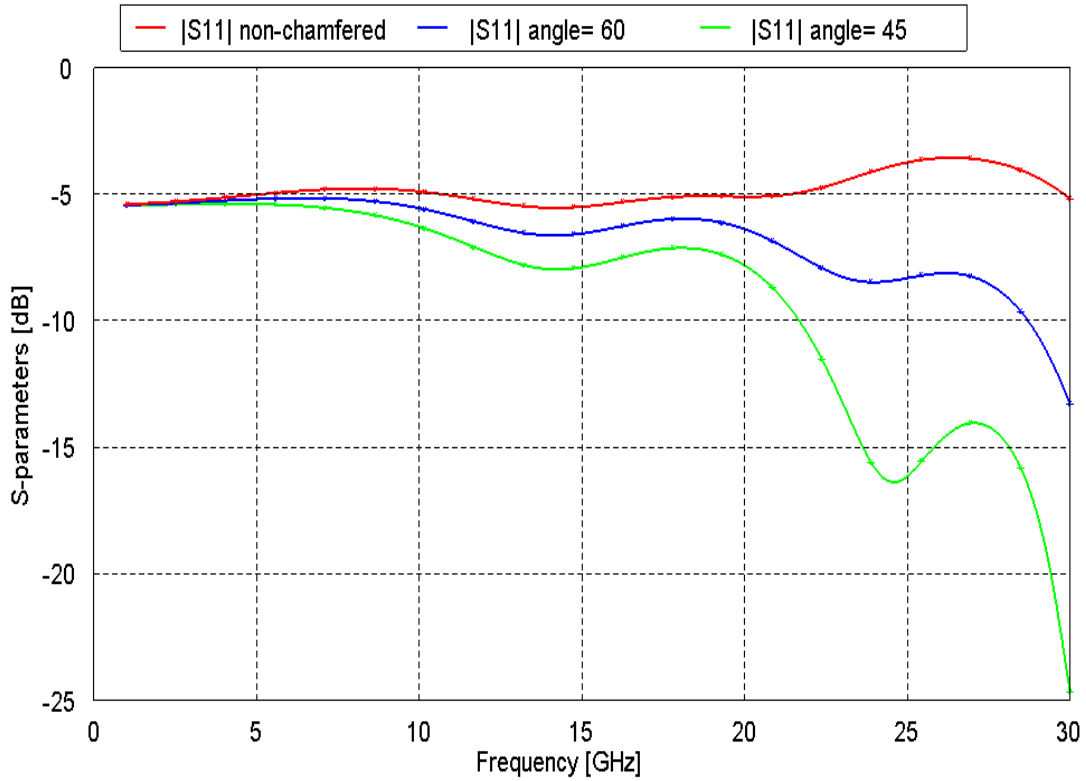

Figure 4.15: Comparison of S-parameters between non-chamfered and chamfered line

In Figure 4.15 we note that when the angle decreases the discontinuity will be decreases.

The electric field in steps without chamfer indicated in the Figures 4.16 and 4.17.

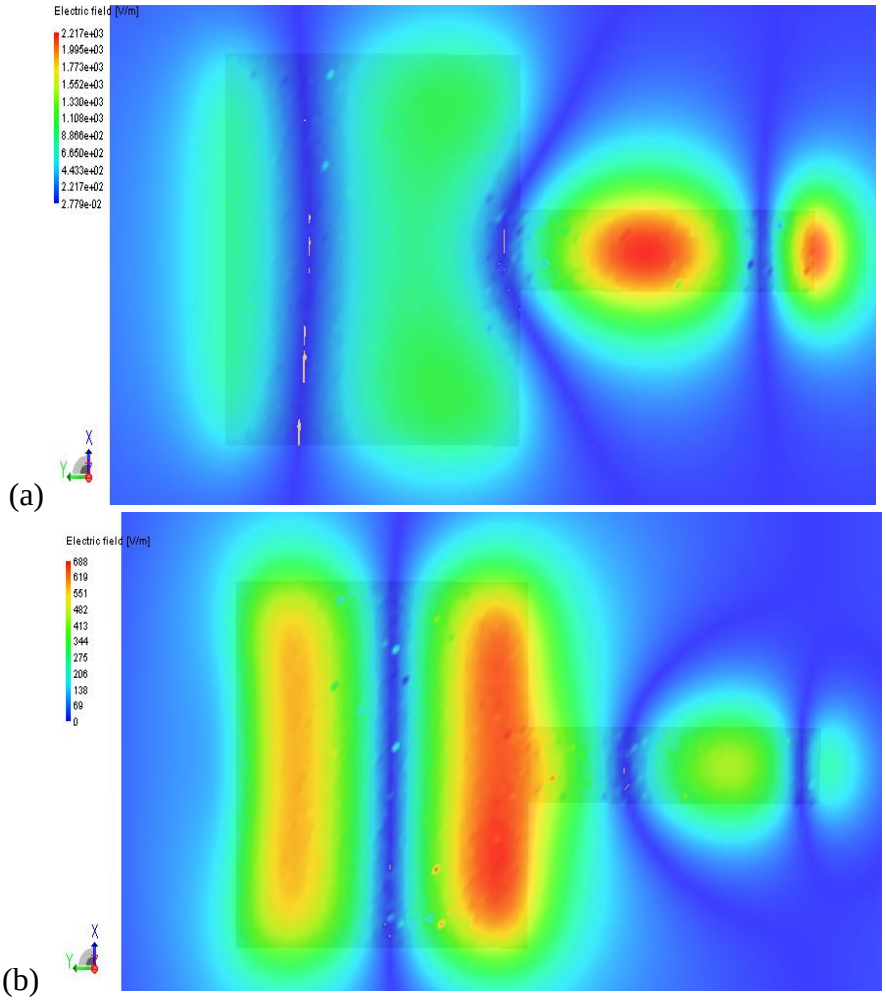

Figure 4.16: Electric field (a) At source step (b) At load step

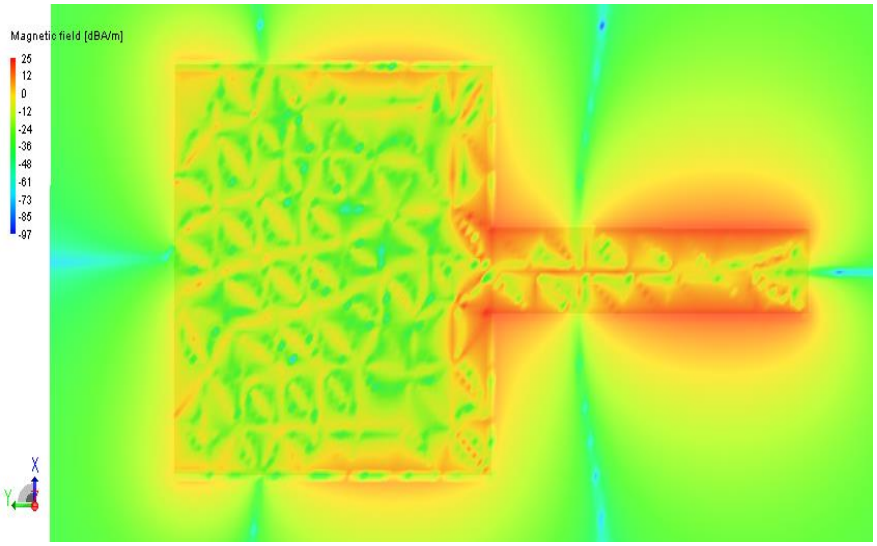

Figure 4.17: Magnetic field non-chamfered step

The electromagnetic field with chamfer by 45^{o} is shown in Figures 4.18 and 4.19.

(a)

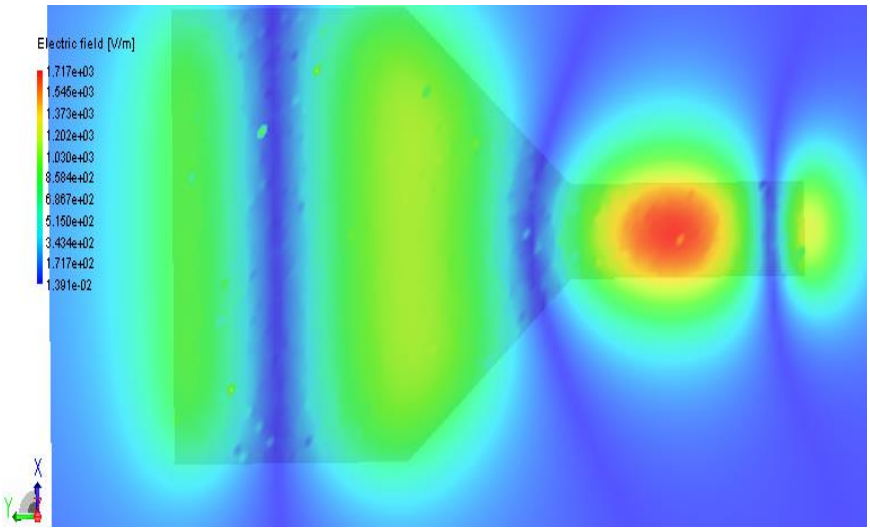

Figure 4.18: Electric field for chamfered step off line

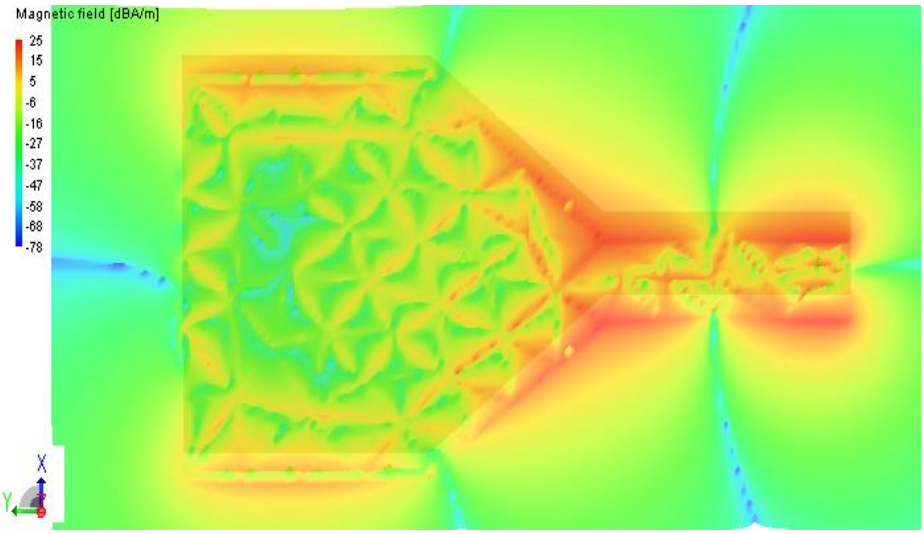

Figure 4.19: Magnetic field for chamfered step

4.4.2.1 Chamfered All Step

New method used to reduce the discontinuity problem in the step-width microstrip lines. This achieve when the chamfered is done to all steps in microstrip lines as shown in Figure 4.20 [10]. The greater improvement in the result would be achieved when this method are used, as indicate in Figure 4.21.

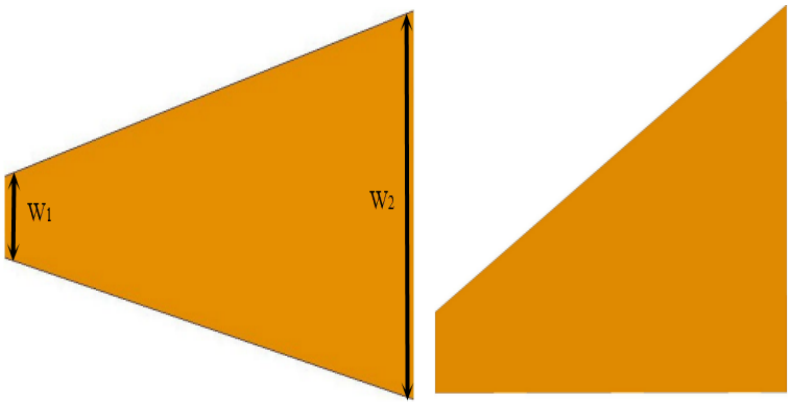

Figure 4.20: Step in width with all step chamfered (a) Two side (b) One side

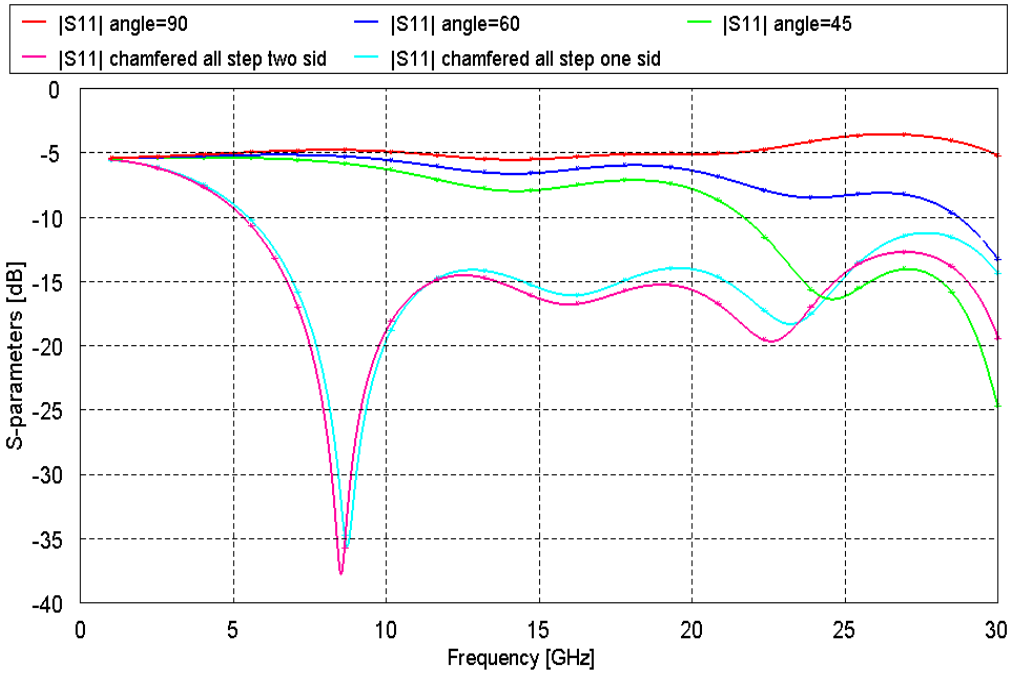

Figure 4.21: Comparing S_{11} between angles and all step chamfered

Figure 4.21 shows that the reflection coefficient S_{11} when chamfered all sides comparing with the angle chamfered which also shows that the results will have a great improvement in the signal transmission.

The electromagnetic field when chamfered all step are shown in Figures 4.22 and 4.23 respectively.

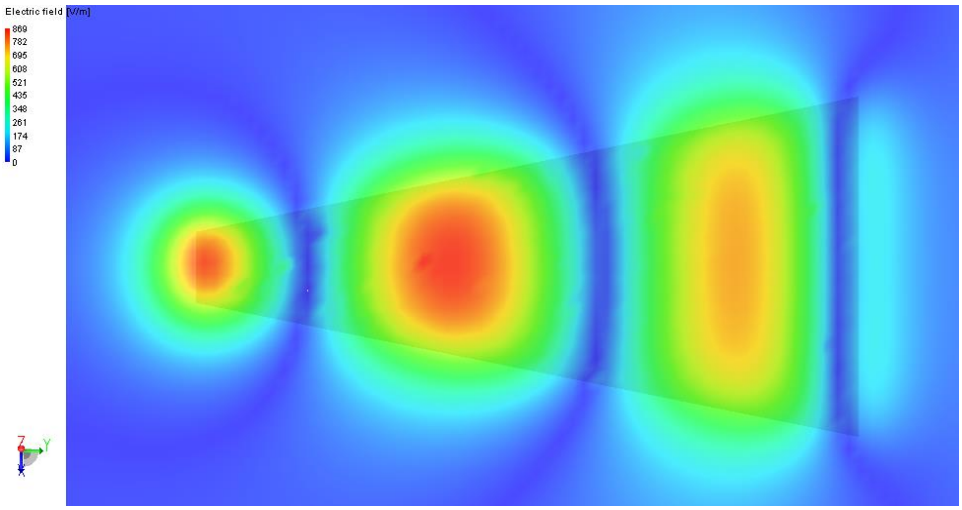

Figure 4.22: Electric field for all step chamfered

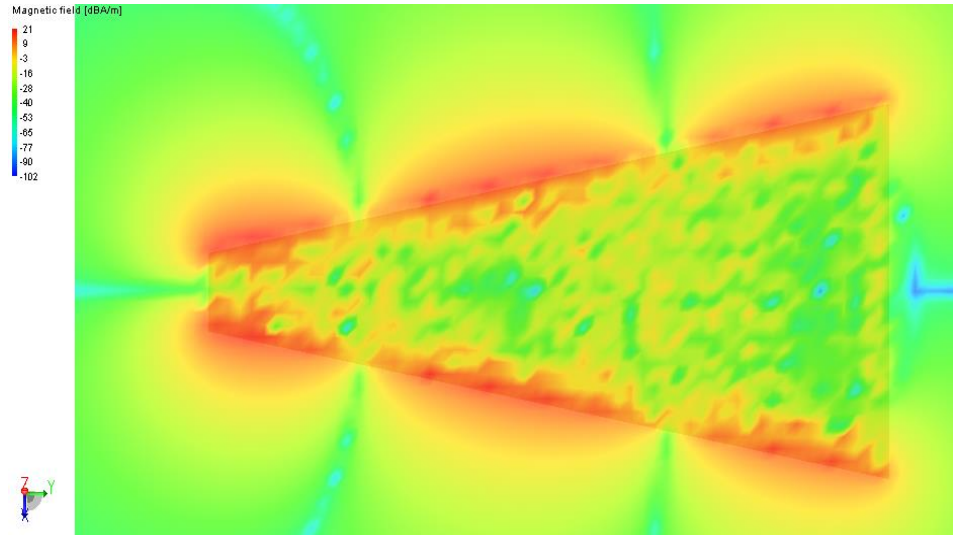

Figure 4.23: Magnetic field for all step chamfered

Chapter 5

CONCLUSION AND FUTURE WORK

5.1 Conclusion

In this thesis, we work on two main microstrip line problems. The first, crosstalk problem between double microstrip lines there is the analysis and simulated by using FEKO 5.5 simulation software. With several previous methods in use, we accommodate new ways of reduction in crosstalk by using novel geometry e.g. using rectangular trace between microstrip lines, use of RVG and CVG with shortened via fence at short line lengths helped us to get better results for (FEXT and NEXT). We compare with past manners to solve this problem; and discover improvement in our results nearly by 7dB, 7dB, and 8dB for FEXT, by using rectangular trace between microstrip lines , RVG and CVG respectively, if this is compared with the result of the design with spacing rule of $S = 4W$. But for NEXT it reduces but slightly range because the NEXT is less effective on signal integrity (SI) at receiver than FEXT.

In the second part, we try to solve the discontinuity problem by using the chamfered method for the bend and step width microstrip lines. Also, novel geometry was proposed to solve this problem by chamfering the sides of the step-in-width microstrip line. A WB of nearly 23GHz within the operating range was observed when compared with the step-in-width without chamfered, and for the bend discontinuity with chamfered ratio 70% , we found out that reflection coefficient was reduced by 4 dB for 19GHz-95GHz *BW* compared with 50% chamfered ratio.

5.2 Future Work

The delay and overshot problems in the lines causes problems especially when the dimensions are very small (Micron levels for the VLSI applications). Codes can be developed to measure the delay and the overshoot and suggest solutions. Similar simulations may be carried out by the stripline.

REFERENCES

[1] Felix D. Mbairi, W. Peter Siebert, and Hjalmar Hesselbom, "High-frequency transmission lines crosstalk reduction using spacing rules," *IEEE transactions on components and packaging technologies,* vol. 31, no. 3, pp. 601-610, 2008.

[2] Indar Surahmat, Sugihartono, Achmad Munir, "Crosstalk analysis of parallel microstrip line using 4-port scattering model," in *International Conference on Electrical Engineering and Informatics*, Indonesia, 2011.

[3] Wen-Tzeng, Huang Ding-Bing Lin and Chen-Kuang Wang and Chi-Hao Lu, "Using rectangular-shape resonators to improve the far-end crosstalk of the coupled microstrip lines," in *Electromagnetics Research Symposium Proceedings*, Morocco, 2011.

[4] George E. Ponchak, Donghoon Chen, Jong-Gwan Yook, and Linda P. B. Katehi, "Filled via hole fences for crosstalk control of microstrip lines in LTCC packages," in *3rd International Wireless Communications Conference (WCC98) Digest*, San Diego, 1998.

[5] Jinsook Kim, Weiping Ni, and Edwin C. Kan, "Crosstalk reduction with nonlinear transmission lines for high-speed VLSI system," in *IEEE Custom Intergrated Circuits Conference (CICC)*, Ithaca, 2006.

[6] Marek-Sadowska, Ashok Vittal and Malgorzata, "Crosstalk reduction for VLSI," *IEEE transactions on computer-aided design of integrated circuits and systems*, vol. 16, no. 3, pp. 290-298, 1997.

[7] Jianbo Maol, Yingshen Xu, Rui Zhang, Mingwu Yangl, and Jinxian Liu, "Analysis of microstrip discontinuities and their compensation via the finite difference time domain method," in *Microwave Technology and Computational Electromagnetics International Conference*, China, 2009.

[8] N. O. Sadiku, Matthew, *Elements of Electromagnetics*, Oxford: Oxford, 2011.

[9] Pathak, Rashmi, "Characterizing losses in microstrip transmission lines," *University of Wisconson-Madison, milwaukee*, 2005.

[10] M. Pozar, david, *Microwave Engineering*, amherst: Wiley, 2005.

[11] Huan-Huan Li, Chen-Jiang GUO, Yu Zhang, "Research of crosstalk reduction between microstrip lines based on high-speed PCBs," in *College of Electronic information, Northwestern Poly technical University*, China, 2010.

[12] Mbairi, F. D., "Some aspect of advanced technologies and signal integrity issues in high frequency PCBs, with emphasis on planar transmission lines and RF/ microwave filters," *KTL information and communication technology, stockholm*, 2007.

[13] Asanee Suntives, Arash Khajooeizadeh, Ramesh Abhari, "Using via fences for crosstalk reduction in PCB circuits," in *University of Alberta*, Canada, 2009.

[14] Li Shufang, Sun Fuxun, "Simulation for crosstalk in coupled microstrip transmission lines," in *Asia-Pacific Conference on Environmental Electromagnetics*, China, 2003.

[15] Rosu, Iulian, "Microstrip, stripline, and CPW design," 2013. [Online]. Available: http://www.qsl.net/va3iul.

[16] W.Tang, Y.L. Chow and K.F. Tsang, "Different microstrip line discontinuities on a single field-based equivalent circuit model," *IEE Proc. Microw. Antennas Propag*, vol. 151, no. 3, pp. 256-262, 2004.

[17] Rakesh chadha, and K. C. Gupta, "Compensation of discontinuity in planare transmission lines," *IEEE traansactions on microwave theory and techniques*, Vols. MTT-30, no. 12, pp. 1151-1156, 1982.